TUNNELING NANOTUBE NETWORKS IN DENDRITIC CELL COMMUNICATION AND HIV-1 TRANS-INFECTION

by

Colleen Rosemarie Zaccard

B.S., Medical Microbiology and Immunology, University of Wisconsin-Madison, 2001

M.S., Bacteriology, University of Wisconsin-Madison, 2008

Submitted to the Graduate Faculty of

Infectious Diseases and Microbiology

Graduate School of Public Health in partial fulfillment

of the requirements for the degree of

Doctor of Philosophy

University of Pittsburgh

2015

UNIVERSITY OF PITTSBURGH

GRADUATE SCHOOL OF PUBLIC HEALTH

This dissertation was presented

by

Colleen Rosemarie Zaccard

It was defended on

April 8, 2015

and approved by

Velpandi Ayyavoo, PhD, Professor and Assistant Chair, Infectious Diseases and Microbiology
Graduate School of Public Health, University of Pittsburgh

Simon Barratt-Boyes, PhD, Professor, Infectious Diseases and Microbiology
Graduate School of Public Health
Professor, Immunology
School of Medicine, University of Pittsburgh

Pawel Kalinski, MD, PhD, Professor, Surgery, Immunology
School of Medicine
Professor, Infectious Diseases and Microbiology
Graduate School of Public Health, University of Pittsburgh

Robbie B. Mailliard, PhD, Research Assistant Professor, Infectious Diseases and Microbiology,
Graduate School of Public Health, University of Pittsburgh

Simon C. Watkins, PhD, Professor and Vice Chairman, Cell Biology
School of Medicine, University of Pittsburgh

Dissertation Advisor: Charles R. Rinaldo, Jr., PhD, Professor and Chairman
Infectious Diseases and Microbiology
Graduate School of Public Health
Professor, Pathology
School of Medicine, University of Pittsburgh

Charles R. Rinaldo, Jr., PhD

TUNNELING NANOTUBE NETWORKS IN DENDRITIC CELL COMMUNICATION AND HIV-1 TRANS-INFECTION

Colleen Rosemarie Zaccard, PhD

University of Pittsburgh, 2015

ABSTRACT

The ability of dendritic cells (DC) to mediate $CD4^+$ T cell help for cellular immunity is guided by instructive signals received during maturation, and the resulting pattern of DC responsiveness to the Th signal, CD40L. Furthermore, the professional transfer of antigenic information from migratory to lymph node-residing DC is critical for the effective induction of cellular immune responses. Here we report that, in addition to their enhanced IL-12p70 producing capacity, human DC matured in the presence of inflammatory mediators of type-1 immunity (DC1) are uniquely programmed to develop networks of tunneling nanotubes (TNTs) in response to CD40L-expressing $CD4^+$ Th cells or recombinant CD40L. This immunologic process of 'reticulation' facilitates intercellular trafficking of endosome-associated vesicles and antigen, and is regulated by the opposing roles of IFN-γ and IL-4. The initiation of reticulation represents a novel helper function of CD40L and a superior mechanism of intercellular communication possessed by DC1, as well as a pathway for exploitation by pathogens for direct cell-cell spread. Importantly, DC1 possess a superior ability to transmit HIV-1 to $CD4^+$ T cells compared to DC2. DC1 highly express Siglec-1, the lectin associated with HIV-1 capture by mature DC, while DC2 fail to do so, indicating differential ability of polarized DC to acquire virus. Furthermore, CD40L signaling is critical for DC1-mediated HIV-1 trans-infection, as demonstrated by the abolition of transmission upon treatment with CD40L-specific blocking antibody. TNT

formation is dependent on F-actin and cholesterol-rich lipid rafts, as DC1 trans-infection was abrogated by pre-treatment with latrunculin A or simvastatin, which depolymerize actin or inhibit cholesterol synthesis, respectively, at concentrations that also inhibited TNT networks. Additionally, HIV-1-like-particle-pulsed DC1 were co-cultured with $CD4^+$ T cells in the setting of reticulation, and live-cell super-resolution imaging revealed strong supporting evidence for TNT-mediated HIV-1 transmission. Finally, high ICAM-1 surface expression was previously linked to enhanced DC1 trans-infection, and we visualized ICAM-1 puncti localization to TNTs. These data demonstrate a role for reticulation in DC1-driven HIV-1 trans-infection in addition to its immunologic function, which impacts public health by providing a rationale for exploration of therapeutic strategies to target this process and interrupt HIV-1 transmission.

TABLE OF CONTENTS

LIST OF FIGURES

PREFACE

I would like to thank past and current members of Dr. Charles Rinaldo's laboratory, including Blair Erdeljac, Diana Campbell, Angela Anthony, and Dr. Ronald Fecek for both technical assistance and daily support. I also thank Deena Ratner, Lori Caruso, and Sharie Ganchua for technical assistance. I am especially grateful to Dr. Simon Watkins, Greg Gibson, Dr. Donna Stolz, and other staff of University of Pittsburgh's Center for Biological Imaging, who provided expertise and support during the many long hours I spent collecting imaging data. I also thank the entire faculty, students, and staff of the Department of Infectious Diseases and Microbiology for an incredible life-altering experience over the past 4.5 years. I would also like to express gratitude to my dissertation committee members, whose intellectual contributions helped to guide not only my project, but also my development as a scientific researcher. Finally, my mentors, Drs. Charles Rinaldo and Robbie Mailliard were both instrumental in my development as a PhD. They offered unwavering encouragement, guidance, and expertise over the years, and I therefore express my most whole-hearted appreciation to them both.

1.0 INTRODUCTION

1.1 DENDRITIC CELL POLARIZATION OF ADAPTIVE IMMUNE RESPONSES

Dendritic cells (DC) play a central role in the initiation and regulation of immune responses. These antigen (Ag)-presenting cells (APCs) bridge the innate and adaptive branches of immunity by gathering pathogen- and tissue-derived environmental cues in the periphery and translating this information into the development of appropriate adaptive responses following their migration to draining lymph nodes [1]. Signals may be derived from pathogen-associated molecular patterns (PAMPs) and endogenous inflammatory mediators, as well as complementary activating signals provided by $CD4^+$ and $CD8^+$ T cells [2, 3]. The combination of exogenous and endogenous activation signals received in the affected tissue during their immature stage results in their differentiation into mature, pre-programmed DC capable of inducing differentially polarized, Ag-specific immune responses. The overarching research goal of this dissertation is to investigate the role of $CD4^+$ T helper (Th) cell-associated CD40 ligand (CD40L) in inducing a novel immunologic process that we have termed 'reticulation', which results in the formation of dynamic networks of filamentous (F)-actin based-tunneling nanotubes (TNTs), in DC programmed by mediators of type-1 immunity. Herein, type-1 immunity is synonymous with T cell-driven responses, in contrast to type-2 immunity, which refers to humoral responses predominantly driven by antibodies (Ab), though it is acknowledged that this is not a strict

demarcation. Furthermore, I will investigate possible functions of inducible TNT networks in the context of DC-mediated orchestration of adaptive immune responses and the role of these conduits in enhanced ability of DC1 to transmit human immunodeficiency virus type-1 (HIV-1) in trans to $CD4^+$ T cells. This research could lead to advancements in our understanding of the function of these TNT networks in DC biology, HIV-1 pathogenesis, and DC-based immunotherapies.

1.1.1 CD40L-mediated T cell help for DC

The ability of DC to drive the appropriate type of adaptive immune response to a pathogen assault is greatly influenced by their interaction with $CD4^+$ Th cells and their responsiveness to Th cell-associated CD40L, a critical factor in 'licensing' or enabling DC to promote cellular immunity [4-6]. CD40L is a cell surface protein of the tumor necrosis factor (TNF) superfamily, which is produced de novo by naïve $CD4^+$ T cells. Additionally, both effector and memory $CD4^+$ T cells store pre-formed CD40L in lysosomal compartments for rapid delivery to the cell surface upon secondary Ag stimulation [7]. The presence of pre-formed CD40L in polarized Th cells raises the possibility that these cells could deliver 'help' for inducing reticulation during short encounters with DC in the periphery, in addition to doing so in their naïve stage during the relatively long lasting interactions required for initiating primary immune responses in lymph nodes. Type-1 polarized DC (DC1) [2], or DC matured under pro-inflammatory conditions by innate immune mediators associated with acute viral infections such as viral RNA [3], type-1 interferons (IFNs) [8], and activated natural killer (NK) cells [9], respond to CD40L by producing enhanced levels of IL-12p70, a key driving factor of Th1-biased cellular immunity [10]. Importantly, the cytokine IFN-γ, which can be secreted by activated effector T cells and

NK cells, represents a central DC1 polarizing factor [11]. Conversely, 'standard' or type-2 polarized DC (DC2) [2], such as those matured in the presence of histamines or prostaglandin E_2 (PGE_2), drive Th2-biased responses, display a diminished capacity to produce IL-12p70 upon CD40 ligation, and are less effective at driving cell-mediated immunity [3, 12]. PGE_2 is a critical homeostatic factor that facilitates acute local inflammation, but conversely has a specialized immunomodulatory role in suppressing Th1-, cytotoxic T lymphocyte (CTL)-, and NK-cell-mediated type-1 immunity, while promoting Th2, Th17, and regulatory T cell responses [13]. While all cell types are capable of secreting PGE_2, this factor is prevalent in the tumor microenvironment and the setting of chronic inflammation. Additionally, uncommitted DC matured in the absence of type-1 or type-2 polarizing factors (DC0) possess migratory capacity and produce intermediate levels of IL-12p70 in response to CD40L [12], but they can be instructed by concurrent helper signals from Ag-stimulated $CD4^+$ and $CD8^+$ T cells to produce high levels of the Th1-promoting cytokine, similar to DC1 [14]. The pre-programming of DC by mediators of type-1 or type-2 immunity dramatically impacts their subsequent responsiveness to CD40L-mediated $CD4^+$ T cell help for the induction of polarized immune responses (Figure 1). **I propose that the selective induction of reticulation in DC1 represents a novel helper function of CD40L, which provides a pathway for Ag or HIV-1 exchange between interconnected DC, and HIV-1 transfer to $CD4^+$ T cells during Ag presentation.**

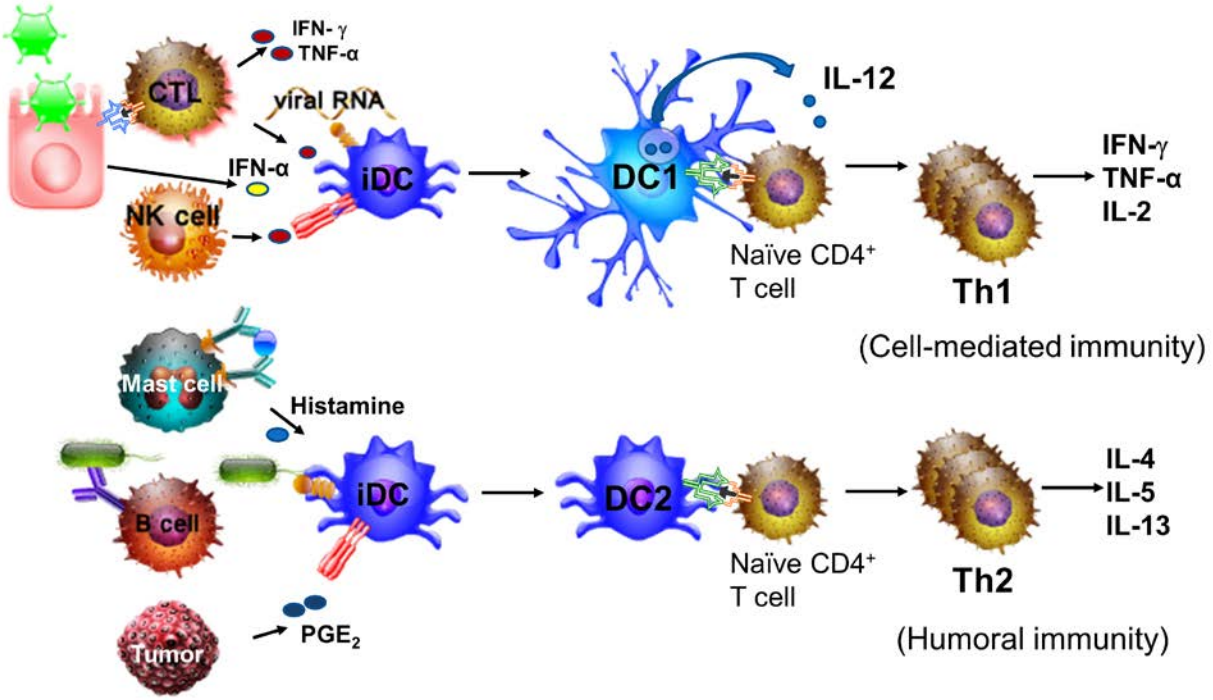

Immature DC can be instructed in the peripheral tissues by signals from intracellular pathogens such as viral dsRNA in combination with NK cell or CTL secreted pro-inflammatory cytokines. The resulting DC1 are capable of initiating Th1 responses, or cell-mediated immunity, which is typified by Th1 cell secretion of IFN-γ and TNF-α. On the other hand, DC2 are programmed by signals from extracellular pathogens in combination histamine from mast cells or PGE_2, which can be produced by all cell types but is prevalent in the setting of cancer and chronic inflammation. The resulting DC2 drive Th2 or humoral immunity, which is characterized by Th2 cell secretion of IL-4, IL-5, and IL-13. Adapted from [3].

Figure 1. DC programming determines their ability to drive polarized adaptive immune responses.

1.1.2 Antigen presentation and transfer by DC

Immature DC (iDC) capture exogenous Ag in the periphery by a number of mechanisms, including phagocytosis, micropinocytosis, and receptor-mediated endocytosis [15]. They next undergo a specific maturation program resulting in expression of lymph node-homing chemokine receptors, co-stimulatory molecules, and cytokines for the initiation of polarized adaptive immune responses [16]. In the regional lymph nodes, mature DC encounter cognate $CD4^+$ T lymphocytes and present processed Ag bound to cell surface MHC class II molecules, which are recognized by specific T cell receptor (TCR) molecules [16]. DC also possess the unique ability to 'cross-present' exogenous Ags from virus-infected or tumor cells in the context of MHC class I for presentation to cognate $CD8^+$ T cells and subsequent initiation of CTL responses [17]. While migratory DC may be essential for initial transportation of Ag to draining lymph nodes, the effective initiation of CTL responses likely requires communication with a subset of lymph node resident DC that possess an enhanced ability to cross-present Ag to $CD8^+$ T cells [18, 19]. DC migration and transportation of Ag to draining lymph nodes is a critical component to this process, but the effective initiation of CTL responses likely involves communication with a subset of lymph node resident DC that possess an enhanced ability to cross-present Ag to $CD8^+$ T cells [18-21]. Transfer of antigenic information between migratory and lymph node-residing DC has been shown to be essential in models of immunity to viruses [21, 22], but the exact mechanisms involved in this antigen exchange are unclear. Ag acquisition by DC through intercellular transfer has been demonstrated through a number of mechanisms including uptake of apoptotic cell debris [23], and DC-derived exosomes [24], as well as direct membrane exchange between DC [25].

One proposed mode of direct intercellular Ag exchange occurs through the facilitation of TNTs, or ultrafine F-actin-comprised membrane protrusions that form direct cytoplasmic connections between proximal and remote cells [26, 27]. In situ imaging studies have revealed that maturing migratory DC undergo dramatic morphological alterations upon entry into lymph nodes, including the formation of extended membrane processes, as they are integrated into a network of lymphoid-residing DC [26], thus supporting the concept of direct Ag transfer. The morphology of standard mature DC generated in vitro is typified by membrane ruffles and short hair-like protrusions, but the extended membrane processes described in vivo are rarely observed [27]. Here I investigate the ability of the Th cell signal, CD40L, to induce uniquely in mature pro-inflammatory DC1 the formation of extensive networks of TNT-like membrane protrusions, in the context of immunity and HIV-1 transmission to $CD4^+$ T cells.

1.2 TUNNELING NANOTUBE-MEDIATED INTERCELLULAR COMMUNICATION IN THE IMMUNE SYSTEM

1.2.1 Diverse modes of intercellular communication in mammalian cells

Multicellular organisms require mechanisms of indirect and direct intercellular communication to orchestrate coordinated cellular processes such as innate and adaptive immune responses. Cross-talk between adjacent and remote cells can occur via secreted proteins such as cytokines, IFNs, and chemokines that are recognized by specific target cell surface receptors for the initiation of signal transduction pathways involved in immune cell growth, differentiation, activation, and migration [28]. Additionally, extracellular membrane vesicles, i.e. exosomes,

derived from the originating cell's plasma membrane or multivesicular bodies, can transfer diverse proteins, lipids, and nucleic acids to target cells for the modulation of immune responses [29]. While secreted proteins and exosomes are able to facilitate both long- and short-range communication, they rely on random diffusion to reach their targets, and additional mechanisms of have evolved to specifically facilitate cross-talk between cells in close contact. For example, narrow channels linking the cytosol of adjacent cells, termed gap junctions, exchange small molecules including ions, metabolites, second messengers, and peptides for the transmission of electrical, metabolic, and immunologic signals [30]. Furthermore, bull's eye shaped supramolecular activation clusters (SMAC) comprised of associated TCR and MHC molecules as well as adhesion molecules can form at the junction between T cell and APC membranes, and these immunologic synapses are required for initiation of adaptive immune responses. Furthermore, trogocytosis, or exchange of plasma membrane fragments from APC to T cells during cell conjugation facilitated by the immunologic synapse, is another form of intercellular communication, which likely contributes to 'fratricide' of CTLs that have acquired MHC class I molecules from target cells [31]. A novel form of direct intercellular communication, termed TNTs or membrane nanotubes, supports both membrane and cytoplasm continuity between adjacent or distance cells and combines various aspects of the fore-mentioned modes of cross-talk [32].

1.2.2 Distinguishing TNTs from other plasma membrane extensions

Mammalian cells have developed a number of distinct plasma membrane protrusions to facilitate processes such as probing of the extracellular environment, cell adhesion, and migration. DC are named for their dendrites, defined as long, adherent, arborizing processes that can facilitate Ag

uptake, processing and presentation, but they can also display diverse membrane structures such as veils, ruffles, stress fibers, and filopodia [16, 27, 33, 34]. DC-derived veils, also termed lamellipodia, are characterized as sheet-like protrusions constructed from a branching network of actin, while stress fibers are contractile structures composed of myosin and actin bundles [34]. On the other hand, filopodia are defined as thin, finger-like protrusions comprised of tight parallel bundles of F-actin, which specialize in probing the environment. Filopodia can serve as precursors of TNTs, but these structures are typically < 10 micrometers (μm) in length, while TNTs can span distances over 100 μm. TNTs are also distinct from all the fore-mentioned types of membrane extensions as they can form direct open-ended cytoplasmic connections and are typically located above the substrate [35].

Many non-immune and immune cell types, including APCs, have been shown to form TNTs in vitro, and these structures support the intercellular transfer of vesicles, organelles, cytoplasmic and cell surface proteins, calcium ion fluxes, electrical signals, as well as some pathogens [35-37]. Although in vitro and in vivo evidence has recently emerged to support a role for TNTs in immune cell communication, transmission of certain pathogens, and chronic diseases such as cancer, very little is known about the function of TNTs in the context of an immune response. Here I review the discovery of TNTs, the processes involved and molecular basis of TNT formation, the diversity of structure and function of these structures in myeloid- and lymphoid-origin immune cells, as well as recent evidence supporting the existence of TNTs in vivo. Finally, the contribution of TNTs to various disease states, with an emphasis on cell-cell HIV-1 transmission, will be appraised.

1.2.3 Discovery of TNTs in vitro

Recent advances in 3 dimensional (3D) live-cell imaging technologies facilitated the discovery of TNTs, which were initially described by Gerdes and colleagues in 2004 as non-adherent ultra-fine tubular structures forming direct intercellular connections between rat pheochromocytoma (PC12) cells [38]. These structures were visualized in PC12 cells, a commonly used neuronal cell model, exposed to fluorescently tagged wheat germ agglutinin, in addition to human embryonic kidney (HEK) and normal rat kidney (NKR) cells. TNTs were typically non-branching, 50-200 nanometers (nm) in diameter and up to a few cell diameters in length, and could connect cells over long distances, resulting in the formation of complex intercellular networks. Importantly, TNTs were readily disrupted by either prolonged exposure to light, chemical fixation, or mechanical stress, explaining in part why they had been previously undiscovered. Time-lapse imaging revealed vesicles traveling at a speed of 25.9 ± 7.9 nm per second (nm/s), and unidirectional cell-to-cell transfer of lysotracker labeled organelles and plasma membrane-associated fusion proteins labeled with farnesylated EGFP via TNTs. Early endosome markers and myosin motor proteins localized to these structures and treatment with the actin-depolymerization drug latrunculin B completely abrogated TNT-mediated organelle exchange, together suggesting an actin-dependent mechanism of transport. Finally, the authors also proposed a ‘filopodia extension model’ of TNT formation, wherein an F-actin-driven protrusion from a donor cell is extended toward a target cell, resulting in fusion with the target cell membrane.

Also in 2004, Davis and colleagues first described TNTs in cultured myeloid- and lymphoid-origin immune cells using resonance scanning confocal microscopy [43]. Specifically, they observed TNTs forming between human peripheral blood-isolated macrophages or murine

macrophage J774 cells, as well as TNTs between human NK and target cells, an EBV-transformed 721.221 human B cell line. Bulges suggestive of intercellular vesicle trafficking were observed along TNTs in J774 cells, and these conduits supported the exchange of DiO labeled vesicles between cells. Furthermore, transfected 721.221 cells readily transferred GPI-GFP, an outer leaflet membrane marker, to interconnected DiD labeled 721.221 cells, demonstrating a novel mechanism of membrane exchange. Importantly, the authors also revealed an alternate mode of TNT formation to the filopodia extension model, when they reported that TNTs were drawn out from NK and target cells that were in close contact, as they subsequently diverged. Since these seminal discoveries, TNTs have been observed in a wide variety cell types, including neuronal, immune, stromal, and cancer cells, and they display great diversity in both structure and function [35, 37, 39, 40].

1.2.4 Mechanisms of TNT formation

TNTs were initially described as F-actin-based ultrafine extensions of the plasma membrane that facilitate the direct transfer of cytoplasmic vesicles, organelles, proteins, and calcium fluxes, as well as cell surface molecules, but the molecular mechanisms of TNT formation were largely unknown. In late 2009, Ohno and colleagues revealed that functional de novo TNT formation in a murine macrophage cell line required interaction of the cytoplasmic protein M-Sec, also known as TNFaip2, with the active Ras-like GTPase RalA, and the exocyst complex [41]. RalA induces filopodia extensions by several mechanisms, including direct binding of filamin for actin filament cross-linking and indirect binding of Cdc42, a member of the Rho small GTPase family also implicated in TNT elongation [41]. Most important for TNT formation and TNT-mediated calcium flux was the upstream effect of M-sec on the RalA-exocyst effector complex. This

complex consists of 8 protein subunits conserved in yeast and mammalian cells, which participates in actin cytoskeleton remodeling and vesicle trafficking by tethering vesicles at the plasma membrane and regulating polarized exocytosis [42, 43]. Intriguingly, M-Sec mRNA was highly expressed in myeloid lineage cells and treatment of a macrophage cell line with lipopolysaccharide (LPS) or IFN-γ strongly induced M-Sec expression, hinting that TNT induction may be linked to myeloid cell inflammation [41]. In 2012, Weiss and colleagues demonstrated that assembly of the multi-protein complex required for TNT formation is facilitated by the transmembrane MHC class III protein Leukocyte Specific Transcript 1 (LST1), which is also highly expressed on myeloid lineage cells such as DC and macrophages [44]. In their model of TNT formation, LST1 serves as a scaffold, first recruiting RalA and filamin to the plasma membrane for actin cross-linking and then facilitating the interaction of M-Sec, RalA, and the exocyst complex (Figure 2). Furthermore, myosin and myoferilin also interact with LST1, and these molecules likely participate in deformation of the plasma membrane and promotion of membrane fusion to form open-ended TNTs. However, M-Sec-mediated TNT formation may be limited to myeloid origin cells as other cell types such as neurons fail to express this molecule; and Gousset et al. [45] recently demonstrated a role for myosin-X-driven dorsal filopodia in TNT development and subsequent vesicle transfer in a mouse neuronal cell line. Actin dynamics and the participation of accessory molecules such as myosin-X in TNT development in myeloid origin cells remain to be explored. Together, these data highlight the possibility that different molecular mechanisms of TNT formation predominate in distinct cell types, which may also vary in their structure and function.

In addition to the described multi-molecular TNT assembly complex, both adhesion molecules and cholesterol-sphingomyelin membrane nanodomains may be required for TNT

formation (Figure 2). Lokar et al. [46] showed in a human urothelial cancer cell line (T24) that the junction proteins N-cadherin and β-cetenin localized to TNTs, and likely anchor the tip of the donor cell extension to the plasma membrane of the recipient cell. In this study, filopodia were defined as < 10 μm in length and originating from the convex edge of the cell, while TNTs were ≥ 10 μm in length and typically originated from the upper rim of the cell. Intriguingly, extension of TNT-like protrusions required the presence of another cell within 100 μM, while filopodia formation occurred independently of proximity of other cells, indicating that the donor cell may have some mechanism for sensing target cells prior to initiating TNT formation. In a related study, T24 cells were treated with ostreolysin, a marker that preferentially binds to cholesterol-sphingomyelin membrane nanodomains, followed by immunostaining and confocal microscopy, which revealed localization of these structures to the length of TNTs [47]. Additionally, depletion of membrane cholesterol using methyl-β-cyclodextrin resulted the retraction of TNTs in this cell type, indicating that cholesterol-rich lipid rafts are necessary for maintenance of TNT stability.

In some cell types, stress, a receptor-ligand interaction, and/or cytokine-induced activation can initiate TNT formation. Zhang and colleagues showed that astrocytes and neurons develop TNTs in response to H_2O_2- or serum depletion-induced stress in a P53 dependent manner [48]. Stressed cells consistently formed TNTs with unstressed cells in co-cultures, and these structures supported the unidirectional transfer of mitochondria, endoplasmic reticulum, golgi, and endosomes to unstressed cells. Co-stimulation with chemokine receptor 1 and FcεR1 along with Ag and macrophage inflammatory protein 1α induced TNTs in mast cells [49]. Inducible TNTs grew out from regions of calcium accumulation in the cytoplasm and were also inhibited by membrane cholesterol depletion. Furthermore, cytokine-induced activation and

engagement of cognate receptor-ligand pairs enhanced TNTs formed between NK and target cells [50]. Together, these data provide us with a partial understanding of the molecular mechanisms of TNT formation, and highlight the possibility that functionally distinct classes of TNTs may exist in different cell types.

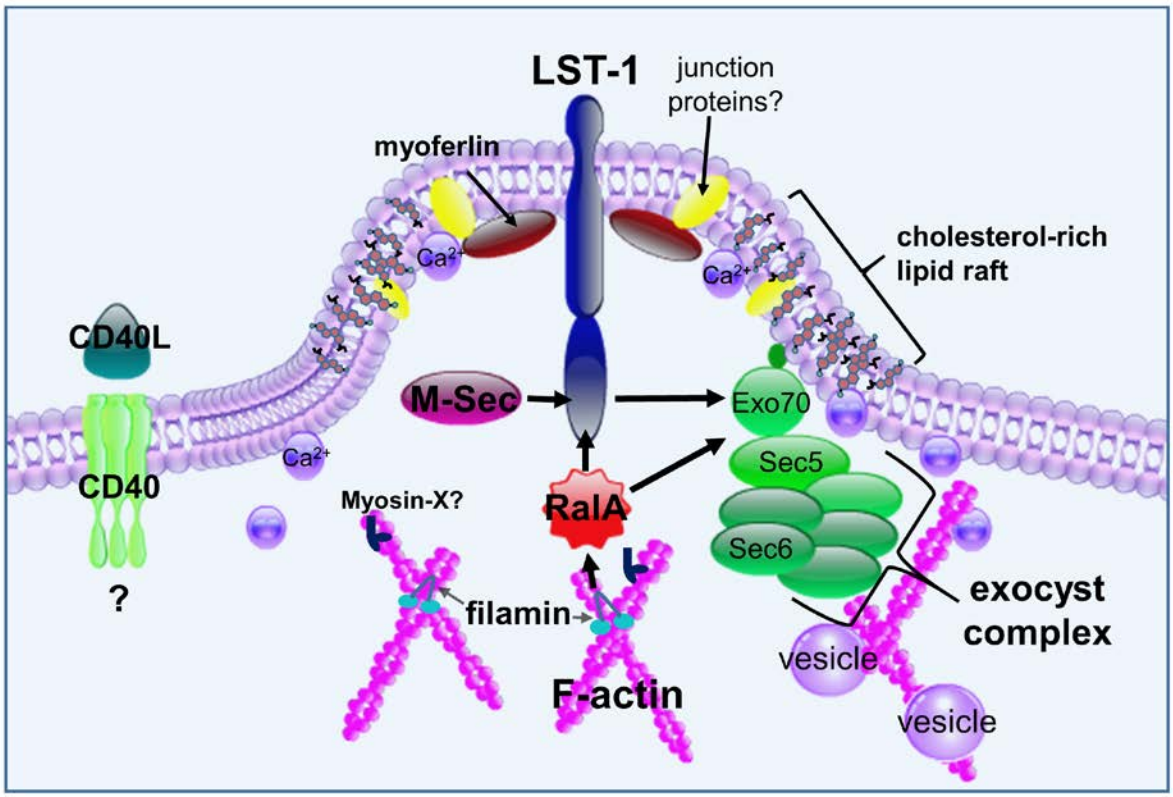

In this recently proposed model of TNT formation, LST1 serves as a membrane scaffold for a multi-protein complex induced by LST1 recruitment of RalA and associated effector, filamin, which leads to actin cross-linking. LST1 next promotes interaction between M-Sec, RalA, and the exocyst complex at the plasma membrane, facilitating the orchestration of actin polymerization and membrane complementation. Considering that the exocyst complex participates in cytoskeletal rearrangements and also targets vesicles to the plasma membrane, this complex may also directly participate in TNT-medicated vesicular trafficking. Additionally, myosin and myoferlin interact with LST-1 at the plasma membrane, and likely induce local membrane deformation, enabling membrane fusion and open-ended TNT formation. Additional studies support a role for myosin-X in F-actin-driven TNT formation, the junction proteins N-cadherin and β-cetenin in anchoring the tip of the donor cell extension to the plasma membrane of the recipient cell, and cholesterol-sphingomyelin membrane nanodomains in TNT stabilization [45-47]. Importantly, distinct cell types may rely on different mechanisms of TNT formation and functionally divergent TNTs may be induced in the same cell type under varying conditions. Actin dynamics during TNT formation are currently poorly understood. This model was adapted from [44].

Figure 2. Current model of the molecular mechanisms of TNT formation.

1.2.5 Heterogeneity of TNT structure and function in immune cells

Diversity of TNT structure and function in the multitude of cell types capable of forming these conduits has been extensively reviewed elsewhere [37, 51-53], and consequently herein I focus on studies that could shed light on the role of TNT networks in the immune system. These structures have been observed to form in vitro between a wide variety of immune cell types, including myeloid lineage monocytes, macrophages, and dendritic cells, lymphoid lineage T cells, as well as between NK cells or CTLs and target cells [35, 54]. However, TNT structure and function differs greatly even between related cell types, and their modes of induction and in vivo function are currently not well understood. The apparent abundance of TNTs in immune cells in vitro and reports of high expression levels of M-Sec mRNA in lymphoid tissues and both M-Sec and LST1 mRNAs in immune cells provide us with a rationale for further investigation of these conduits in an immunologic context [41, 44]. Importantly, early in vitro and in vivo evidence suggests a role for mediators of acute inflammation in the induction of TNTs in myeloid origin cells. The field of TNT-based intercellular communication is young, and an improved understand of how these conduits function in the context of an immune response as well as in DC-mediated HIV-1 transmission are the principle goals of this dissertation.

1.2.5.1 Myeloid lineage cells

Critical insight into inducible TNT function in myeloid cells was provided by Watkins and Salter in 2005. Using differential interference contrast (DIC) and confocal imaging, they showed that these conduits mediate the transmission of calcium ion fluxes, a critical early step in cell activation, between fura-2-labeled human monocyte-derived iDC and THP-1 monocytes in response to mechanical stimulation or *Escherichia coli* supernatants [55]. Previously, they

demonstrated that iDC responded to a soluble bacteria-derived factor by forming extensive membrane veils, which served to capture and transport bacteria to the cell body for subsequent internalization [33]. The current study additionally revealed how novel TNT-like extensions participate in transmitting pathogen-inducible activation signals. Gap junction and extracellular ATP inhibitors failed to affect TNT-mediated flux transmission, while physical disruption of the connections completely abolished calcium fluxes. TNTs were more frequent between cells in close proximity, and they typically extended from the lower region of the cell body and were occasionally detected above the substrate. Furthermore, the fluid phase marker lucifer yellow readily transferred to multiple connected cells via TNTs while a marker of particulates spread only to adjacent cells that formed multiple direct connections, suggesting that small soluble molecules may transfer more readily than larger particulates. In a study of cultured neuroblastoma and HEK cell lines, TNT-mediated calcium ion fluxes were not dependent on passive diffusion, but they could be actively propagated by inositol triphosphate (IP_3), and immunostaining revealed localization of IP_3 receptors along the length of TNTs [56]. Further study is required to determine the role of IP_3 in facilitating calcium fluxes in myeloid cells, but utility of TNT-mediated calcium fluxes for instigating a coordinated multicellular response to pathogen-related signals in iDC is evident.

In 2006, Davis and colleagues demonstrated the existence of functionally distinct types of TNTs in human monocyte-derived macrophages [57]. Thin TNTs were described as those with a diameter < 0.7 μm that contained only F-actin and participated in capture and surfing of bacteria along the length of the structures for internalization by phagocytosis at the cell body. Macrophages were surface biotinylated and time-lapse confocal imaging of streptavidin-coated beads on thin TNT surfaces revealed unidirectional constitutive flow at a rate of 0.13 ± 0.02

μm/s. On the other hand, thick TNTs (≥ 0.7 μm) were comprised of both F-actin and microtubules and supported the bidirectional trafficking of vesicles such as DiD-labeled vesicles and lysotracker labeled-lysosomes, at an average rate of 1 μm/s. Importantly, the trafficking of LAMP-1^+ endosomes or lysosomes and larger organelles such as mitochondria were all observed trafficking between cells via thick TNTs only, but they failed to support bacteria surfing on the surface. Whereas the previously described ultrafine TNTs were relatively transient, thick TNTs could persist for a few hours. Both thin and thick TNTs were typically non-branching, and the 2:1 ratio of thin to thick TNTs was relatively unchanged by culture on glass, fibronectin, or collagen. The existence of these two functionally distinct classes of TNTs in DC, a related myeloid origin cell type that also functions in Ag presentation, remains to be explored.

A 2012 study by Weiss and colleagues demonstrated another potential function of TNTs in both myeloid origin cells and HeLa cells, which is the intercellular transfer of vesicles containing MHC class I molecules, and to a lesser extent, surface-bound MHC class I molecules [58]. Monocytes were treated with TPA to induce macrophage differentiation and iDC were exposed to TNF-α and IFN-γ containing cocktails to generate mature DC. Inflammatory stimuli increased LST-1 protein expression in both mature DC and HeLa cells, confirming a role for these mediators in TNT induction. Transfected HeLa cells readily transferred the trans-membrane fusion protein HLA-A2-EGFP to differentially labeled target HeLa cells, and this phenomenon was effectively blocked by treatment with latrunculin A and enhanced by overexpression of LST-1. EGFP was not detected in isolated exosome fractions and transfer of a soluble variant of HLA-G, HLA-Gas-EGFP was less efficient, indicating the exchange involved endocytic vesicles. This study provides only indirect evidence for MHC exchange in myeloid

origin APCs, but it nevertheless highlights a possible function of TNT networks, which is the facilitation of 'crossdressing' or the exchange of MHC-Ag complexes between remote APCs.

The function of TNTs in iDC patrolling the tissues likely involves the sensing of pathogen- and/or host-derived danger signals for the transfer of Ag-related information or the induction of early cell activation, allowing a rapid, multicellular response by APCs to trauma or infection. In support of this supposition, Chinnery, Pearlman, and McMenamin provided in 2008 the first in vivo evidence of a network of TNTs connecting remote DC in inflamed mouse corneas [59]. Up until this point, a paucity of evidence for the existence and function of TNTs in vivo led some members of the scientific community to question whether these conduits were merely an in vitro artifact as opposed to a versatile, ubiquitous, and previously unknown mode of intercellular communication. While shorter TNTs were expressed by GFP^+ MHC class II^+ putative DC in the periphery of inflamed and to a lesser extent in naïve corneas, MHC class II^+ DC of the central region of inflamed corneas uniquely formed extremely long and highly curved or winding TNTs, on average 151 ± 16 μm, with a maximum length of 333 μm. The average diameter of TNTs found in corneas was 0.64 ± 0.04 μm and localized beading or bulging along the length and base of TNTs, which is a marker of TNT-mediated vesicle trafficking in vitro [57], was also observed. TNTs were not detected in macrophages stained with CD11b-, CD68- or CD69-specific mAbs. Both LPS and injury significantly increased TNT expression in MHC class II^+ DC in the central compared to naïve cornea, highlighting a potential link between inflammation and TNT formation for the first time in vivo [51]. Furthermore, the predominance of extremely long and highly curved TNTs in the central region of the cornea, where DC are very sparse, indicates that TNTs may pass messages in the setting of inflammation to induce a rapid and coordinated response by resident DC. Importantly, this group also observed TNT-like

structures that appeared unconnected to a second cell, which perhaps represented disrupted TNTs or those in the process of seeking target cells. On the other hand, those apparently unconnected TNTs could have been interacting with an unlabeled and therefore undetectable cell type in their system, such as nerve or stromal cells.

Importantly, Blanco and Saban utilized intravital multiphoton imaging of CX3CR1-Cre Ross-tdTomato or -GFP chimeric mice to report that bone marrow (BM)-derived mononuclear phagocytes form a vast and complex network of TNTs across the normal cornea, which supported the bidirectional exchange of the tdTomato reporter protein between interconnected cells [60]. Furthermore, they introduced donor CX3CR1-Cre Rosa-tdTomato cells to transgenic Thy-1 eYFP hosts to visualize tdTomato$^+$ BM-derived cells in TNT-mediated physical contact with Thy-1$^+$ nerve cells at the axon terminals, which originated in the trigeminal ganglion of the brain. Importantly, these BM-derived and nerve cell networks were detected in other mouse tissues, including the skin, intestine, and peritoneum, indicating that they could be ubiquitous in certain mammalian compartments in the steady state. The cornea, skin, and intestine are all thin and permeable barriers to the exterior of the body that have sensory or food absorption functions, but they are also associated with specialized and compartmentalized mucosa-associated lymphoid tissue (MALT) [61-63]. These sites represent common portals of entry for pathogens, perhaps necessitating a rapid response via close communication between sparse local DC and the nervous system. Together, these data provide convincing new evidence of a system of DC-derived TNTs in tissues in vivo that interfaces directly with nerve networks in the MALT, but their exact immunologic function remains to be explored.

While TNT participation in the transmission of signaling fluxes has been well described in iDC [28], little information exists concerning the nature of their induction in mature migratory

DC, or their role in initiating and maintaining polarized adaptive immune responses via cross-talk with lymphoid origin cells in lymph nodes. Preliminary evidence suggests a role for the key $CD4^+$ Th cell signal, CD40L, in the induction of TNTs in DC matured in the presence of mediators of type-1 immunity. **Herein, I investigate the ability of CD40L and polarized Th cell cytokines to induce and regulate the formation of TNT networks, or reticulation, in mature differentially programmed DC. Furthermore, I reveal a novel function of these conduits, the direct exchange of Ag between interconnected DC for the induction of T cell responses, which may be critical for efficient DC1-mediated instigation of type-1 adaptive immune responses.**

1.2.5.2 Lymphoid lineage cells

Davis and colleagues initial description of TNTs in immune cells included early evidence for an immunologic function of TNTs. HLA-Cw6 localized to long TNTs formed between human peripheral blood NK cells and HLA-Cw6-GFP transfected 721.221 target cells as they moved apart, indicating that immunologic synapses can be maintained by these structures over relatively long distances [64]. In 2009, they extended these observations to show that NK cell-derived TNTs formed connections with other NK cells, as well as mouse mastocytoma cells, and human monocyte-derive THP-1 cells [50]. The development of TNTs upon divergence of NK and target cells was time-dependent, and cell contact time of at least 10 minutes (min) was required. Importantly, these structures contained a junction which inhibited the free diffusion of both cytoplasmic and membrane-associated proteins. The majority of TNTs contained α-tubulin in addition to F-actin, indicating the presence of microtubules, similar to thick TNTs described in macrophages [57]. The frequency of TNT formation was amplified by treatment of NK cells with the activating cytokines IL-2, IL-12, IL-15, or IL-18, and depended on engagement of

cognate receptor-ligand pairs, including NKG2D-MICA and lymphocyte function-associated Ag 1 (LFA-1)- intercellular adhesion molecule 1 (ICAM-1). Proximal NK cell signaling proteins were recruited to the TNT junctions, which implies the existence of immunologic synapses at these sites. Polarized target cells were observed moving along TNTs toward NK cells, with their uropods oriented in the direction of the cell motion, contrasting with the orientation typically observed during cell migration, and the targets were lysed upon close contact with the connected NK cell. Strikingly, the majority of target cells remotely connected to NK cells via long-range TNTs were also lysed from a distance.

The previously discussed findings provide compelling evidence of a role for TNTs in facilitating long-distance killing of target cells by NK cells, and these conduits may also facilitate interactions between CTLs and target cells. Indeed, a study of the immunologic synapse formed between CTLs and target cells unexpectedly revealed the unidirectional transfer of target cell membrane proteins to CTLs from the point of close contact, as well as long processes extending from the target to the CTL, presumably upon separation of the cell conjugates after direct membrane fusion at the region of close contact [65]. The authors speculated that acquisition of target cell proteins, i.e. MHC class I molecules, could make these CTLs susceptible to 'fratricide', or killing by other CTLs of the same specificity.

A 2010 study conducted by Esposti and colleagues was the first to show that the Fas/CD95 surface receptor, which mediates rapid apoptosis in diverse cell types, induces TNT development between T cells [66]. Fas activation with FasL or an antagonist Ab prompted TNT formation in both the human Jurkat J6.1 T cell line and primary $CD4^+$ T cells isolated from human peripheral blood, which occurred prior to caspase activation and peaked within 20-30 min. Treatment with TRAIL, a similar ligand of widespread death receptors, also induced TNT

formation and death receptor ligation-mediated TNT formation was blocked by an inhibitor of Rho GTPases, which regulates actin, and secramine A, a specific inhibitor of Cdc42. These inducible conduits supported the bidirectional exchange of membrane components such as endogenous FasL as well as exosome-like vesicles, cytosolic YFP, and active caspases, indicating they were open-ended conduits. TNTs were abrogated by actin inhibitors, and they failed to support the exchange of mitochondria, perhaps indicating that these inducible conduits did not contain microtubule tracks that facilitate transportation of large cytoplasmic structures. Importantly, TNT formation was severely impaired in activated T cells from autoimmune lymphoproliferative syndrome (ALPS) patients, an uncommon genetic disease in which defects in Fas signaling manifest as an autoimmune disorder, highlighting a possible link between this disease and the loss of Fas-stimulated TNT networks in vivo. This study provides further evidence of T cell 'fratricide' facilitated by TNT connections, in this case induced by death receptors.

Davis and colleagues reported a small percentage of cultured Jurkat T cells and peripheral blood-isolated PMA- and ionomycin-activated primary human and mouse T cells were connected by TNTs [67]. These structures had an average length of 22 ± 3 μm, but were up to 100 μm in length, and typically formed single connections between cells. These structures contained F-actin, but not microtubules, unlike those described in macrophages and NK cells [50, 57]. This study provided further evidence that TNT formation by the cell divergence mechanism is dependent on the duration of close contact between cells, as only contacts sustained for more than 4 min typically led to TNT development as cells moved apart. Furthermore, utilization of a 3D mimic of the extracellular matrix led to formation of even longer TNTs on average 38.4 ± 7.6 μm, which often curved in order to bypass obstructions to connected

cells. Importantly, unlike the open-ended Fas-inducible TNTs, the observed structures displayed a distinct junction, which could move bidirectionally along the length of these structures. Although large transmembrane molecules such as GFP-labeled ICAM-1 and HLA-Cw or small cytoplasmic could localize to TNTs, they failed to traffic seamlessly to interconnected cells. Furthermore, the conduits failed to flux calcium, but readily transferred HIV-1 in a receptor-dependent manner, indicating that these structures are not only morphologically, but also functionally distinct from open-ended TNTs described elsewhere.

While studies of T cell-APC interactions via TNTs are currently lacking, one study conducted by Kloog and colleagues in 2013 revealed that TNTs formed between Ag-presenting B cells and Jurkat cells in vitro facilitated the transfer of fluorescently labeled H-Ras, a small GTPase that localizes to the inner membrane leaflet [68]. Spinning-disk confocal imaging revealed that GFP-H-RasG12V transfected 721.221 B cells in contact with Jurkat cells > 5 min formed TNTs upon separation of conjugated cells. The resulting TNTs were made up of membrane from either B cells or Jurkat cells, or they were comprised of membranes from both cell types. FRAP-based imaging techniques indicated that H-Ras-containing membrane patches moved freely by lateral membrane diffusion along donor B cell TNTs, but recipient Jurkat T cell TNTs contained a junction that prevented diffusion of membrane patches. Nevertheless, breakage of TNTs often resulted in B cell-originating membrane patches retained on the surface of the Jurkat cells. These data indicate that plasma membrane-anchored proteins originating from APCs can traverse the length of TNTs, and despite the presence of a junction, can be left behind upon TNT disruption and incorporated into the T cell membrane. This study provides the first evidence of a mechanism of membrane protein exchange between B and T cells, however

the ability of myeloid-derived APCs such as DC and macrophages to form TNTs with T cells and transmit membrane or cytoplasmic components remains to be elucidated.

1.2.6 TNTs: A multifarious mode of intercellular communication

We have outlined the multitude of recently described TNT functions in immune cells, including the direct exchange of calcium ions, vesicles, organelles, and surface proteins (Figure 3). Importantly, TNT networks may represent the most mechanistically diverse form of intercellular communication yet discovered, as evidence suggests these conduits can work cooperatively with numerous other modes of cell-cell communication, including receptor-ligand signaling, immunologic synapses, gap junctions, and vesicular trafficking [35, 37]. Investigations of TNTs between NK and target cells revealed that direct interaction between surface cell receptors and ligands can occur between the leading edge of a donor cell TNT and the target cell membrane [50]. Furthermore, Gerdes and colleagues used optical membrane potential measurements and mechanical stimulation to reveal TNT-mediated bidirectional electrical coupling in NRK cells, which was dependent on interposed gap junctions [36]. NRK cell conduits displayed membrane continuity on only one end of the TNT, while the other end exhibited a Cx43-positive border, and co-localization studies revealed the existence of both connexin-containing TNTs that participated in electrical coupling, and connexin-deficient TNTs that failed to facilitate electrical coupling. These interposed TNTs and gap junctions facilitated targeted and rapid signaling between cells up to 100 μm apart. On the other hand, Watkins and Salter demonstrated that TNT-mediated calcium fluxes between human iDC or monocytes occurred independently of gap

junctions [55], and so the ability of TNTs from myeloid-derived cells to support electrical coupling remains unclear.

New evidence also suggests a cooperative relationship between TNT- and exosome-mediated pathways of intercellular communication. Exogenous melanoma-derived exosomes enhanced TNT formation in lipid raft-enriched melanoma cells, and TNTs facilitated their direct cell-cell transfer [69]. Furthermore, the authors concluded that exosomes may act as a chemotactic stimuli for TNT development. Cholesterol-rich lipid rafts were also detected 2-fold higher in TNT-containing mesothelioma cells compared to TNT-deficient cells, providing further evidence that these lipid-raft enriched membranes can serve as a biomarker for TNT-positive cells. Additionally, exosomes from chronic myeloid leukemia cells induced TNTs that facilitated their direct cell-cell trafficking in remodeling umbilical endothelial cells [70]. DC-derived exosomes, typically 50 to 100 nm in diameter, vary in function depending on the activation state of the originating cell, and these structures can induce either immune activation or tolerance [71], but also support HIV-1 transmission to $CD4^+$ T cells [72]. A possible connection between these two modes of intercellular communication in myeloid cells could therefore have critical implications in the fields of basic immunology, vaccine development, as well as HIV-1 immuno-pathogenesis.

The function of diverse TNT-mediated cargo exchange between interconnected cells depends on nature of the cargo, the cell types involved, and the surrounding environment in which the cell-cell interaction occurs in vivo. Furthermore, the current literature suggests that distinct classes of TNTs can incorporate other known forms of direct and indirect intercellular communication [37, 73], providing impetus for further study of these conduits in the context of immunity. We postulate that TNT-mediated intercellular communication in myeloid origin DC

likely has a critical purpose in the setting of acute inflammation such as the activation of multiple nearby cells for a rapid multicellular response to a pathogen assault, or Ag exchange for amplification of DC-mediated immune responses. However, TNTs can represent a double-edged sword in the context of certain neurological disorders, cancer, and HIV-1 transmission.

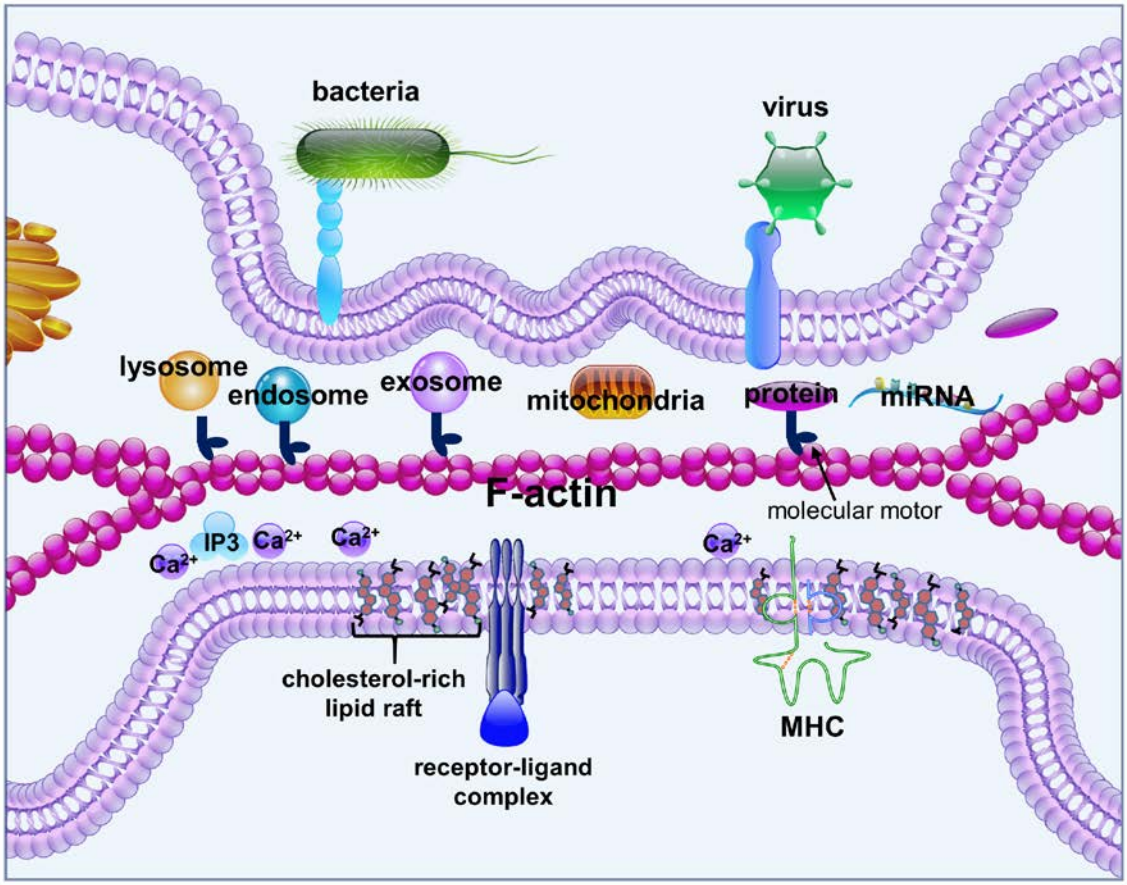

Representation of the diverse cytoplasmic and plasma membrane-conjugated cargoes that can be directly transported between interconnected cells via TNTs. Lysosome-, endosome- and exosome-associated vesicles, which can contain a wide variety of molecules, can be transported from donor to recipient via molecular motor proteins. Large organelles such as mitochondria, and cytosolic proteins, small molecules such as calcium ions, and microRNAs can be also be exchanged via these conduits. Additionally, cholesterol-rich membrane patches, membrane-associated receptor-ligand complexes, MHC molecules, and pathogens bound to capture molecules can be transported along the outside of TNTs. Electrical signals in association with gap junctions can also be transmitted via TNTs in some cell types (not depicted) [36, 73]. Notably, functionally distinct classes of TNTs comprised of F-actin alone or F-actin and tubulin as well as open- and closed-ended TNTs have been observed, and these structures differ in their ability to transmit specific cargoes. Thus, TNTs represent an extremely complex and diverse mode of intercellular communication that can support the direct exchange of cargoes, the identity of which in part determines the functional consequence for the target cell. Adapted from [73].

Figure 3. TNTs support the direct intercellular exchange of diverse cargoes.

1.3 TUNNELING NANOTUBES AND DISEASE

The diversity in structure and function demonstrated by TNTs, as well as their distribution across a wide variety immune and non-immune mammalian cell types, indicates an important role for TNT networks in coordinating multicellular functions in mammalian cells. Intriguingly, bacteria, which were previously thought to communicate primarily by way of secreted factors, were recently shown to form membrane TNT-like connections that are structurally distinct from conjugative pili [74]. These conduits supported the direct exchange of antibiotic resistance genes between *Bacillus subtilis* and *Staphylococcus aureus* and also between *S. aureus* and *E. coli*, two evolutionarily distant species. Even internal membrane-containing viruses were recently observed to form proteo-lipidic tubes in vivo that can pierce gram-negative bacteria envelopes and support delivery of viral genomes [75]. Importantly, TNTs have been implicated in the context of certain chronic diseases in mammals, as they facilitate tumor development and the direct cell-cell spread of prions as well as HIV-1.

1.3.1 Cancer

The most convincing in vivo evidence for the existence of TNTs in the setting of cancer in was provided by Lou et al. [76] in 2012, when they visualized TNTs in human mesothelioma and lung adenocarcinoma tumor samples via confocal microscopy. These conduits were additionally observed in vitro in mesothelioma cell lines and primary mesothelioma cells. TNT formation was enhanced by culture in low-serum, acidic growth media and these structures supported the unidirectional and bidirectional exchange of mitochondria, vesicles, and proteins, similar to non-cancer cell types [35, 37]. Intriguingly, TNTs formed between mesothelioma cells or normal

mesothelial cells, but failed to develop between malignant and normal cells, indicating selective TNT-mediated cross-talk between discrete cell populations in the context of cancer. Additionally, TNTs formed along the leading invasive edge of mesothelioma cells in vitro, which could indicate a role for these structures in disease progression. Furthermore, exogenous tumor cell exosome-mediated stimulation of TNT formation in mesothelioma cells provided the first evidence of a cooperative relationship between exosomes and TNTs [69]. A more in depth characterization of TNTs by Lou and colleagues revealed a higher frequency of TNTs in malignant versus benign mesothelioma cells, as well as the potentially novel function of these structures in an model of pleural/peritoneal effusion, which is the tethering of suspended, non-malignant cells to adherent cells or the pleural lining [77]. This same research group observed TNTs ex vivo in both human ovarian adenocarcinoma tumor explants and demonstrated TNT-mediated exchange of oncogenic microRNAs between ovarian cancer cells in vitro, and also between osteosarcoma and stromal cells [78]. These findings indicate a role for TNTs in the interaction between cancer cells and their surroundings, which may be important for tumor development, progression, and recurrence.

1.3.2 Neurological disorders

The class of neurodegenerative disorders termed transmissible spongiform encephalopathies (TSEs) are initiated by pathogenic isoforms (PrPSc) of a host-encoded cellular protein (PrPc), also commonly known as prions [79]. Normal isoforms can be found on the cell surface of lymphoid and neuronal cells, and consumption of contaminated food leads to PrPSc amassing in lymphatic tissues prior to invading the central nervous system (CNS). PrPSc likely acts as a catalyst for conversion of normal to the pathogenic isoform, eventually leading to accumulation

of aberrant proteins in the brain and neurodegenerative disease, but the mode of initial prion transport to and within the CNS remains to be elucidated. In 2010, Langevin et al. [80] first demonstrated that bone-marrow-derived DC can be hijacked to spread prions to neuronal cells. DC rapidly internalized PrPSc upon exposure to infected brain homogenates and catabolized the aggregates, prior to transferring them directly to cerebellar neurons via TNTs in a co-culture system. Furthermore, lysosomal vesicles containing fluorescently tagged endogenous or exogenous PrPSc were exchanged between neurons via TNTs at a speed that indicated an actimyosin-dependent transport mechanism [79]. Together, these data highlight a role for TNTs in both the initial conveyance of PrPSc to the CNS and subsequent spread of these proteins in neurons in the CNS.

1.3.3 HIV-1 transmission

HIV-1 is a retrovirus that selectively infects and eventually depletes $CD4^+$ T cells, and in the absence of antiretroviral treatment (ART) results in collapse of the immune system and acquired immune deficiency syndrome (AIDS) [81]. Over 35 million people in the world are currently living with HIV-1, which has caused at least 39 million deaths since the epidemic was officially recognized in 1981 [82]. HIV-1 is capable of infecting APCs such as macrophages and DC as well as $CD4^+$ T cells, albeit with widely varying efficiency, and unchecked infection also has deleterious effects on B cell responses, leading to the impairment of both cellular and humoral immune responses [83]. Myeloid-derived APCs are probably among the earliest targets of HIV-1 infection due to their localization to mucosal tissues and participation in Ag acquisition at these sites [84]. An exhaustive review of the mechanisms of HIV impairment of the immune system is beyond the scope of this dissertation, and I will instead focus on the role of TNTs in direct cell-

cell HIV-1 transmission. While TNTs facilitate direct and indirect intercellular communication, they can also be hijacked by intracellular pathogens such as HIV-1 to spread rapidly to distant cells, allowing them to circumvent diffusion limited spread while avoiding the inhospitable extracellular milieu.

Monocytes and macrophages are considered to be important targets of HIV-1 infection in vivo, and may provide a reservoir for the virus during ART [85]. Eugenin, Gaskill, and Berman showed in 2008 that HIV-1 infection increases the frequency of TNTs in human monocyte-derived macrophages and that HIV-1 particles localize to these structures [86]. The authors categorized 'short' TNTs with an average length of 30 μm and 'long' TNTs with an average length of 150 μm, and these TNT types were distinct from filopodia, which were typically 5 μm in length. They observed immunolabeled HIV-1 p24 in both intracellular vesicles as well as TNT-like processes. Infected macrophages displayed a 60-70% increase in short TNTs and a 20-25% increase in long TNTs, compared to that of uninfected macrophages. Furthermore, the peak of TNT formation was 2-3 days (d) post-infection, which correlated with active virus replication. Finally, virus particles appeared to be inside of short TNTs, but surfed along the outside of narrower, long-range TNTs, hinting that the mechanism of virus transfer may differ depending on the class of TNT involved.

In 2011, Kadiu and Gendelman conducted in depth proteomic, biochemical, and imaging studies to show that endocytic trafficking drives intercellular HIV-1 spread in human monocyte-derived macrophages through TNT-like connections they termed bridging conduits [87], the equivalent of thick TNTs described previously in this cell type [57]. They confirmed that HIV-1 infection increases TNT formation in macrophages and identified endosome, golgi, and endoplasmic reticulum (ER) proteins in the proteome of the conduits, and confirmed the

presence of these markers as well as ER and Golgi-associated HIV-1 envelope (Env) and capsid core (Gag) proteins within these structures via immunostaining and confocal imaging [87]. Infectious HIV-1 particles underwent retrograde transport from early/recycling endosomes to the trans-golgi following endocytosis. In a related study, Kadiu and Gendelman showed that viral RNA and proteins could be sequestered in multiple endocytic compartments within conduits, with a preference for multivesicular body-Rab11 recycling endosomes [88]. Transport of virus components through the conduits was dependent on the integrity of both endocytic and actin-myosin networks, and facilitated HIV-1 spread to neighboring uninfected macrophages. The authors noted the absence of mature HIV-1 virions within endosomes in the conduits, and postulated that TNT-mediated HIV-1 spread could involve shuttling of disassembled viral cargoes, which are still capable of initiating infection, to uninfected cells.

Although HIV-1 apparently utilizes endocytic vesicular trafficking to mediate virus transmission to neighboring, uninfected macrophages, monocyte-derived DC are highly resistant to HIV-1 cis-infection [89], and the mechanisms of transfer could also conceivably differ. DC instead are thought to carry intact virus to regional lymph nodes where they transmit virus in trans to $CD4^+$ T cells [90], but the mechanisms underlying this process and the role of trans-infection in in natural infection are fiercely contested. DC-mediated HIV-1 transmission via TNTs is not well studied, and herein I attempt to fill this perceived gap in the current literature.

Nef, a membrane-associated accessory protein conserved in HIV-1, HIV-2, and SIV, plays a central role in viral pathogenesis and disease progression as it modulates cell surface receptors to escape immune detection, regulates T cell activation, and enhances virus infectivity, replication, and transmission [43, 91]. In addition to down-regulation of CD4, CD3, and MHC class I, and modulation of T cell signaling pathways, this protein has been shown to facilitate

virus transmission by inducing of multivesicular bodies and TNT formation via interaction with the exocyst complex [43]. Although HIV-1 does not directly infect B cells, untreated infection nevertheless indirectly leads to a multitude of B cell-intrinsic humoral defects in part by Nef-mediated inhibition CD40L-driven $CD4^+$ T cell help [83]. In 2009, Cerutti and colleagues revealed an abundance of $CD68^+$ macrophages containing p24 and Nef, often proximal to pre-class-switched Nef^+ IgD^+ B cells, in follicular and extra-follicular regions of infected lymphoid tissues from chronically infected patients [92]. HIV-1-infected macrophages inhibited B cell IgG2 and IgA class switching via Nef in vitro, as well as Nef-induced long-range TNT development between infected THP-1 cells or primary macrophages and B cells. In addition to Nef^+ vesicles budding from the membrane of THP-1 cells, Nef localized along the length of TNTs or within bulges indicative of TNT-mediated vesicular trafficking. Examination of systemic and intestinal follicles additionally revealed Nef-containing conduits formed between macrophages and Nef^+ B cells, providing in vivo evidence of a role for TNT-mediated Nef transfer from infected macrophages in promoting B cell dysfunction in the context of HIV-1 infection.

Gabuzda and colleagues shed light on the mechanisms of Nef-mediated TNT induction when they identified an association between Nef and 5 components of the exocyst complex, EXOC1-4 and EXOC6, in Jurkat T cells by tandem mass spectrometry and co-immunoprecipitation assays [43]. The association was dependent Nef-induced activation of Pak2, a kinase involved in actin cytoskeleton dynamics and T cell signaling. Bioinformatics analysis of the Nef-exocyst interactome identified functional linkages between RalA, the adaptor protein 2 complex, Pak2, vav/Cdc42, and Nef and the exocyst complex. Furthermore, mutations targeting Nef association with Pak2 and shRNA-mediated EXOC2 depletion substantially

inhibited Nef-induced enhancement of TNT formation in Jurkat cells. Considering the central role of the exocyst complex in both TNT formation and vesicle secretion at the plasma membrane, direct interaction between Nef and this multi-protein complex likely facilitates direct spread of HIV-1 virions as well as HIV-1-associated immunosuppressive proteins via TNTs and vesicles.

Davis and colleagues showed that TNTs formed between HIV-1-infected Jurkat and uninfected Jurkat T cells, and while infection did not induce TNT formation, their existing TNTs supported the direct transfer of nascent virions to uninfected T cells over long distances [67]. Co-localized Gag and Env proteins suggestive of late stage virus were detected in TNTs connecting infected and uninfected Jurkat cells after only 1 h of co-incubation. Furthermore, co-localized HIV-1 proteins were also observed in uninfected target cells that were physically connected to infected cells by TNTs, but not in unconnected target cells. Laser scanning confocal microscopy revealed trafficking of Gag-GFP recombinant HIV-1 virions between infected and uninfected Jurkat cells at an average speed of 0.08 ± 0.03 $\mu m/s^{-1}$, which is consistent with actin-mediated movement, but is considerably faster than filopodia-driven intercellular trafficking of murine leukemia virus. Gag transfer was eliminated when cells were separated by a trans-well system or when TNTs were broken by shaking. While blocking CD4 or the gp120 subunit of Env with respective specific Abs failed to inhibit TNT formation or localization of Gag to TNTs, either treatment precluded passage of Gag to uninfected target cells. Furthermore, transmission was substantially inhibited in a CD4-deficient T cell line. Taken together, these data indicate that TNTs likely serve as a receptor-dependent route for direct high-speed transmission of HIV-1 between $CD4^+$ T cells.

In this dissertation, I will investigate the ability of HIV-1 to utilize CD40L-inducible TNT networks to spread between interconnected DC and also to facilitate DC1-mediated HIV-1 trans-infection of $CD4^+$ T cells. Our research group recently showed that HIV-1 can selectively utilize CTL helper activity in the absence of killing as a means to induce and program DC1, which also expressed enhanced numbers of membrane extensions capable of efficiently mediating HIV-1 trans-infection of $CD4^+$ T cells [93, 94]. These data demonstrate a scenario in which HIV-1 could perpetuate a positive feedback loop that promotes acute inflammation and TNT networks, a setting which also likely facilitates high-speed cell-cell transmission. Clearly, TNTs represent a double-edged sword in the context of an immune response to HIV-1 infection, and further investigation is needed to determine if we can safely and effectively target these novel conduits to disrupt HIV-1 transmission in vivo.

1.4 DC-MEDIATED HIV-1 TRANS-INFECTION OF $CD4^+$ T CELLS

In addition to supporting direct intercellular communication in DC1, TNT networks may play a role in the DC-mediated transmission of pathogens such as HIV-1. Intriguingly, the cell-cell transmission of HIV-1 can be 100-1000 times more efficient than transmission of cell-free virus [95]. DC are considered early targets of HIV-1 transmission due to their localization to mucosal surfaces where they efficiently capture Ag at the immature stage, together with their unique ability to migrate to the lymph node upon maturation and present Ag to T cells as they integrate into resident DC-comprised intercellular networks [84]. DC are highly resistant to cis-infection due to complex factors such as expression of HIV-1 restriction factors, degradation of internalized virions by iDC, and down-regulation of the CCR5 co-receptor upon maturation. In

striking contrast, DC have demonstrated a unique ability to acquire, carry, and transmit intact HIV-1 virions to $CD4^+$ T cells in vitro [90]. This phenomenon may have important implications, considering that $CD4^+$ T cells are the primary target of HIV-1 infection in vivo, and eventual depletion of this cell type leads to collapse of the immune system in the absence of ART. In a process termed trans-infection, migratory DC are thought to capture HIV-1 virions at the site of primary infection, which remain in infectious form during DC migration to the draining lymph nodes, where DC transmit them to susceptible $CD4^+$ T cells across the virologic synapse. The virologic synapse occurs at the site of contact between 2 cells upon recruitment of viral molecules Env and Gag together with adhesion molecules such as ICAM-1, lipid raft markers, and tetraspanins on the donor cell, and CD4, CCR5 or CXCR4, talin, actin, and LFA-1 on the target cell [96]. The polarization of these molecules results in formation of a characteristic ring-shaped structure at the interface between donor and target cells. Furthermore, $CD4^+$ T cells may actively participate in HIV-1 acquisition by extending TNT- or uropod-like membrane protrusions into virus-containing crypts, onto which the virus is readily transferred [97]. Studies in iDC suggest that cell surface C-type lectin receptors such as DC-specific intercellular adhesion molecule-3-grabbing non-integrin (DC-SIGN), also known as CD209, mediate capture of virions via interaction with the viral Env protein gp120 and subsequently internalize and sequester them in non-classical endosomal tetraspanin-rich vesicles [98]. Endocytosed virions can be redirected to the secretory pathway and the resulting highly infectious exosomes provide a possible pathway for transmission to $CD4^+$ T cells that occurs independently of direct contact with DC [72]. Alternatively, HIV-1 can localize to complex, surface-accessible invaginations of the cell membrane before virions are directed to the virologic synapse, where they are transferred to $CD4^+$ T cells upon close contact by a receptor-dependent mechanism [99]. More recent

studies have revealed that HIV-1 capture by mature DC is mediated by the cellular sialic-acid-binding immunoglobulin-like lectin 1 (Siglec-1), which binds to host-derived gangliosides on the viral membrane, as opposed to the viral Env glycoprotein [89]. The transmission of HIV-1 by professional APC such as DC in the absence of cis-infection results in a dramatic burst of viral replication in $CD4^+$ T cells [100]. However, the mechanisms of HIV-1 transfer from DC to T cells and the role of this process in natural HIV-1 infection are fiercely debated [72, 99, 101-104].

1.4.1 DC-T cell interactions via membrane protrusions at the virologic synapse

DC-T cell interactions at the virologic synapse have been extensively studied with various live- and fixed-cell imaging technologies, however these studies typically include only iDC or standard mature DC. Piguet and colleagues recently showed that Env engagement of DC-SIGN induced membrane extensions in iDC through activation of Cdc42 in a signaling cascade involving Src kinases, Pak1, and Wasp [105]. Ion abrasion scanning electron microscopy (IA-SEM) revealed that the DC-T cell contact areas with the initial appearance of thin filopodia are actually extended membrane sheets, which enveloped the T cells. Felts et al. [106] used advanced imaging techniques, including IA-SEM and stimulation emission depletion (STED), for 3D visualization of virologic synapse formation between mature DC and $CD4^+$ T cells. STED is one of the rapidly emerging super-resolution technologies that transcends the diffraction limit, allowing visualization of individual virions in close proximity, and unlike electron microscopy, can be used to image live cells. The authors observed extensive sheet- or ruffle-like membrane extensions on the DC surface that folded back onto the membrane surface and trapped virions in surface accessible compartments or crypts. Upon close-cell contact and formation of

the virologic synapse, these sheets appeared to envelop T cells and protect the cell-cell contact zone from the extracellular environment. Synapse formation was dependent on actin rearrangements, and involved interdigitation between the DC membrane and filopodia-like extensions originating from the T cell and extending into the virus-containing crypts. These findings are consistent with previous reports demonstrating that $CD4^+$ T cells actively participate in HIV-1 acquisition by extending thin membrane protrusions into virus-containing crypts, along which the virus surfs toward more proximal regions of the cell body, where they undergo receptor-mediated fusion, as evidenced by inhibition of infection by treatment with CD4 blocking mAb [97].

Importantly, DC used for 3D visualization of the DC-T cell virologic synapse in the fore-mentioned study were matured using a PGE_2-containing cocktail, which is known to induce type-2 polarization [12, 107]. Cultured iDC described in the literature exhibit substantial membrane ruffles and very few extended membrane processes, while standard mature DC form only short membrane projections, and these morphologies are both dramatically different from the long interdigitating processes characteristic of DC found in peripheral tissues and lymph nodes [27]. Our initial observations suggest profound differences in the membrane morphologies of mature DC1 and DC2, which are even more pronounced upon secondary stimulation by CD40L-expressing Th cells. PGE_2-matured DC2 are fairly round, typically display membrane ruffles and very few dendrites, and CD40L activation induces only short membrane projections. On the other hand, DC1 are larger, display long ultra-fine membrane protrusions, and CD40L activation induces many more dynamic extended membrane processes of varying diameters. Consequently, I propose that HIV-1 may utilize different mechanisms for direct cell-cell spread than those described in these earlier studies in DC programmed in the presence of mediators of type-1

immunity, which develop in the setting of acute viral infection. I intend to fill this apparent gap in the literature by observing DC1-$CD4^+$ T cell interactions and subsequent HIV-1 transmission using super-resolution imaging modalities in the context of reticulation, wherein DC1 uniquely form extensive networks of TNT-like membrane processes in response to CD40L-expessing $CD4^+$ T cells.

1.4.2 HIV-1 trans-infection and disease progression

HIV-1-infected non-progressors (NP), who can inhibit disease progression for many years in the absence of therapy, are a heterogeneous cohort, and slow disease progression has been attributed to diverse viral, immunologic, and genetic factors, including polymorphisms in the cellular HIV-1 co-receptor [108]. A recent study by Ayyavoo and colleagues also linked slow disease progression to polymorphisms in the HIV-1 accessory protein Vpr in variants isolated from NP, which resulted in enhanced virus replication [109]. In a recent investigation conducted by our research group that was led by Rappocciolo, iDC and B cells derived from a subset of NP lacked the ability to trans-infect $CD4^+$ T cells due to increased levels of the reverse cholesterol transporter ABCA1, which resulted in a paucity of APC cholesterol [110]. Strikingly, cholesterol levels and cis-infection of $CD4^+$ T cells were comparable to that of HIV-1 progressors (PR) and sero-negative donors, and cholesterol reconstitution in the APC restored their trans-infection ability. These data demonstrate for the first time a probable relationship between HIV-1 disease progression and APC-mediated trans-infection.

Cholesterol-rich lipid rafts have been implicated as a biomarker for TNT development [69], and our unpublished findings demonstrate that polarized DC1 from these same NP display an impaired ability to respond to CD40L by forming TNT networks. This information, in

combination with evidence for augmented trans-infection by DC upon CD40 ligation [111], and Th1 depletion in long term HIV-1 infection [112], provide a rationale to further investigate CD40L-induced reticulation in inflammatory DC1 as a potentially important pathway for DC-mediated HIV-1 transmission. I speculate that DC1 induction of Th1-biased responses creates a positive IFN-γ-driven feedback loop wherein Th1 cells selectively induce more DC1, which not only enhance inflammation, but also directly facilitate virus spread via TNT networks to both resident DC and susceptible $CD4^+$ T cells.

1.4.3 HIV-1 trans-infection and DC maturation state

The maturation state of DC is thought to be critical in determining the ability of this cell type to support trans-infection, as mature DC are more efficient than iDC at transmitting virions to $CD4^+$ T cells in part due to their up-regulation of molecules required for T cell activation [100]. Furthermore, a previous report by Berkhout and colleagues demonstrated that DC1 are superior mediators of trans-infection compared to DC2, which transmit HIV-1 inefficiently, and DC0, which display an intermediate ability to transmit virus, similar to iDC [113]. DC1 trans-infection ability correlated with high surface expression of ICAM-1, also known as CD54, compared to other DC types; and Ab blocking of ICAM-1 substantially reduced both DC1- and iDC-mediated HIV-1 transmission. Furthermore, DC-SIGN expression was highest on iDC, rather than DC1, indicating that enhanced DC1 trans-infection was related to their ability to transmit the virus to T cells, rather than their ability to acquire the virus. However, this study was conducted prior to the revelation that Siglec-1, not DC-SIGN, mediates HIV-1 capture in mature DC. I will therefore determine the surface expression of Siglec-1, in addition to ICAM-1, on differentially-matured DC used in trans-infection experiments. These results overall suggest that

the well-established interaction between ICAM-1 on DC1 and LFA-1 on T cells is important for efficient DC-mediated HIV-1 transmission. However, I propose that TNT- and ICAM-1-mediated enhancement of virus transmission by DC1 are not mutually exclusive concepts. Comrie, Boyle, and Burkhardt very recently demonstrated that DC maturation induces changes in the expression and activation of moesin and α-actinin-1, which associate with actin filaments and the cytoplasmic domain of ICAM-1, thereby constraining its lateral movement and promoting ICAM-1 clustering and LFA-1-dependent T cell activation [114]. These data demonstrate a role for F-actin-driven cytoskeletal alterations and the formation of ICAM-1 puncti on mature DC in promote T cell priming. Considering this in combination with evidence of ICAM-1 participation in DC1 trans-infection, I will determine if ICAM-1 clusters localize to CD40L-induced DC1-derived TNTs. This phenomenon may provide greater opportunity for contacts between DC1 and T cells, and subsequently directly enhance virus transmission.

While DC1 promote Th1 responses and are the most efficient mediators of HIV-1 transmission, a study by Jong and colleagues indicates that mature DC transmit HIV-1 to subsets of T effector memory cells, including Th1, Th2, and unbiased Th0 cells, with equal efficiency [115]. Using a single cycle virus transmission assay and either R5 or X4 HIV-1, the authors showed no significant difference in the ability of Th subsets to be infected by mature, polarized DC and no preference for DC0, DC1, or DC2 to transmit virus to their corresponding Th type. However, in all cases DC1 was the most efficient mediator of trans-infection compared to DC2, which were inefficient, and DC0 which displayed an intermediate trans-infection ability. Interestingly, an R5-tropic virus was preferentially transmitted to T_{EM} cells, while an X4 virus was most efficiently transferred to naive Th cells. The current literature demonstrates that differences in the ability of mature, polarized DC types to transmit HIV-1 is related to some

quality of the DC rather than differential susceptibility of the T cells, I will therefore focus my investigation on delineating the unique characteristics of DC1 that influence their enhanced trans-infection ability.

1.4.4 A role for inducible TNT networks in DC1-mediated trans-infection?

The ability of HIV-1 to circumvent CTL-mediated recognition and elimination by frequently mutating and generating variant strains in response to host immune selective pressure is well known [116]. Intriguingly, our research group's recent study showed that CTL-driven epitope divergence resulted in surviving HIV-1 epitope variants that could selectively utilize CTL helper activity in the absence of killing as a means to induce and program DC1, which were capable of efficiently mediating HIV-1 trans-infection of $CD4^+$ T cells [93, 94]. These cross-reactive CTL-programmed DC1 were able to secrete high levels of pro-inflammatory cytokines such as IL-12p70 and IL-6, as well as a wide range of chemokines, including CCL4, CCL5, CXCL9, and CXCL10. This chemokine profile could allow CTL-programmed DC1, which also displayed a heightened ability to develop far-reaching networks of TNT-like extensions, to preferentially attract activated $CD4^+$ Th cells.

These data and my initial findings that Th cell-associated CD40L induces an even more extensive interconnected network of TNTs uniquely in DC1, provides a rationale for studying the role of these conduits in mediating enhanced DC1 trans-infection. Furthermore, the diversity of TNT-mediated intercellular communication, from the facilitation of membrane-bound vesicle transport inside TNTs to pathogen surfing and immunologic synapse formation between donor and target cell membranes on the outside of TNTs, hints that reticulation may represent a multifaceted mechanism of HIV-1 transmission by DC1. I hypothesize that the ability of

differentially polarized migratory DC to transmit HIV-1 to interacting $CD4^+$ T cells is dictated in part by their unique responsiveness to $CD4^+$ Th cell-associated CD40L, which induces uniquely in DC1 the development of extensive TNT networks, as well as high IL-12p70 production for the polarization of Th1- and CTL-biased adaptive immune responses.

2.0 HYPOTHESES AND SPECIFIC AIMS

2.1 AIM 1

Identify and quantitatively characterize a novel aspect of CD40L-mediated $CD4^+$ T cell help, the induction of TNT networks, in DC programmed by mediators of type-1 immunity. Hypothesis: CD40L induces in DC programmed by mediators of type-1 immunity the development of complex networks of open-ended TNTs. In Aim 1, I will investigate the ability of the Th cell-associated CD40L to induce reticulation, or the development of extensive TNT networks, in differentially programmed DC. I hypothesize that the unique responsiveness of DC1 to CD40 ligation results in the formation of dynamic and extensive interconnected networks of TNTs, in addition to high IL-12p70 production. Morphological alterations resembling TNTs appear to develop exclusively in DC1 when they are activated by CD40L-expressing $CD4^+$ T cells, while DC2 fail to develop these extensions. I will show that the unique ability of DC1 to respond to CD40L-mediated activation is imprinted on iDC during maturation by exposure to mediators of type-1 immunity, while DC2 are refractory to the induction of this process. Advanced 3D imaging analysis software will be utilized to quantitate and characterize CD40L-induced alterations in the membrane morphologies of representative DC types from independently tested, healthy donors.

2.1.1 Aim 1a.

Generate differentially polarized DC from human monocytes using the αDC1 cytokine-based cocktail [8] or PGE_2-based cocktail [117], confirm their functional phenotype, and use bright field microcopy to determine the differential ability of DC1 and DC2 to form TNT-like membrane extensions upon co-culture with autologous Ag-stimulated $CD4^+$ T cells.

2.1.2 Aim 1b.

Confirm surface expression of CD40L on Ag-stimulated $CD4^+$ T cells as well as constitutive surface expression of CD40 on differentially programmed DC by flow cytometry, and show that abrogating CD40L signaling with a CD40L-specific blocking mAb substantially inhibits the formation of TNT-like extensions in DC1. Additionally, I will demonstrate the ability of CD40L-expressing J558 cells or recombinant human (rh) CD40L protein to induce membrane extensions in DC1, similar to CD40L-expressing $CD4^+$ T cells.

2.1.3 Aim 1c.

Perform quantitative assessment of cell membrane morphologies, including the total cell surface area and parameters associated with TNT-like extensions, in individual representative resting and CD40L-activated DC1 and DC2 from 3 independent, healthy donors using IMARIS 3D imaging analysis software. Quantitative data will be statistically analyzed using a one way analysis of variance (ANOVA) or unpaired student t tests, and significance determined at an α of 0.05.

2.1.4 Aim 1d.

Utilize additional strategies to generate DC1 aside from the αDC1 cocktail, including cellular methods such as co-culture of iDC with 2 signal-activated NK cells [9] or activated $CD8^+$ T cells [14], and several alternate methods to generate DC0 and DC2 [12], and assess their reticulation ability in response to CD40L. DC types will be stimulated with rhCD40L for 18 hours (h), followed by cell surface staining and high resolution confocal imaging to reveal intricately branching networks of TNT-like extensions in DC1.

2.2 AIM 2

Investigate the role of polarized Th cell cytokines in the regulation of DC reticulation, and demonstrate that this process provides a functional pathway for Ag exchange between interconnected DC1.

Hypothesis: The immunologic process of DC reticulation is regulated by the opposing roles of the Th1 cytokine, IFN-γ, and the Th2 cytokine, IL-4. The resulting network of TNTs enhances intercellular communication and facilitates the direct hand-off of Ag between interconnected DC1, but can also be hijacked by pathogens such as HIV-1 for direct cell-cell spread. I will investigate the role of helper signals from distinct $CD4^+$ T cell subsets in the regulation of the reticulation process. I will also utilize advanced imaging techniques to confirm that the observed structures are indeed open-ended conduits supporting the exchange of endosome-associated vesicles and bacterial or viral pathogens between DC1, similar to previous descriptions of TNTs

in myeloid origin cells. Furthermore, a potentially important immunologic function of these reticulating DC1 will be investigated, which is the facilitation of direct Ag exchange for enhanced induction of Ag-specific T cell responses between interconnected DC.

2.2.1 Aim 2a.

Investigate the role of the Th1, Th2, and regulatory T cell cytokines, IFN-γ, IL-4, and IL-10, respectively, in the regulation of the CD40L-induced reticulation process in differentially polarized monocyte-derived DC by adding cytokines alone or in combination with rhCD40L, to representative differentially programmed DC types. Quantitative data will be expressed as the percentage of reticulation positive cells and statistical significance determined using the Fishers exact test.

2.2.2 Aim 2b.

Demonstrate that $CD1c^+$ $HLA\text{-}DR^+$ myeloid DC isolated directly from human peripheral blood can be induced to form TNT networks by CD40L in an IFN-γ-dependent manner, analogous to the behavior of monocyte-derived DC.

2.2.3 Aim 2c.

Utilize high resolution imaging techniques to capture the process of reticulation in representative DC1, or the development of networks of TNT-like connections, over time. I will also demonstrate that the observed structures are open-ended conduits that support the bi-directional

transfer of endogenous components such as endosome-associated vesicles between interconnected DC1.

2.2.4 Aim 2d.

Investigate the ability of resting versus CD40L-activated 'donor' DC1 and DC2 to transfer exogenous yellow-green (YG)-labeled nano-beads representing Ag to differentially labeled respective 'recipient' DC1 or DC2 using live-cell time-lapse confocal imaging and flow cytometry. I will also demonstrate the CD40L-dependent transfer of cytomegalovirus (CMV) and varicella zoster virus (VZV) peptide pools or whole protein tetanus toxoid (TT) Ags from reticulating donor DC1 to differentially labeled recipient DC1 in direct co-cultures or trans-wells. Recipient DC1 from direct co-cultures will be sorted by flow cytometry, using the acquisition of YG beads from donor DC1 as a marker for intercellular exchange. Differences in the ability of sorted YG^+ and YG^- recipient DC1 to drive antigen-specific T cell responses will be assessed using our established 10 day extended DC-T cell stimulation and IFN-γ ELISPOT assay [118].

2.2.5 Aim 2e.

Demonstrate using previously described imaging modalities that the CD40L-induced TNT networks can be utilized by pathogens such as HIV-1 for direct high-speed spread between interconnected DC1.

2.3 AIM 3

Quantitatively assess the ability of mature differentially programmed DC to transmit HIV-1 to CD4$^+$ T cells in trans, and investigate the possible mechanisms of enhanced DC1-mediated transmission, including CD40L-inducible TNT networks.

Hypothesis: Previous studies demonstrated that DC1 are superior mediators of HIV-1 trans-infection compared to iDC and other mature DC types [113, 115]; and I propose that this ability is related to the enhanced number of TNTs formed by DC1 as a result of their programming by type-1 inflammatory mediators and their resulting unique responsiveness to CD40L. I will first demonstrate the differential ability of mature DC types, including DC0, DC1, and DC2, to transmit HIV-1 to susceptible, autologous CD4$^+$ T cells utilizing our established in vitro trans-infection model [93, 110, 119]. Next, I will investigate the mechanisms underlying enhanced DC1 trans-infection by determining expression of the primary HIV-1 capture molecule in mature DC, Siglec-1, in addition to DC-SIGN on DC types. The contribution of CD40L and CD40L-inducible TNT networks to virus transmission will be investigated by abrogating CD40L-CD40 signaling with anti-CD40L blocking mAb, and by blocking TNTs with actin depolymerization or cholesterol depletion drugs, at concentrations that also inhibit TNT networks. Furthermore, I will investigate the ability of inflammatory DC1 to transmit HIV-1 to autologous CD4$^+$ T cells in the setting of reticulation using live-cell super-resolution imaging techniques. I showed previously that CD40L-induced morphological changes result in dramatically increased surface area and spatial reach of individual DC1 and formation of an intricate network of TNTs, and postulate that these membrane protrusions enhance DC-T cell contacts and DC1-mediated transmission. Importantly, a previous report related enhanced trans-infection to high surface expression of ICAM-1 on DC1 compared to DC2 [113]. I propose that this and the inducible

TNT-mediated mechanism of trans-infection are not mutually exclusive. I will use live-cell super-resolution microscopy to reveal the presence of ICAM-1 puncti along TNTs, which likely directly enhances DC-T cell interactions and further promotes trans-infection. I propose that inducible TNT networks facilitate interactions with adjacent and remote $CD4^+$ T cells, in addition to spreading the virus among interconnected DC1, and subsequently enhance DC1-T cell HIV-1 transmission.

2.3.1 Aim 3a.

Assess the ability of representative mature DC types, including DC0, DC1, and DC2 to mediate transmission of HIV-1 BaL, an R5 tropic virus, to autologous PHA and IL-2 pre-activated $CD4^+$ T cells using our established in vitro trans-infection model [93, 110, 119]. The primary readout of infectivity will be estimated by determining the percentage of live HIV-1 Core Ag positive $CD4^+$ T cells at d 6 and d 8 post virus-exposure by intracellular staining (ICS) with an HIV-1 core Ag-specific mAb, followed by flow cytometric analysis.

2.3.2 Aim 3b.

Delineate the role of CD40L-inducible TNT networks in the enhanced ability of DC1 to transmit HIV-1 in trans to susceptible $CD4^+$ T cells by adding blocking agents in our in vitro trans-infection model. DC types will first be assessed for their surface expression of candidate molecules involved in either the acquisition of HIV-1 or DC-T cell interactions, including DC-SIGN, Siglec-1, and ICAM-1, in addition to the maturation marker CD83 and co-stimulatory molecule CD86, using flow cytometric methods [113]. We will determine the impact of T cell-

associated CD40L on DC1 trans-infection by inhibition of signaling with a CD40L-specific blocking mAb. The impact of TNT networks on enhanced DC1 trans-infection will be directly assessed by conducting blocking studies with latrunculin A, an actin depolymerization drug which is typically used to inhibit TNTs in previous studies [49, 58, 76], or simvastatin, a clinically approved drug which inhibits cholesterol biosynthesis [120], at concentrations which also substantially inhibit TNT networks.

2.3.3 Aim 3c.

Utilize super-resolution live-cell imaging technologies to visualize the interaction between reticulating DC1 pulsed with EGFP-labeled HIV-1-like particles and autologous $CD4^+$ T cells to provide supporting evidence of TNT-mediated HIV-1 transfer to $CD4^+$ T cells via TNTs. Furthermore, I will determine if ICAM-1 puncti localize to these CD40L-inducible structures, thereby further enhancing DC1-$CD4^+$ T cell contacts and HIV-1 trans-infection. Imaging studies will be conducted using live-cell super-resolution structured illumination microscopy (SIM) or stimulated emission depletion (STED).

3.0 MATERIALS AND METHODS

3.1.1 Isolation of human primary cells

Whole blood products (buffy coats) from healthy, anonymous donors were purchased from the Central Blood Bank of Pittsburgh. Autologous $CD14^+$ monocytes, $CD3^+$ T cells, $CD4^+$ T cells, $CD8^+$ T cells, and myeloid blood-derived DC were isolated from PBMC by density gradient separation [121] followed by immunomagnetic negative selection of the respective cell types (EasySep: STEMCELL Technologies Inc., Vancouver, BC, Canada).

3.1.2 Generation of DC

Monocytes were cultured for 5–7 d at 37°C in IMDM (Gibco, Life Technologies, Grand Island, NY) supplemented with 10% fetal bovine serum (cIMDM) in the presence of GM-CSF and IL-4 (both 1000 IU/ml; R&D Systems, Minneapolis, MN). DC generated under serum free conditions using either AIM-V (Gibco) or Cellgenix base media were also tested and yielded similar results (data not shown). On d 5, iDC were differentially exposed to activation factors for 48 h. For mature DC1, the activation factors consisting of combinations of either polyisosinic:polycytidylic acid [poly(I:C)] (20 μg/ml), IFN-α (3,000 units/ml), TNF-α (50 ng/ml), IL-1β (25 ng/ml), and IFN-γ (1,000 IU/ml) [8], LPS (250 ng/ml) and IFN-γ (1,000

IU/ml), or R848 (2.5 μg/ml) (Enzo Life Sciences, Farmingdale, NY) and IFN-γ (1000 IU/ml). Alternatively, DC1 were generated by co-culturing iDC with IL-18-primed NK cells in the presence of IL-15 (1 ng/ml) [9], or $CD8^+$ T cells in the presence of staphylococcal enterotoxin B (SEB) (1 ng/ml) [14] (Sigma-Aldrich, Saint Louis, MO). Mature, low IL-12p70 producing DC2 were generated using a modified version of a previously described cocktail consisting of TNF-α (50 ng/ml), IL-1β (25 ng/ml), and PGE_2, (10^{-6} mol/L) [8], a combination of LPS (250 ng/ml) and PGE_2 (10^{-6} mol/L) [12], or R848 (2.5 μg/ml) and PGE_2 (10^{-6} mol/L). Monocyte-derived DC0 were generated by exposure to TNF-α, LPS, or R848 alone for 24 h [12, 14]. Similarly, freshly isolated blood-derived myeloid DC were treated for 24 h with TNF-α prior to secondary stimulation.

3.1.3 CD40L-induced activation of mature DC

Differentially matured DC were stimulated for 24 h with either rhCD40L (0.5 μg/ml) (MegaCD40L; Enzo Life Sciences) or CD40L-expressing J558 (J558-CD40L) cells (Dr. P Lane, University of Birmingham, United Kingdom) [12], which were added to DC cultures at a 1:1 ratio. Where specified, IL-4 (5000 IU/ml), IL-10 (0.1 μg/ml), or IFN-γ (5000 IU/ml) was also included during CD40L stimulation.

3.1.4 Detection of DC IL-12p70 production

DC were harvested, washed, and plated in 96 well flat bottom plates ($3x10^5$ cells/well), and stimulated with either J558-CD40L cells or rhCD40L. IL-12p70 was measured in 24 h

supernatants using the MSD electrochemiluminescence detection system (MesoScale Discovery, Rockville, MD) or IL-12p70 ELISA (Thermo Fisher, Bartlesville, OK).

3.1.5 $CD4^+$ T cell activation

$CD4^+$ T cells were cultured for 2 d at 1×10^6 cells/ml in cIMDM supplemented with phytohemagglutinin (PHA) (Sigma-Aldrich) and IL-2 (Chiron, Emeryville, CA) at 37°C in 5% CO_2 as described previously prior to use in HIV-1 trans-infection or live-cell super-resolution imaging experiments.

3.1.6 DC-T cell co-cultures

Differentially matured DC (1.25×10^5 cells/ml) were co-cultured with $CD4^+$ or $CD8^+$ T cells (3.75×10^5) cells/ml in the presence of absence of SEB (1μg/ml). When used, CD40L-specific blocking mAb (Enzo Life Sciences) or control mAb of the same isotype (BD Biosciences, San Jose, CA) were added to the cultures. Bright field microscopic images (400X) were collected from 5-10 randomly selected fields in independent experiments from 3 healthy donors.

3.1.7 Microarray analysis of DC gene expression

Representative DC1 and DC2 were generated and Qiagen RNeasy kit (Qiagen, Valencia, CA) used to isolate mRNA followed by a direct hybridization assay using the Ilumina Human T-12 Expression BeadChip Kit (Ilumina, San Diego, CA), which contains >47,000 probes corresponding to roughly 35,000 genes. Data analysis was conducted using Genome Studio

software, and the data were additionally VST-transformed to obtain normalized mRNA expression levels.

3.1.8 Flow cytometry

The following immunostaining Ab reagents were used for flow cytometry analysis: Mouse-anti-human CD83-PE, CD86-PE, OX40L-PE, CD40L-PE, CD3-FITC, CD4-APC , CD8-APC, CD19-PE, CD3-PE, HLA-DR-FITC, ICAM-1-PE (CD-54) (all from BD Biosciences), CD40-PE, CD56-PE (Beckman Coulter, Indianapolis, IN), CCR7-FITC, DC-SIGN –FITC (CD209) (R&D Systems), CD14-PE, CD1c-PE (Miltenyi Biotech, San Diego, CA), Siglec-1-488 (CD169) (Serotec) and the respective matched isotype controls (BD Biosciences). Prior to analysis for expression of CD40L, isolated $CD4^+$ and $CD8^+$ T cells were stimulated for 24 h with anti-CD3/CD28 activating Dynabeads (Gibco, Life Technologies) to mimic interaction with DC. Purity was determined by the exclusive expression of either CD4 or CD8 on the $CD3^+$ gated lymphocytes. Purity of isolated $CD4^+$ T cells used in trans-infections was determined after 2 d of PHA and IL-2 activation by the same staining strategy. Purity of blood-isolated DC was delineated using the following gating strategy: lineage (CD3, CD14, CD19, CD56)$^-$ and $CD1c^+$ HLA-DR^+. Analysis was performed using the BD Biosciences LSR Fortessa Cell Analyzer and FlowJo version 7.6 software.

3.1.9 Immunocytochemistry

3.1.9.1 Fixed cell

DC1 were transferred to chambered borosilicate cover-glass slides (Lab-Tek, Thermo Fisher Scientific, Rochester, NY) and treated with rhCD40L or media for 18-20 h prior to processing. Samples were fixed and permeabilized with 0.1% Triton X-100 and non-specific mAb binding blocked with 2% BSA. Primary mouse anti-human early endosomal Ag 1 (EEA1) or isotype control mAb (1.25 μg/ml) (BD Transduction Laboratories, San Jose, CA) were added, followed by secondary goat-anti-mouse Alexa-Fluor 488-conjugated Ab and rhodamine-conjugated phalloidin (Molecular Probes, Invitrogen, Eugene, OR) to label primary mAb and filamentous F-actin, respectively. Nuclei were stained with Hoeschst stain (Invitrogen, Life Technologies).

3.1.9.2 Live cell

Live DC1 were first stained with 10 μg/ml rabbit polyclonal ICAM-1-specific primary Ab (Abnova, Taipei, Japan) at for 1 h, washed and stained with secondary goat-anti-rabbit 555-conjugated Ab or secondary Ab alone for 1 h at 37°C and 5% CO_2. Non-specific mAb binding was blocked using media containing 25% FBS. DC1 were washed and exposed to 6.55 ng/ml HIV-1-like particles or media for 2 h at 37°C, washed extensively with cold media, and then transferred to glass-bottomed imaging dishes with No. 1.5 cover-slips (MatTek Corporation, Ashland, MA). DC1 were treated with rhCD40L for 10-12 h prior to staining for 2 h with 1 μM SiR-actin (Spirochrome AG, Stein am Rhein, Switzerland) at 37°C and 5% CO_2, and imaging.

3.1.10 Microscopy

3.1.10.1 DIC, confocal, and standard bright field

Live-cell differential interference contrast (DIC) and standard or scanning confocal images were collected using a Nikon Eclipse Ti and Photometrics Evolve camera system with a Nikon Apo TIRF 60x Oil DIC N2 objective lens with a numerical aperture (NA) of 1.49; and NIS-Elements software was used to collect and analyze data. Additionally, images of fixed cells were collected on the Olympus Fluoview 1000 microscope system with Olympus 60x objective lens (NA=1.4). Standard bright field images were collected using a Leica DM IL LED using a Leica HI Plan I Ph2 40x objective lens (NA=0.5) using a Leica EC3 Camera system, and images were analyzed using Leica Application Suite software. Live cell cultures were maintained in an imaging chamber at 37°C and 5% CO_2 in media (cIMDM) during image acquisition, while fixed cells were maintained in PBS.

3.1.10.2 Super-resolution

N-SIM

Super-resolution images were collected in 3D SIM mode using live cells maintained at 37°C in media using the AAA Nikon SIM and camera system at 100x magnification and 0.12 µm slices. Image reconstruction and analysis was carried out using NIS-ELEMENTS software.

STED

Super-resolution images were collected on live cells maintained at 37°C using a Leica TCS SP8 STED 3X system. Images were deconvolved using Leica Application Suite software.

3.1.10.3 SEM

Mature DC1 were plated to glass coverslips and then fixed with 2.5% gluteraldehyde prior to standard processing of SEM samples, and imaging using a JSM 6335F SEM.

3.1.11 Morphological analysis of DC by high resolution imaging

DC (1.25×10^5 cells/ml) were cultured in glass-bottomed microwell imaging dishes (MatTek Corporation, Ashland, MA). Time-lapse live-cell DIC imaging was captured at time points and durations specified, with illumination intervals ranging from 2 to 6 min. For confocal imaging experiments, DC were either maintained in media alone (resting) or exposed to rhCD40L for 18 to 20 h, followed by surface staining using anti-human HLA ABC:Alexa Fluor 488 Ab (AbD Serotec, Raleigh, NC) as previously described [55, 64], and cell nuclei were stained with HCS Nuclear Mask Red Stain (Invitrogen, Life Technologies). To quantitate total cell surface area and membrane morphologies, cell cytoplasms were additionally stained with 0.39 μg/ml (0.4 μM) CFSE (Molecular Probes, Invitrogen), and IMARIS imaging software (Bitplane, South Windsor, CT) was used for data analysis. Individual cells were considered reticulation+ if they displayed ≥ 5 thick TNTs with a length of at least 10 μm. The full analysis was conducted in IMARIS on 3 independent donors, and subsequent assessment of reticulation+ cells was conducted by acquiring ≥ 10 image fields at 40x using the Leica DM IL LED and camera system, and scoring reticulation+ cells by hand.

3.1.12 Peptide and protein antigens

The following Ag sources were used at the concentrations listed in the described Ag transfer experiments: 0.2 μg/ml of CMV Ag (a pool of 9- to 12-mer peptides that comprise the CMV portion of the common control CMV, EBV, and influenza A virus peptide pool [122]); 0.4 μg/ml of varicella zoster virus (VZV) Ag (18mer overlapping peptide pool spanning the entire glycoprotein E; Sigma-Aldrich); and 0.5 μg/ml of tetanus toxoid (TT) Ag (whole protein; Astarte Biologics, Bellevue, WA).

3.1.13 Intercellular bead and antigen transfer

'Donor' DC1 and DC2 were generated by pulsing iDC with 40 nm yellow-green (YG) latex nano-beads (Molecular Probes, Invitrogen) at 1×10^{10} beads/ml and exposed them to the respective polarizing cocktails. For Ag transfer experiments, CMV, VZV, and TT Ags were added along with the beads and again after 24 h. Donor DC containing beads and 'recipient' DC lacking beads were labeled with cyanine dyes (Cy)5 or Cy3 dye (GE Health Care, Piscataway, NJ), respectively, for 20 min at room temperature. Donor and recipient DC1 or DC2 were harvested, washed 5 times, and co-cultured for 20 h in the presence or absence of rhCD40L. Where stated, a 0.45 μm trans-well system (Corning Costar, Tewksbury, MA) was used to separate co-cultured DC. Bead transfer to recipient DC was assessed by flow cytometry, as well as by live-cell confocal microscopy.

For Ag transfer experiments, donor DC1 were co-cultured with Cy5-labeled recipient DC1 for 20 h in the presence of rhCD40L. Cy5-labeled recipient DC1 were then differentially

sorted based on YG bead expression (as a marker for donor to recipient DC1 intercellular exchange) using a BD FACS Aria IIu cell sorter. Sorted YG^+ (bead-containing) and YG^- (bead-deficient) recipient DC1 were used as Ag-presenting stimulators of autologous T cell responses in a modified version of the previously described extended in vitro sensitization and IFN-γ ELISPOT assay [118]. Briefly, the sorted DC1 and autologous $CD3^+$ T cells were co-cultured for 10 d at a DC:T cell ratio of 1:10, with rIL-2 (100 IU/ml; Novartis, New York, NY) added on d 3. The cultured T cells (3×10^4/well) were tested by ELISPOT for reactivity to the individual CMV, VZV, and TT Ags in the presence of autologous monocytes (5×10^4/well). Spots were counted using an automated ELISPOT reader (AID), and expressed as mean Ag specific IFN-γ spot forming units (SFU) per 10^5 cells, subtracting values from Ag negative control wells.

3.1.14 Detection of intercellular trafficking of pathogens

3.1.14.1 Bacteria transfer studies

DC1 were cultured in imaging dishes and stimulated with CD40L for 8-10 h, prior to placement into the imaging chamber, which was maintained at 37°C and 5% CO_2. Live EGFP-expressing bacteria (*E. coli* strain BL21DE3) suspensions were prepared by picking a green isolated colony, and suspending it in 200 µl cIMDM. Ten µl of the *E. coli* mix was then injected into the media directly above cells. Cultures were incubated for 2 h to allow bacteria to settle in the proximity of the DC monolayer, and sequential images were generated using confocal resonance scanning methods.

3.1.14.2 Virus-like particle transfer studies

DC1-DC1

HIV-1-like particles were generated by transfecting 293T cells with pGag-EGFP, pRev, pGag/Pol, and pHXB2-Env using polyjet reagent (SignaGen Laboratories, Gaithersburg, MD) per manufacturer's instructions. Seventy-two h post-transfection, supernatants were collected, spun at 3000 rpm for 10 min and filtered through a 0.22 μm filter to remove cellular debris. Particles were concentrated by ultracentrifugation and resuspended in PBS. Virus titer was quantitated by p24 ELISA. Cy5-labeled donor DC1 were pulsed with 26.2 ng/ml HIV-1-like particles for 1 h and then washed extensively to remove unbound particles. Recipient DC1 were labeled with Cy3 and co-cultured in imaging dishes with donor DC1 the presence of CD40L for 8-12 h or 18-22 h prior to live-cell, time-lapse confocal imaging.

DC1-$CD4^+$ T cell

Prior to live-cell super-resolution imaging, DC1 were stained with Cy5 and exposed to HIV-1-like particles, as described previously DC1 were co-cultured with Cy3-labeled, autologous 1-2 day PHA and IL-2 activated $CD4^+$ T cells in glass-bottomed MatTek imaging dishes at a 1:5 ratio for 1-2 h.

3.1.15 Inhibition of TNT networks

3.1.15.1 Actin depolymerization

Mature DC1 were harvested and plated at 0.25 million cells/ml in a final volume of 0.2 ml/well of a flat-bottomed 96 well plate. Media alone or latrunculin A (Invitrogen, Molecular Probes) was added to the cell suspensions at a final concentration of 100 nM, the lowest concentration

that effectively inhibited DC1 reticulation. After 24 h culture, images were collected and individual image fields (≥ 10/condition) scored for % reticulation+ cells, as described previously.

3.1.15.2 Inhibition of cholesterol synthesis

Immature DC were treated with cytokine-containing maturation cocktail to generate DC1 along with 20 mM simvastatin (Sigma) in IMDM + 10% charcoal stripped FBS for 2 d prior to harvest and CD40L activation for 24 h, followed by collection of images (≥ 10/condition) for quantitation as before.

3.1.16 HIV-1 cis- and trans-infections

3.1.16.1 HIV-1 virus and core Ag ELISA

HIV-1 BaL, an R5-tropic virus, was propagated in PHA- and IL-2-activated HIV-naïve PBMC, as previously described [123], and virus titer (pg/ml) determined by HIV-1 p24 Ag Capture Immunoassay kit (SAIC-Frederick, MD). This immunoassay was also used where specified as an alternate surrogate marker of virus infectivity in cis-infection experiments.

3.1.16.2 HIV-1 exposure and co-culture of $CD4^+$ T cells and DC

Immature DC and differentially programmed mature DC (5×10^5) were exposed to 5, 12.5, or 50 pg of HIV-1 as specified for 2 h at 37°C at 5% CO_2. PHA- and IL-2-activated $CD4^+$ T cells were incubated with media (uninfected) or 5, 12.5, 50, or 500 pg HIV-1 per 1×10^6 cells as specified also for 2 h at 37°C at 5% CO_2. DC types and $CD4^+$ T cell controls were washed extensively in cold media to remove unbound virus prior to co-culture of DC with uninfected autologous $CD4^+$ T cells at a 1:10 ratio (10,000:100,000 per well) or culture of DC alone (10,000

per well) or T cells alone (100,000 per well) and media, for a total volume of 200 µl/well in round-bottomed 96 well plates. DC types all had comparable % viability, as determined by trypan blue dye exclusion.

3.1.16.3 Intracellular HIV-1 core antigen staining and flow cytometry

For cis- and trans-infections, each culture condition was set-up in triplicate, and cells harvested from individual wells were combined for ICS core Ag detection and flow cytometry. Briefly, cells were harvested at d 6 and d 8 and surface stained with Aqua Live/Dead® Fixable Dead Cell Stain (Molecular Probes, Life Technologies) followed by anti-CD3-APC mAb (BD Pharmingen), permeabilized with FACS™ Permeabilizing Solution 2 (BD Biosciences) and ICS with Coulter Clone KC-57-FITC (Beckman Coulter, Fullerton, CA), a mAb with broad specificity for the 55 kD precursor protein, the 39 and 33 kD intermediates, and 24 kD HIV-1 core Ag protein, prior to fixation with 2% PFA, and flow cytometric analysis.

3.1.17 Statistics

Quantitative IMARIS data were analyzed using one way ANOVA or unpaired student t tests (with Welch's correction for unequal standard deviation (SD), when necessary), and significance determined at α of 0.05. Data are represented as mean ± SD, as specified. For experimental data generated by exposing DC types to CD40L ± IL-4, IL-10, or IFN-γ, or DC1 + CD40L + blocking agents (simvastatin or latrunculin A), the percentage of reticulation positive cells ± standard error (SE) is from 1 representative of 3 donors tested (>50 cells assessed/condition), and statistical significance was determined using Fisher's exact test. This method was also used to assess percentage reticulation+ DC1 and DC2 generated from monocytes of HIV-1^+ PR and NP, and

results similarly reflect one representative of 3 donors tested. YG^+ versus YG^- recipient DC conditions in the Ag transfer studies reflect 2 independent experiments that are represented as mean ± SE; statistical comparisons were performed using unpaired student t tests. Statistical significance of DC1 vs. DC2 HIV-1 trans-infection was calculated for 3 independent donors using an unpaired t test ± SE, as specified.

4.0 RESULTS

4.1 AIM 1

Identify and quantitatively characterize a novel aspect of CD40L-mediated $CD4^+$ T cell help, the induction of TNT networks, in DC programmed by mediators of type-1 immunity.

4.1.1 Aim 1a. Interaction with $CD4^+$ T cells induces membrane extensions in DC1

Autologous monocyte-derived human DC were used as Ag presenting cells to stimulate $CD4^+$ and $CD8^+$ T cell subsets to study the in vitro T cell activation potential of differentially polarized mature DC. Our method for generating mature DC1 utilized the previously described αDC1 cocktail, consisting of poly(I:C), TNF-α, IL-1β, IFN-α, and IFN-γ [8]. These DC1 were characterized by expression of CD83, $CD86^{high}$, and CCR7, and their enhanced IL-12p70 production capacity when subsequently exposed to CD40L (Figure 4A). In contrast, DC2 were generated using a previously described cytokine cocktail consisting of IL-1β, TNF-α, IL-6 and PGE_2 [12], and characterized by their surface expression of CD83, $CD86^{high}$, CCR7, and OX40L, and their diminished capacity to produce IL-12p70 (Figure 4A). Using standard bright field microscopy, we observed that DC1, but not DC2, developed TNT-like membrane extensions when co-cultured for 24 h with $CD4^+$ T cells in the presence of the Ag surrogate, SEB (Figure

4B). Importantly, the formation of these membrane bridges required the presence of Ag as well as $CD4^+$ T cells, and did not occur in co-cultures containing $CD8^+$ T cells (data not shown (d.n.s.)).

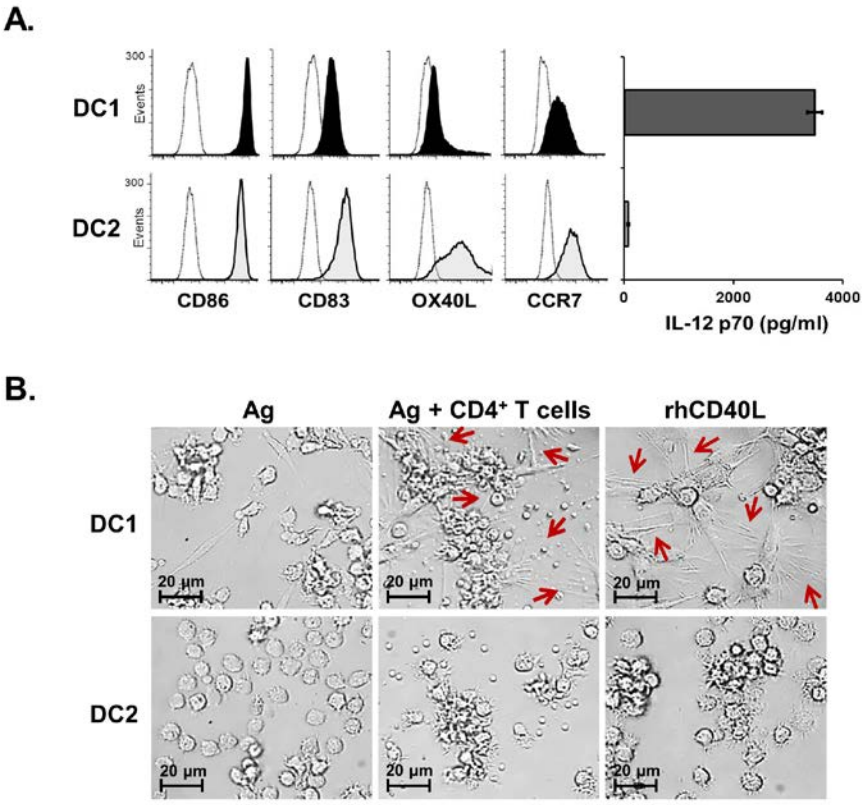

$CD4^+$ Th cells induce TNT-like networks upon co-culture with Ag-bearing DC1, but not DC2. (A) DC1 and DC2 were harvested and analyzed by flow cytometry for the following cell surface markers: CD83, CD86, CCR7, and OX40L (left panel). IL-12p70 production of DC1 and DC2 in response to secondary rhCD40L stimulation was determined by MSD electrochemiluminescence (right panel). (B) Bright field images (400X) of mature DC1 or DC2 co-cultured in the presence of SEB alone (left panels) or with $CD4^+$ T cells (middle panels), or rhCD40L (right panels) for 24 h. Red arrows highlight TNT-like extensions displayed by the Ag-loaded DC1 cultured with $CD4^+$ T cells or DC1 cultured with rhCD40L.

Figure 4. $CD4^+$ T cells induce TNT-like connections in Ag-loaded DC1, but not DC2.

4.1.2 Aim 1b. The induction of TNT-like protrusions in DC1 is CD40L-dependent

We next sought to determine why these morphological changes were unique to DC1 co-cultured with $CD4^+$ T cells, but not $CD8^+$ T cells. We investigated the role of the DC-activating molecule CD40L in our system since its expression is rapidly induced on $CD4^+$ T cells, but not $CD8^+$ T cells, upon Ag-specific activation [8]. When anti-CD40L blocking mAb was added to 24 h DC1-$CD4^+$ T cell co-cultures, the formation of the membrane extensions was inhibited (Figure 5A). Furthermore, CD40L expression on the $CD4^+$ T cells was demonstrated by their stimulation with anti-CD3/CD28 activating beads (Figure 5B, left). Moreover, both DC1 and DC2 comparably expressed the ligand's receptor CD40 (Figure 5B, right), eliminating the possibility that the differences of DC1 and DC2 to CD40L were related to differential receptor expression. To test whether this effect on DC1 was CD40L-dependent and could occur independently from other T cell-derived factors, differentially activated DC were exposed to either a J558-CD40L cell line or the control CD40L-deficient J558 cells. When stimulated with the J558-CD40L cells, DC1 developed membrane protrusions similar to those induced by the $CD4^+$ T cells (Figure 5C). However, this did not occur with exposure to the CD40L-negative J558 control cells (Figure 5C); and once again, DC2 failed to develop these formations (d.n.s). We also tested the direct effect of adding rhCD40L to DC types (Figure 4B), which induced a similar network of TNT-like membrane processes in DC1, but not DC2, in up to 25 donors tested. Together, these data definitively show that the Th cell factor CD40L is an inducer of the described morphological alterations occurring exclusively in DC1.

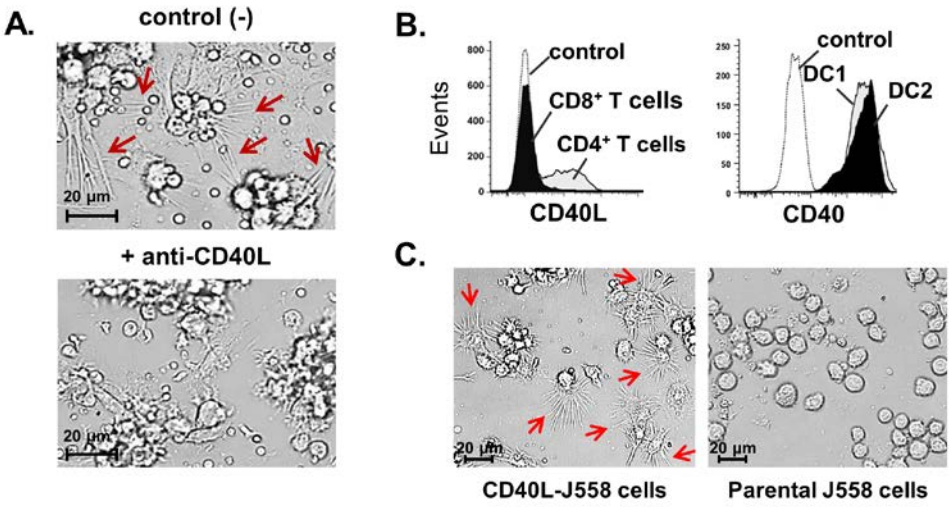

(A) 24 h co-cultures of SEB Ag-presenting DC1 and $CD4^+$ T cells in the presence of control mAb (top) or CD40L blocking mAb (bottom). (B) Flow cytometric analysis showing the differential surface expression of CD40L on 24 h CD3/CD28-activated $CD4^+$ and $CD8^+$ T cells (left panel), and comparable surface expression of the receptor CD40 on DC1 and DC2 (right panel). (C) DC1 co-cultured with either a J558-CD40L cell line (left panel) or the control parental CD40L-deficient J558 cell line (right panel) for 20 h and analyzed by bright field microscopy (400X) for the presence of induced TNT-like protrusions (red arrows). (A-C) Data are representative of 6 independent experiments using cells from 3 healthy donors.

Figure 5. $CD4^+$ T cell-associated CD40L induces networks of TNT-like extensions in DC1.

4.1.3 Aim 1c. CD40L-induced TNT networks dramatically enhance the surface area and reach of DC1 compared to DC2

Live-cell confocal fluorescence microscopy revealed that DC1 develop extensive networks of TNT-like processes in response to CD40 ligation (Figure 6A), which we termed 'reticulation', and we next used IMARIS 3D imaging analysis software to quantitate the morphological changes observed in the DC types (Figure 6B). This evaluation showed that the total cell surface area was dramatically increased in CD40L-activated DC1 compared to resting DC1, and to a lesser degree in DC2 upon activation (Figure 6C). Importantly, a highly significant difference in surface area was shown between DC1 and DC2 following rhCD40L treatment (Figure 6C).

In their resting state, we found that 27.2% of DC1 already displayed ≥ 5 long, ultrafine, non-branching TNTs similar to those previously described in iDC [55], while only 2.4% of resting DC2 displayed multiple TNTs (Figure 6D). CD40L-activated DC1 displayed a substantial increase in TNT-like extensions, which varied widely in length, diameter, and complexity, established multiple linkages between neighboring cells, and were occasionally detected above the substratum. In contrast, CD40L-activated DC2 were typically smaller and more rounded than DC1, and displayed membrane ruffling as opposed to TNT-like extensions.

For analysis of the more complex membrane formations, we characterized each 'filament' (Figure 6B, middle panel), defined as a group of connected dendrite- and TNT-like segments that branched from a single origin point at the edge of the cell body. The analysis showed that 100% of CD40L-activated DC1 displayed a reticulate membrane morphology (≥5 filaments per cell), compared to 16.7% of CD40L-activated DC2 (Figure 6E). Furthermore, CD40L-induced membrane extensions dramatically extended the spatial reach of DC1 compared to DC2 (Figure 6F), as determined by measuring the shortest distance from the origin point to the

distal terminal point of each filament (Figure 6B, right panel). Among the reticulation+ cells, filaments expressed by DC2 tended to be lesser in number, shorter in length, and displayed less complexity of branching than that of DC1 (Figure 6G-6J).

A previous study of the molecular mechanisms of TNT formation demonstrated that assembly of the multi-molecular complex composed of M-Sec, RalA, and the exocyst complex is orchestrated by the transmembrane scaffold protein, LST1, which was found to be highly expressed on myeloid lineage cells [44]. We therefore investigated LST-1 gene expression levels from representative DC1 and DC2 using a genome-wide transcriptional profiling approach. In support of the imaging-based approach to TNT quantitation in DC1 and DC2, the VST-normalized mRNA expression levels showed equal or greater expression of LST-1 variants in DC1 vs. DC2, with 2 of the 4 variants being expressed more than 10-fold higher by DC1 (Figure 7).

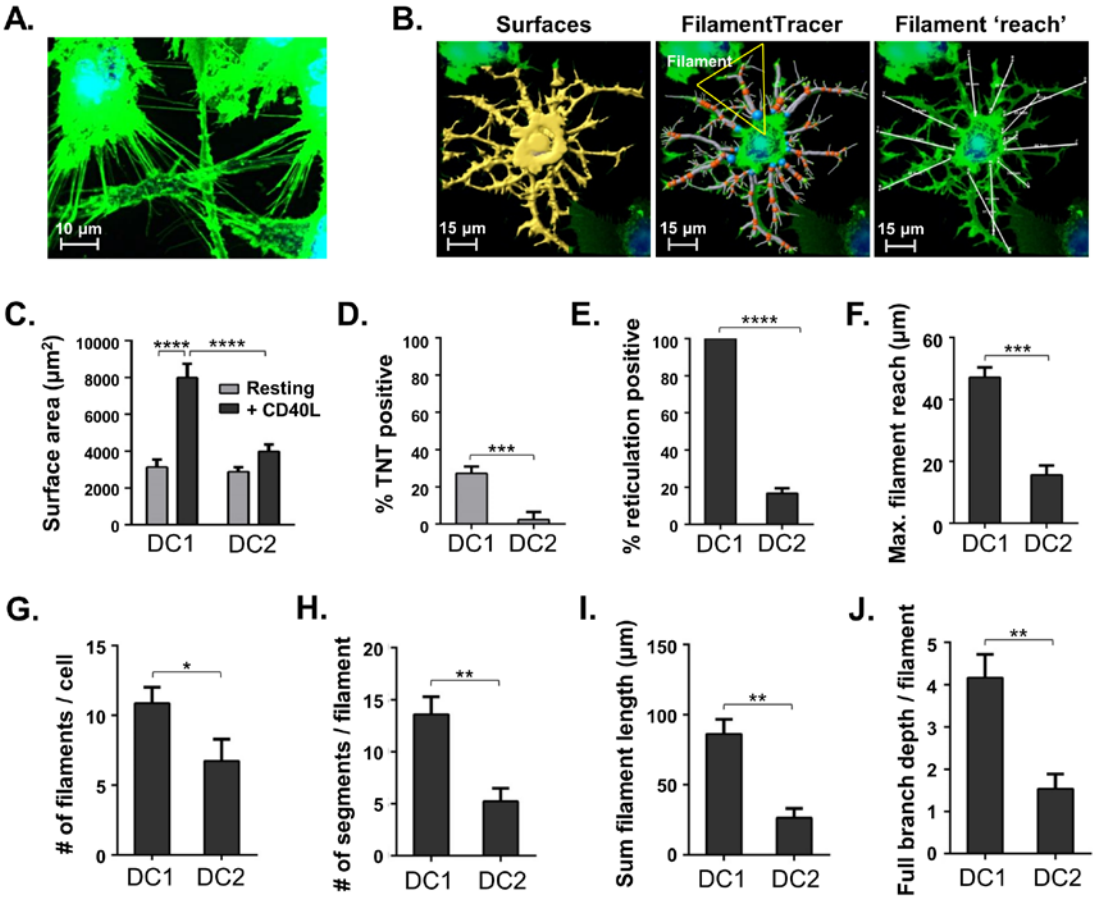

(A) Representative Z-series projection image revealing a network of TNT-like membrane connections in fluorescently labeled DC1. (B) Representative Z-series projection images of a CD40L-activated DC1 analyzed using the IMARIS 'Surfaces' program to determine total cell surface area (left panel), and IMARIS 'FilamentTracer' to trace the pathway of each 'filament' branch extending from a single origin (blue spheres) at the edge of the cell body (middle panel). Individual segments begin at an origin or branch point (orange spheres) and end at the next branch or terminal point (green spheres). Spatial 'reach' was defined as the shortest distance from a filament origin to the distal terminal point of that filament (right panel; white lines connecting 2 points). (C) Total cell surface area comparisons of resting and CD40L-activated DC1 and DC2. (D) Comparison of percentage 'TNT+' resting DC1 and DC2 (media only), defined as those expressing ≥ 5 individual TNTs per cell that were each > 5.0 µm in length. (E) Comparison of percentage 'reticulation+' CD40L-activated DC1 and DC2, delineated as those displaying ≥ 5 filaments per cell that were each > 10.0 µm in sum segment length. (F) 'Maximum reach' of filaments, defined as the shortest distance (µm) from the origin to the farthest terminal point of a filament. (G) Graphical depiction of the mean number of filaments per cell in reticulation+ DC1 compared to DC2. (H) Graph of the mean number of segments per filament in individual reticulating DC1 versus DC2. (I) Mean filament length per cell, defined as the sum length (µm) of its segments, graphically depicted in reticulating DC1 compared to DC2. (J) Graph of the mean full branch depth of filaments per cell, delineated as the maximum number of bifurcations from the origin point to a terminal point in an individual filament, in reticulation+ DC1 versus DC2. (C-J) Data were generated from randomly chosen image fields (20-30 per donor) and represented as mean ± SD of 3 healthy donors independently tested. P-values < 0.0001, < 0.001, < 0.01 and < 0.05 are represented by ****, ***, **, and *, respectively. (F-J) Complex membrane filaments, displayed by 100% of individual CD40L-activated DC1 and 16.7% of DC2, were analyzed using IMARIS.

Figure 6. CD40L-induced TNT networks greatly increase surface area and reach of DC1.

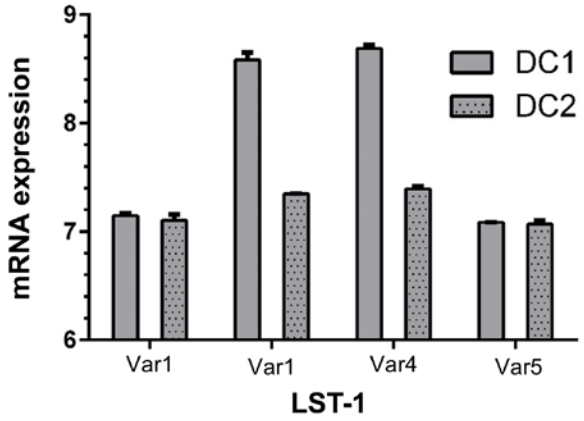

Representative DC1 and DC2 were generated using αDC1 or PGE_2-based cocktails, respectively and mRNA extracted for direct hybridization using the Ilumina HumanT-12 Expression BeadChip Kit, which contains > 47,000 probes corresponding to roughly 35,000 genes. Analysis was conducted using Genome Studio software, and data were additionally VST-transformed to obtain normalized mRNA expression levels. Importantly, a 1 unit difference (i.e. 7.0 to 8.0) represents nearly a 10-fold difference in gene expression. LST-1 expression levels were greater than 10-fold higher on DC1 compared on DC2 for 2 of the 4 LST-1 variants. The graphs represent 2 replicate samples ± SE.

Figure 7. LST-1 mRNA expression levels are higher in DC1 than DC2.

4.1.4 Aim 1d. CD40L-induced reticulation is a general characteristic of DC1

We were curious whether the CD40L-induced TNT networks was related to the particular cocktail(s) of activation factors used in our initial experiments, or if this was in fact a general characteristic of DC1. While a variety of pathogen- or host-derived signals can induce DC maturation, the presence of either IFN-γ or PGE_2 during the maturation process is particularly important for driving differential DC polarization [2, 9, 12, 14, 124]. To further explore the role of these key polarization factors in priming DC for reticulation, we tested the CD40L effect using alternative methods for generating DC0, DC1, and DC2 from iDC precursors utilizing different TLR agonists, such as LPS (TLR4) or R848 (TLR7/8) alone, or in combination with IFN-γ or PGE_2, respectively [12, 125, 126]. DC1 generated using these alternative methods not only produce high levels of IL-12p70 in response to secondary CD40L stimulation (Figure 8), but they also formed extensive TNT networks, while DC2 failed to do so, and non-polarized DC0 displayed an intermediate morphology (Figure 9A-9B). Additionally, we tested other previously published cellular methods to induce DC1, using either activated NK cells [9] or Ag-stimulated $CD8^+$ T cells [14, 93]. As was found with the other DC1 types, both NK cell- as well as $CD8^+$ T cell-induced DC1 responded to secondary CD40L stimulation by forming networks of TNTs (Figure 9C). Together, these data highlight that reticulation is indeed a characteristic trait of DC matured under type-1 inflammatory conditions, while PGE_2-exposed DC2 are refractory to the reticulation process.

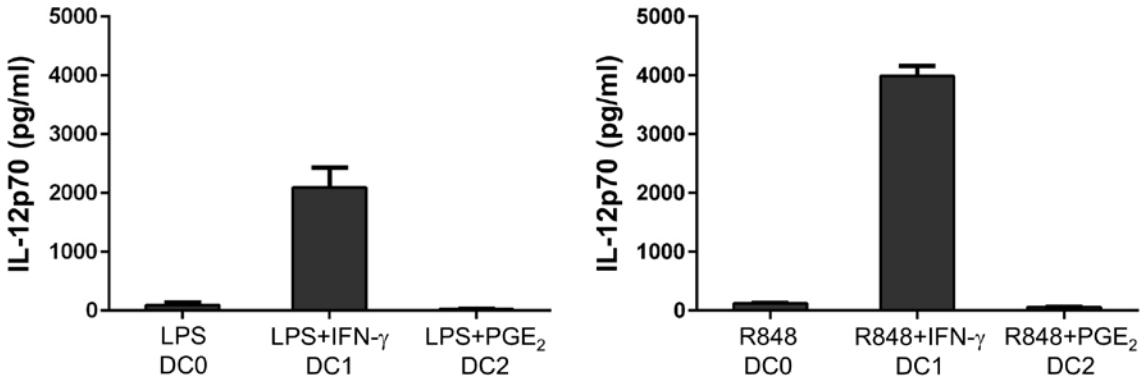

Differentially polarized DC0, DC1, or DC2 were generated using LPS- or R848-based maturation cocktails. Similar to the previously described methods, LPS-programmed DC (left) and R848-programmed DC types (right) were stimulated with rhCD40L for 24 h and IL-12 production was measured by IL-12p70 ELISA. Data are represented as the mean pg/ml ± SE of 2 duplicate experiments from one representative of 3 donors independently tested.

Figure 8. DC1 generated by alternative methods produce high levels of IL-12p70 in response to CD40L.

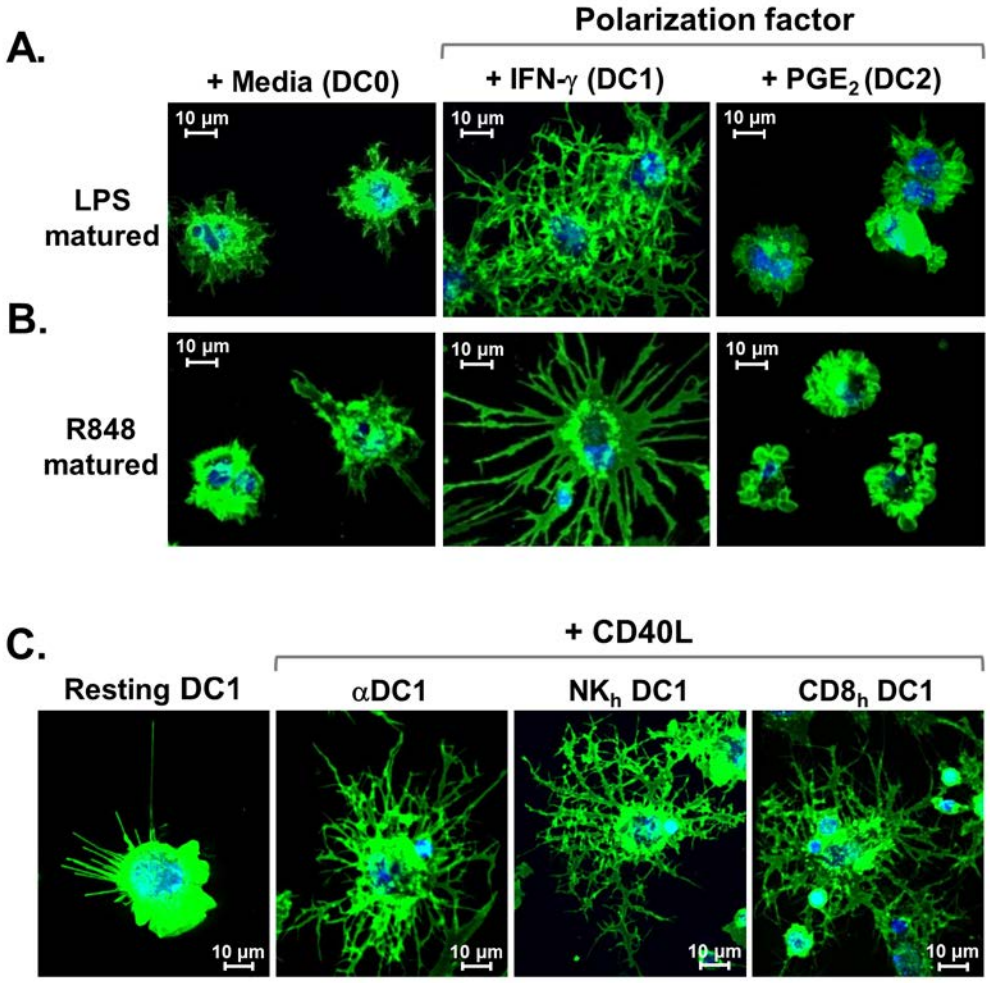

(A-C) 3D reconstruction images (600X) of differentially matured DC stimulated for 20 h with rhCD40L prior to labeling the cell surface with MHC class I mAb (green) and labeling nuclei (blue), followed by live-cell confocal imaging. Data are representative of 6 independent experiments conducted using DC from 3 healthy donors. (A) Membrane morphologies of mature CD40L-activated DC0, DC1, and DC2 propagated using LPS alone, LPS + IFN-γ, or LPS + PGE_2, respectively. (B) Mature CD40L-treated DC0, DC1, and DC2 generated by the respective use of R848 alone, R848 + IFN-γ, or R848 + PGE_2. (C) Cell morphologies of DC1 treated with media alone or CD40L. DC1 were generated using the αDC1 cytokine-based cocktail (first two panels on left), or induced by 48 h co-culture of iDC with either 2-signal activated NKh cells (middle) or SEB-activated $CD8^+$ T cells (right).

Figure 9. CD40L-induced reticulation is a trait of DC matured by type-1 inflammatory mediators.

4.1.5 Permissions

Figures 4-6 and 9 were originally published in *The Journal of Immunology*. Zaccard CR, Watkins SC, Kalinski P, Fecek RJ, Yates AL, Salter RD, Ayyavoo V, Rinaldo CR, Mailliard RB. 2015. CD40L Induces Functional Tunneling Nanotube Networks Exclusively in Dendritic Cells Programmed by Mediators of Type 1 Immunity. J. Immunol. Feb 194(3):1047-1056; published ahead of print December 29, 2014, doi:10.4049/jimmunol.1401832. Copyright © [2015] The American Association of Immunologists, Inc.

4.2 AIM 2

Investigate the role of polarized Th cell cytokines in the regulation of DC reticulation, and demonstrate that this process provides a functional pathway for Ag exchange between interconnected DC1.

4.2.1 Aim 2a. Opposing roles of IFN-γ and IL-4 in regulating CD40L-inducible reticulation

We demonstrated quantitatively that CD40L-induced reticulation was dose-dependent, with significantly higher percentages of reticulation+ cells detected in both DC0 and DC1 compared to the media only controls, using concentrations as low as 0.05 μg/ml (Figure 10A-10B). In accordance with live-cell imaging data, DC1 displayed a dramatically enhanced ability, while DC0 demonstrated an intermediate propensity to form TNTs. Pre-programmed DC1 can be generated from iDC by treatment with maturation factor(s) in combination with IFN-γ, but concomitant activation of mature non-polarized DC0 with IFN-γ and CD40L can also induce high IL-12 production, similar to that of DC1 treated with CD40L alone [14, 121]. We speculated that IFN-γ might act in an analogous fashion, along with CD40L, as a co-stimulator of the reticulation process in DC0. Therefore, we tested the co-stimulatory effect of this Th1-associated cytokine, as well as the respective Th2- and regulatory T cell-associated cytokines, IL-4 and IL-10 [3], on reticulation in TNF-α-matured DC0. We found that, in addition to augmented IL-12p70 production (d.n.s.), IFN-γ co-stimulation enhanced the ability of DC0 to reticulate in response to CD40L (Figure 10A). Intriguingly, co-exposure of DC0 to CD40L and

IL-4 substantially reduced the percentage of reticulation+ cells, while IL-10 had no significant impact on reticulation (Figure 10A). We next investigated the effect of these differential Th cell-associated cytokines on CD40L-induced reticulation in pre-programmed DC1, and revealed an even more substantial inhibitory effect of IL-4 on this process (Figure 10B). Again, the addition of IL-10 had no significant impact on the ability of DC1 to reticulate. Taken together, these data indicate opposing roles for the Th1 cytokine, IFN-γ, and the Th2 cytokine, IL-4, in regulating the CD40L-inducible process of reticulation.

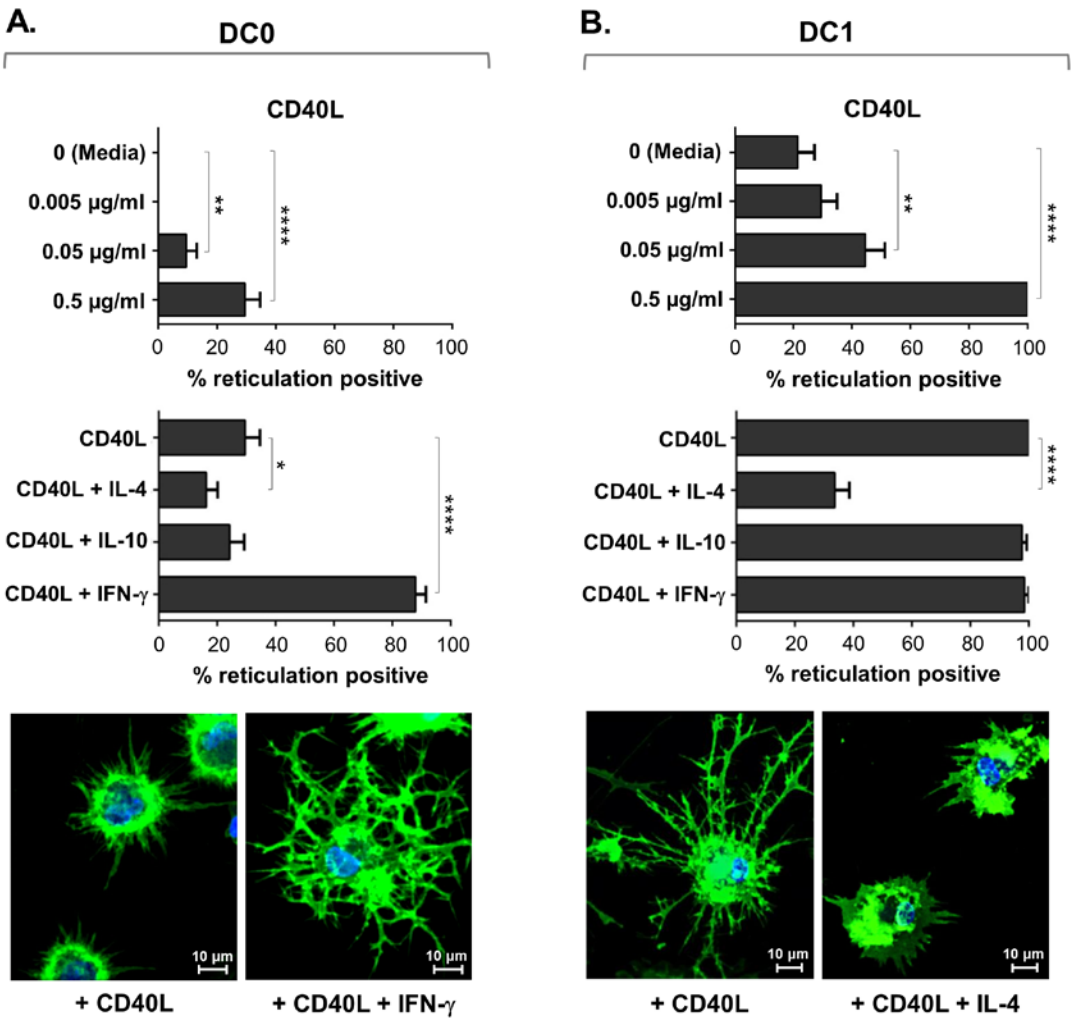

(A) Graphical display of the percentage of reticulation+ TNF-α-matured DC0 after 20 h exposure to varying doses of rhCD40L alone (top left), or in combination with IL-4, IL-10, or IFN-γ (middle left). Also shown are representative confocal images (600X) of DC0 stimulated with rhCD40L alone or in combination with IFN-γ and then surface labeled with MHC class I-specific mAb (green) and nuclear labeled (blue) (lower left). (B) Graphical depiction of percentage reticulation+ αDC1 after 20 h exposure to varying doses of rhCD40L alone (upper right), or combined with IL-4, IL-10, or IFN-γ (middle right). Additionally shown are representative confocal images (600X) of DC1 stimulated with rhCD40L alone or in combination with IL-4 (lower right). (A-B) Quantitative data, displayed as percentage positive ± SE, are representative of 3 healthy donors independently tested twice per donor.

Figure 10. Reticulation is enhanced by the Th1 cytokine IFN-γ, and inhibited by Th2-associated IL-4.

4.2.2 Aim 2b. IFN-γ dependent reticulation of blood-isolated DC in response to CD40L

The method of generating DC from monocytes in vitro allows for sufficient cell numbers to be obtained for research studies and clinical applications [1], and represents an established model for migratory DC that arise in vivo from the differentiation of monocyte precursors [22, 127]. Nevertheless, we were interested to see if DC isolated directly from human peripheral blood could be induced to form TNT networks by CD40L in an IFN-γ-dependent manner, analogous to the behavior of monocyte-derived DC. $CD1c^+$ $HLA\text{-}DR^+$ myeloid DC were isolated from fresh PBMC by magnetic bead enrichment and matured with TNF-α for 24 h prior to treatment with media, rhCD40L, or IFN-γ + rhCD40L, followed by live-cell confocal imaging. Although low cell numbers limited the scope of these experiments, we established that concomitant exposure of TNF-α-matured, myeloid DC to the Th1 cytokine IFN-γ enhanced the formation of networks of ultrafine TNTs in response to CD40L (Figure 11). TNTs observed in peripheral blood DC tended to be thin and non-branching, as opposed to the complex structures observed in monocyte-derived DC, but these structures established multiple intercellular connections and were frequently detected above the substratum, similar to those observed in monocyte-derived DC1.

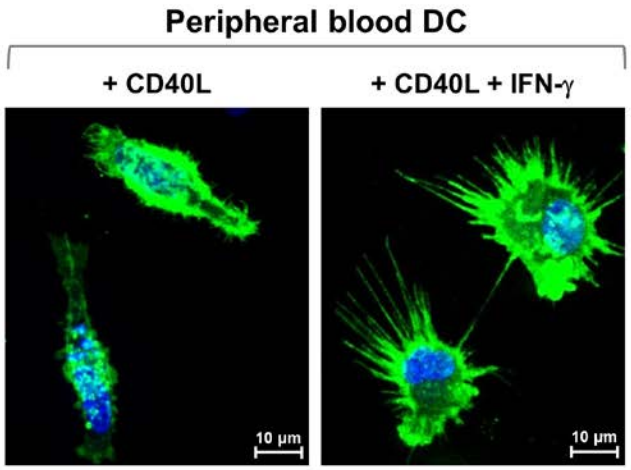

Z plane reconstruction image (1000X) of TNF-α-treated, human peripheral blood-isolated myeloid DC (lineage-, HLA-DR+ and CD1c+) following 20 h activation with rhCD40L alone or in combination with IFN-γ. Confocal mages are representative of 3 healthy donors independently tested.

Figure 11. IFN-γ-dependent reticulation of peripheral blood-isolated DC in response to CD40L.

4.2.3 Aim 2c. Reticulation supports the direct transfer of cellular contents between DC1

TNTs described in the current literature can establish both membrane and cytoplasm continuity between connected cells, which in turn provides a pathway for direct intercellular communication [35]. Indeed, TNTs facilitate the direct exchange of organelles and both cytoplasmic and membrane-associated components [35, 58]. We therefore speculated that the reticulation process allows for efficient transfer of cellular contents between proximal and remote DC1. We first used high resolution DIC imaging to capture the formation of the TNT-like networks over time, and to search for visual evidence of the trafficking of cellular content between live DC via CD40L-induced TNTs. In doing so, we were able to clearly observe the dynamic immune process of reticulation, whereby DC actively formed numerous membrane extensions within hours of exposure to rhCD40L, ultimately establishing a network of interconnected processes between proximal and remote DC (Figure 12A). Live-cell imaging demonstrated both the 'filopodia extension' and 'diverging cells' model of TNT development, although the filopodia extension mechanism appeared to predominate. Intriguingly, when DC1 and DC2 were differentially labeled and imaged over time in the presence of CD40L, DC1 became integrated into a vast intercellular network that inhibited their mobility, but they continued to interact with adjacent cells via dynamic membrane extensions. On the other hand, DC2 rapidly migrated around the DC1 networks, and exhibited rapidly probing into the DC1 network via shorter membrane protrusions (d.n.s.).

In addition to capturing the development of TNT networks in DC1 over time, DIC imaging revealed a number of endogenous vesicles could be seen traveling rapidly from one cell to another through these structures (Figure 12B). We hypothesized that the membrane conduits facilitate direct DC-DC transfer of vesicles such as endosomes, which has been shown in other

cell types [38, 57]. To address this possibility, we fixed CD40L-stimulated DC1 and stained them with EEA1-specific mAb and Rh-Phalloidin for labeling endosomes and F-actin-based TNTs, respectively. Early endosome localization within CD40L-induced TNTs (Figure 12C) was clearly detected by confocal microscopy, despite the disruption of the majority of fine membrane extensions by the fixation and staining process. These data indicate that DC1 can utilize the process of reticulation to exchange vesicular cargoes between interconnected cells.

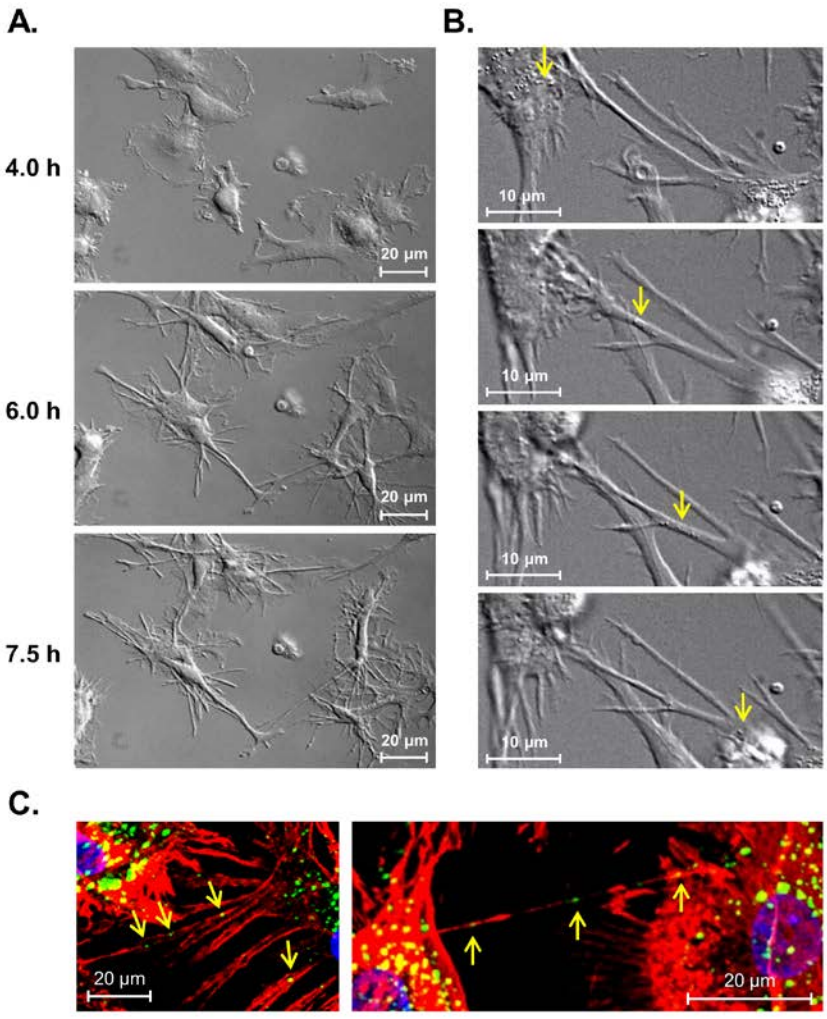

A) Sequential still frames of DC1 actively reticulating from 4 to 7.6 h post-addition of rhCD40L, captured by live-cell, time-lapse DIC imaging (600X). (B) Sequential frames of high resolution, time-lapse DIC imaging (600X) of live 8 h rhCD40L-stimulated DC1 showing endogenous vesicles (arrows) trafficking between neighboring cells through CD40L-induced TNTs. (C) Confocal reconstruction images (1000X) revealing early endosome- (green, arrows) and F-actin-containing TNTs (red) and nuclei (blue) in fixed CD40L-activated DC1. Data are representative of 3 donors independently tested.

Figure 12. Reticulation supports direct trafficking of endogenous components between DC.

4.2.4 Aim 2d. DC1 Reticulation facilitates functional exchange of exogenous antigens

4.2.4.1 Inducible TNT networks facilitate the direct exchange of beads between DC1

In order to test if exogenous material could also be acquired and subsequently exchanged between DC1 by the same mechanism, we pulsed iDC with YG-labeled nano-beads representing Ag or media alone, and added maturation factors to generate DC1. Bead-containing 'donor' DC1 and bead deficient 'recipient' DC1 were labeled with Cy5 and Cy3, respectively, and co-cultured the DC for 20 h in the presence or absence of rhCD40L. Using time-lapse confocal imaging of live cells, beads were observed localizing to TNTs of donor DC1, and rapidly traversing the length of these structures (Figure 13A). Furthermore, the pathway of individual beads could be traced as they traveled through blue donor DC1 membrane extensions into the recipient cell, where they finally collected in the cell body (Figure 13B). In addition to the transfer of cytoplasmic beads, we also frequently observed the bidirectional transfer of Cy3- or Cy5-labeled membrane patches to differentially labeled DC1 via TNTs (d.n.s), as has been observed in other immune cell types [68].

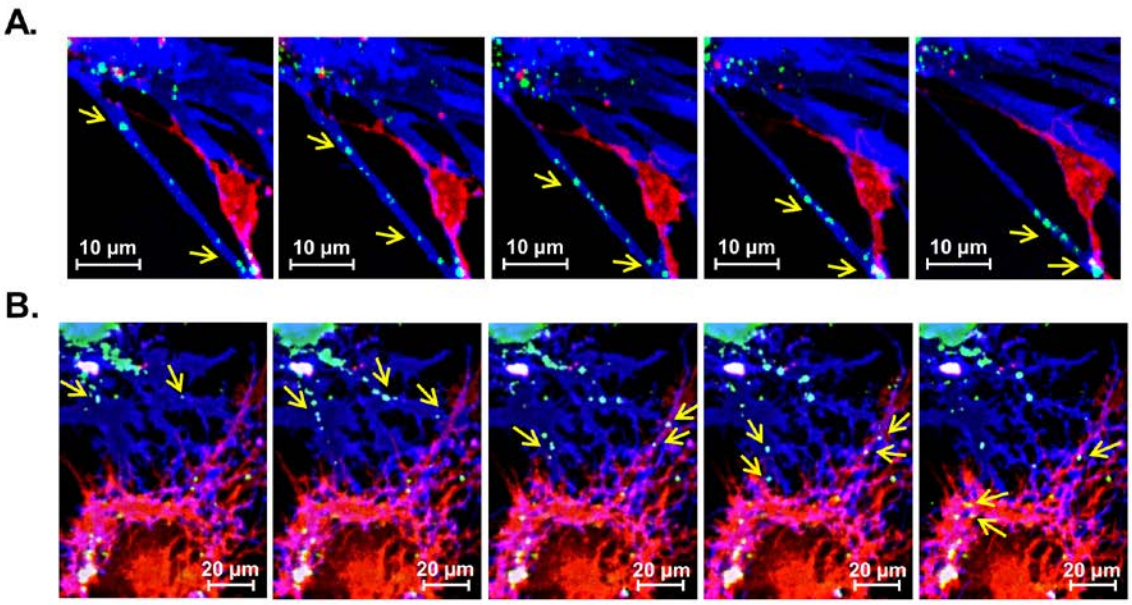

(A-B) Cy5-labeled (blue), YG latex bead (40 nm)-containing donor DC1 were co-cultured with the non-bead-containing, Cy3-labeled (red) recipient DC1 for 20 h in the presence or absence of rhCD40L. Data are representative of 2 donors independently tested. (A) Montage of time-lapse, confocal imaging (600X) showing beads (green; arrows) moving rapidly through donor DC1 TNTs (blue) over a time span of 28 min. (B) Montage tracing the pathway of beads (green; arrows) traveling from the cell body of donor DC1 (blue), through donor cell TNTs and into the connected recipient DC (red), where they finally collect in the recipient cell body.

Figure 13. CD40L-induced reticulation facilitates the intercellular transfer of exogenous Ag.

4.2.4.2 Antigen exchange via the reticulation process induces specific T cell responses

In parallel to, and in support of the live-cell imaging studies, bead transfer between CD40L-activated DC1 or DC2 was quantified by flow cytometry. Immature DC were again pulsed with YG-beads and matured to achieve their DC1 or DC2 status, and Cy5-labeled donor DC types were co-cultured with respective bead-deficient recipient Cy3-labeled DC1 or DC2 for 20 h in the presence or absence of rhCD40L. The transfer of labeled beads from donors to recipients was enhanced in CD40L-activated DC1 compared to resting DC1, and in CD40L-activated DC1 compared to activated DC2 (Figure 14A). While a small fraction of DC2 recipients in the CD40L-activated conditions also acquired beads, the mean fluorescence intensity (MFI) of the bead-containing DC1 recipients was nearly 4 fold greater than that of the DC2 recipients, indicating a higher number of beads transferred to recipient DC1 on a per cell basis (Figure 14B).

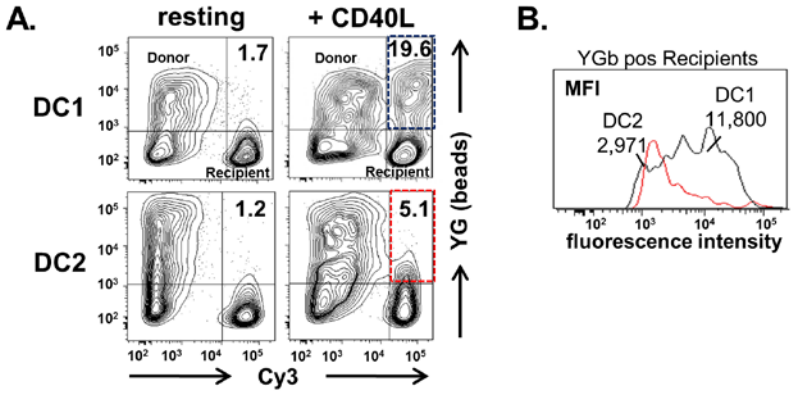

Cy5-labeled, YG latex bead (40 nm)-containing donor DC1 or DC2 were co-cultured with the respective non-bead-containing, Cy3-labeled recipient DC1 or DC2 for 20 h in the presence or absence of rhCD40L. (A) Subsequent flow cytometric analysis determined the percentage of bead positive recipients in resting and CD40L-exposed co-cultures (B) MFI of YGb positive recipient DC1 (black line) versus DC2 (red line) from the respective CD40L-treated conditions.

Figure 14. Reticulation facilitates the exchange of beads between interconnected DC1.

We next evaluated the ability of recipient DC1 to functionally utilize and present Ags acquired from donor DC1 following reticulation. Briefly, we pulsed iDC with a combination of CMV, VZV, and TT Ags in addition to YG nano-beads during their exposure to type-1 polarizing maturation factors to generate Ag- and bead-loaded donor DC1. These donor DC1 were co-cultured with Cy5-labeled recipient DC1 in the presence of rhCD40L for 20 h. Using the YG beads from donor DC1 as a marker for CD40L-induced intercellular exchange, two distinct populations of recipient DC1 (YG^+ and YG^-) were isolated by FACS sorting. The sorted YG^+ and YG^- recipient DC1 were assessed for their differential capacity to drive Ag-specific recall responses in autologous T cell using an established 10 d in vitro sensitization assay followed by an IFN-γ ELISPOT readout. Sorted YG^+ transfer recipient DC1 displayed an enhanced ability to drive Ag-specific T cell responses compared to YG^- DC1 (Figure 15A).

Conversely, recipient DC1 separated from reticulating donor DC1 using a trans-well system in parallel co-cultures failed to generate substantial Ag-specific T cell responses (Figure 15B), indicating that the functional transfer of Ag during the reticulation process was contact dependent.

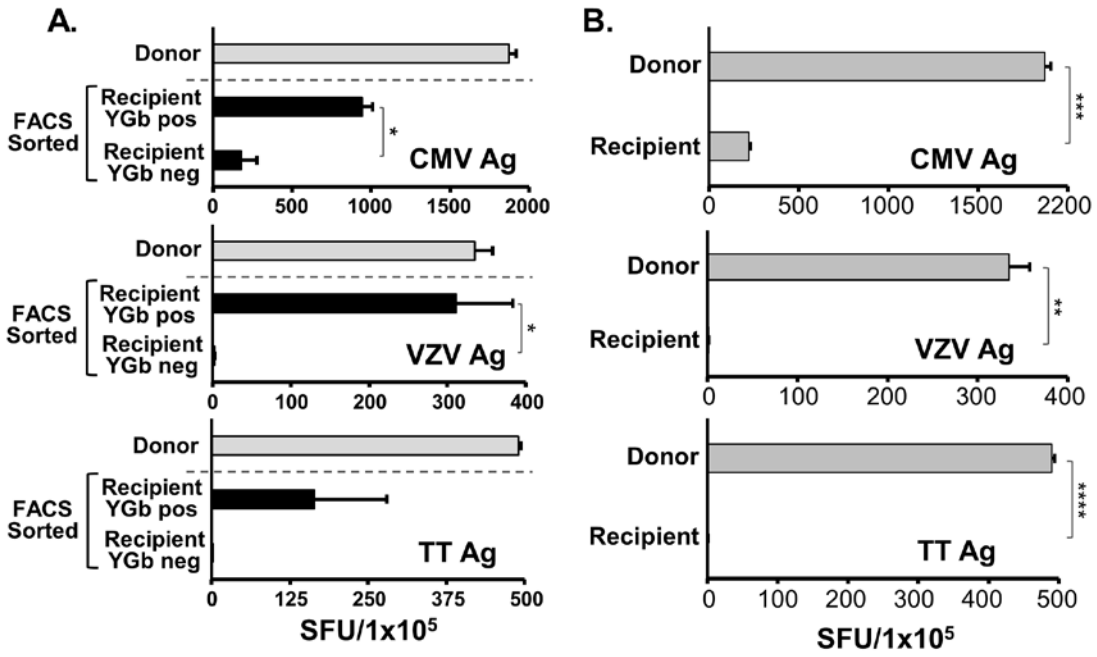

(A) IFN-γ ELISPOT assays measuring Ag-specific recall responses of cultured T cells following their in vitro sensitization with FACS sorted, YG bead/Ag positive and negative recipient DC1. Data are represented as mean ± SE of 2 independent experiments. (B) IFN-γ ELISPOT assays measuring Ag-specific recall responses of cultured T cells following their in vitro sensitization with YG bead- and Ag-containing donor DC1 or recipient DC1 separated from reticulating donor DC1 by a trans-well system. Data are represented as mean ± SD of 2 replicate experiments and p-values < 0.0001, < 0.001, < 0.01 and < 0.05 are represented by ****, ***, **, and *, respectively.

Figure 15. Reticulation facilitates Ag transfer from donor to recipient DC for induction of Ag-specific T cell responses by a contact dependent mechanism.

4.2.5 Aim 2e. DC reticulation facilitates intercellular trafficking of microbial pathogens

While the CD40L-mediated induction of TNT networks likely plays an important role in intercellular communication or Ag transfer between interconnected DC, current literature suggests that bacterial [57] as well as viral pathogens such as HIV-1 [35, 86, 88] can exploit TNTs for direct cell-to-cell transmission. We hypothesized that CD40L-induced reticulation in DC1 could similarly provide an efficient pathway for intercellular trafficking of microbes. In order to determine if direct cell-cell bacterial transfer can occur via CD40L-induced TNT networks, we first injected a suspension of live EGFP-expressing *E. coli* into DC1 cultures following their 10 h stimulation with rhCD40L. Time-lapse confocal resonance scanning was conducted 2 h later to capture the trafficking of live bacteria between DC1. Similar to what has been described in macrophages [57], this experimental strategy clearly revealed bacteria rapidly 'surfing' along the outside of TNT-like membrane bridges from one cell to another (Figure 16A). Notably, individual bacterium could simultaneously travel in opposite directions along the same TNT, as well as change directions in mid-transfer. CD40L-induced extensions were also observed capturing bacteria and drawing them toward the cell body for subsequent internalization (d.n.s.), similar to the veil-mediated capture of bacteria previously described in iDC [33]. These data reveal a mechanism by which CD40L-activated DC can use TNT-like extensions to probe for pathogens in tissues, or a pathway by which bacteria can spread from cell-cell over long distances, potentially facilitating their dissemination.

To confirm that DC reticulation could also support intercellular trafficking of viral pathogens, we pulsed Cy5-labeled DC1 with EGFP-expressing HIV-1-like particles and co-cultured these donor DC with Cy3-labeled recipient DC1. The DC co-cultures were then stimulated with rhCD40L for either 10 or 20 h prior to live-cell confocal microscopy. Maximum

intensity projection images revealed particle localization to TNTs of the reticulating donor cells that connected with recipient cell bodies at both 10 h (Figure 16B) and 20 h time points (Figure 16C). Furthermore, HIV-1-like particles were frequently detected at the interface between donor cell TNTs and recipients, prior to their transfer to recipient cell bodies, up to 24 h after the donor DC first acquired the particles (Figure 16C). Together, these findings demonstrate that the induction of DC reticulation by CD40L can facilitate rapid and direct spread of pathogens such as bacteria or HIV-1 between interconnected immune cells.

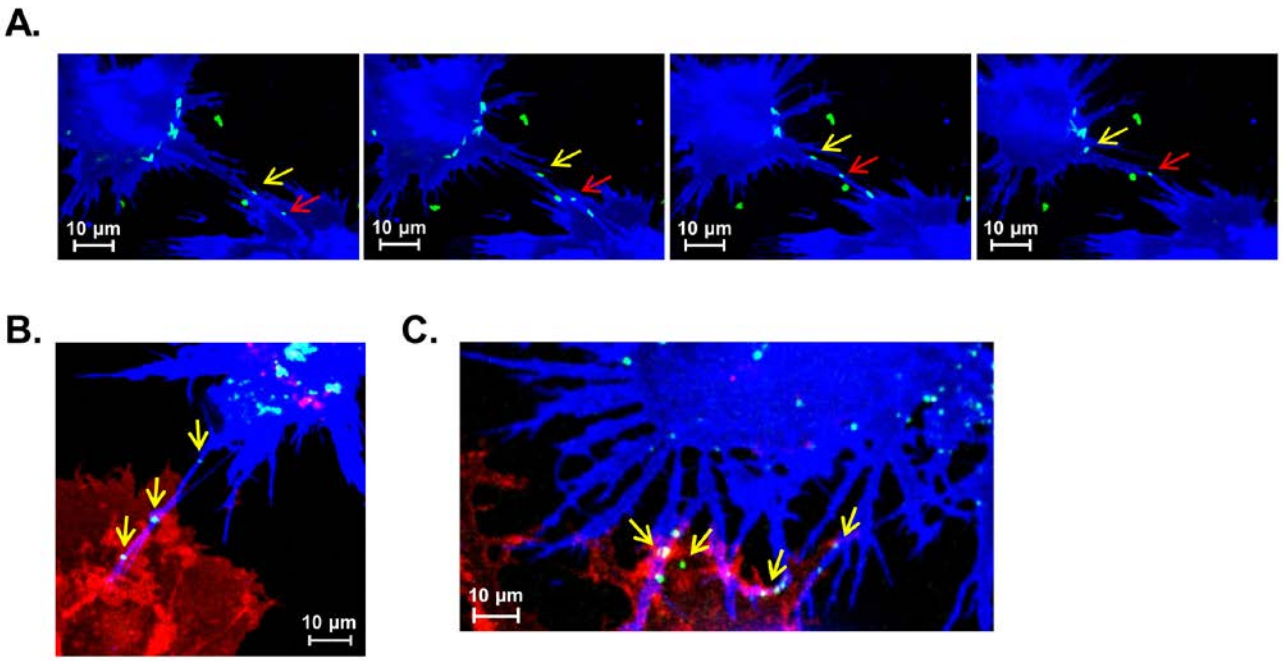

(A) DC1 monolayers that had been stimulated with rhCD40L for 10 h were exposed to EGFP-expressing *Escherichia coli* for 2 h. Subsequent time-lapse confocal resonant scanning microscopy shows individual bacterium (green) trafficking bi-directionally along CD40L-induced TNTs (arrows) between mature DC1. (B) Donor DC1 (blue) pulsed with EGFP-expressing HIV-1-like particles (green) were co-cultured with recipient DC1 (red) in the presence of CD40L for 10 h prior to live-cell imaging. HIV-1-like particles localizing to a donor cell TNT (arrows) that has formed a connection with a recipient cell body. (C) At 20 h post-CD40L stimulation, HIV-1-like particles could be detected at the interface between blue donor cell TNTs and red recipient cells (arrows), prior to their subsequent transfer to recipient cell bodies. (A-C) Imaging data are representative of 3 donors independently tested.

Figure 16. Pathogens can utilize inducible TNT networks for direct intercellular spread.

4.2.6 Permissions

Figures 10-16 were originally published in *The Journal of Immunology*. Zaccard CR, Watkins SC, Kalinski P, Fecek RJ, Yates AL, Salter RD, Ayyavoo V, Rinaldo CR, Mailliard RB. 2015. CD40L Induces Functional Tunneling Nanotube Networks Exclusively in Dendritic Cells Programmed by Mediators of Type 1 Immunity. J. Immunol. Feb 194(3):1047-1056; published ahead of print December 29, 2014, doi:10.4049/jimmunol.1401832.

4.3 AIM 3

Quantitatively assess the ability of mature differentially programmed DC to transmit HIV-1 to $CD4^+$ T cells in trans, and investigate the possible mechanisms of enhanced DC1-mediated transmission, including CD40L-inducible TNT networks.

4.3.1 Aim 3a. Differentially programmed DC display dramatically different HIV-1 trans-infection abilities

4.3.1.1 DC1 are superior conveyers of HIV-1 to $CD4^+$ T cells compared to DC2

We established previously that the interaction between CD40L-expressing $CD4^+$ Th cells and DC1 uniquely induces reticulation, which may facilitate migratory DC1 integration into the resident DC network in lymph nodes and support Ag or HIV-1 exchange between interconnected DC. We next investigated the possibility that HIV-1 can exploit this process for direct, high-speed transmission to its primary target, $CD4^+$ T cells. $CD4^+$ T cells were first isolated from frozen PBMCs, pre-activated for 2 d with PHA and IL-2, and high purity was determined by staining for the markers CD3, CD4, and CD8, followed by flow cytometry (Figure 17A). We then conducted a dose-response experiment of $CD4^+$ T cell cis-infection using R5 HIV-1 BaL. Supernatants were collected for HIV-1 core Ag ELISA and cells for ICS with a fluorescently-labeled HIV-1 core Ag mAb and flow cytometric analysis, which represents another established surrogate marker of infectious HIV-1 titer [115, 128-130]. The staining and gating strategy for the ICS core Ag and flow cytometric detection method is outlined in Figure 17B. For this and all subsequent cis- and trans-infections, each culture condition was set-up in triplicate, and cells harvested from individual wells were combined for ICS core Ag-based detection of HIV-1

infection. We found a correlation between HIV-1 core Ag ELISA and ICS core Ag detection methods at d 6 (Figure 18), and d 8 post-infection (d.n.s). Considering the power of single cell analysis offered by the flow cytometry-based assay, we chose this as our primary detection method in subsequent experiments. Furthermore, we henceforth show only the earliest time point at which cis- and trans-infection could be consistently detected (d 6), in order to minimize the possibility of de novo-produced virions from trans-infected $CD4^+$ T cells in turn cis-infecting more T cells, which would falsely inflate the percentage of trans-infected cells detected in these conditions.

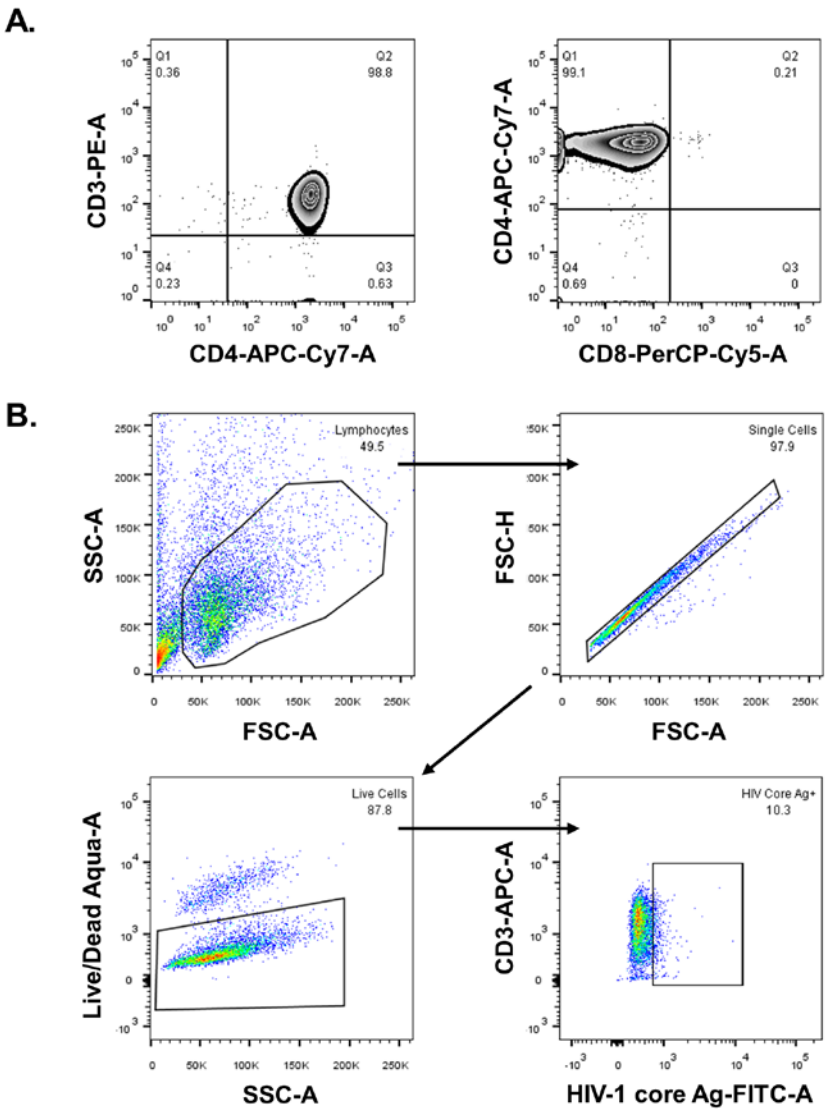

(A) Isolation of $CD4^+$ T cells by magnetic bead enrichment (negative selection) resulted in a highly pure population of $CD4^+$ T cells as determined by double staining for CD3/CD4 and CD4/CD8. (B) For determination of percentage HIV-1 core Ag+ $CD4^+$ T cells in both cis- and trans-infection experiments, the gating hierarchy is described above. The T cell marker CD3 was chosen over CD4 due to the well-known ability of HIV-1 Nef to down-regulate CD4 expression during infection [91], similar to a related study [115]. We observed a trend toward $CD3^{low}$ vs. $CD3^{high}$ in the HIV-1 core Ag+ cells, similar to that of CD4 (d.n.s.). Although not as well understood, down-regulation of CD3 by Nef has also been reported [91]. Considering also the high purity of pre-isolated $CD4^+$ T cells, we chose to include the $CD3^{low}$ population in our HIV-1 core Ag+ gate in both cis- and trans-infections.

Figure 17. $CD4^+$ T cell purity and gating strategy for detection of HIV-1 core Ag+ T cells.

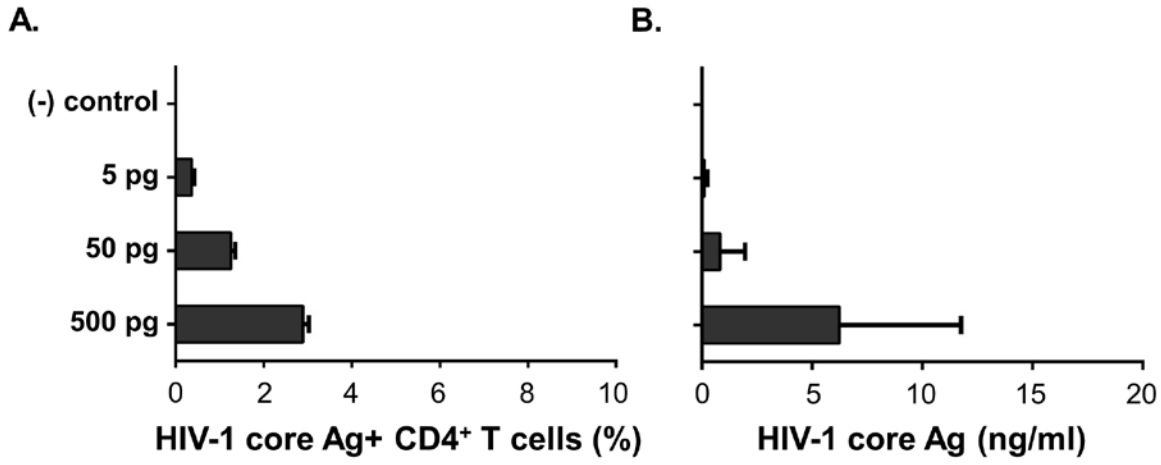

(A) $CD4^+$ T cells were exposed to media alone (- control), or cis infected with 5, 50, or 500 pg R5 BaL HIV-1 for detection of HIV-1 core Ag+ cells using a flow cytometry-based detection method, in which cells from triplicate experiments were combined for staining. (B) Concurrently, cell supernatants were harvested and analyzed for extracellular p24 content (ng/ml) in duplicate. Cells and supernatants were collected at d 6 post-infection. (A-B) High correlation was observed between the two surrogate methods of HIV-1 infectivity, validating the use of ICS/flow cytometry as the primary detection method in future experiments.

Figure 18. Dose response of $CD4^+$ T cell HIV-1 cis-infection using ICS- or ELISA-based core Ag detection methods.

We next assessed the ability of iDC and representative mature DC1 and DC2 generated using the αDC1 or PGE_2-based cytokine cocktails, respectively, to mediate transmission of 50 pg HIV-1 BaL to autologous pre-activated $CD4^+$ T cells using our established in vitro trans-infection model [93, 110, 119]. Briefly, DC types were exposed to specified amounts of HIV-1 in low volume media for 2 h at 37°C in 5% CO_2, and then washed extensively to remove unbound virus prior to co-culture with uninfected $CD4^+$ T cells at a 1:10 DC:T cell ratio. To control for possible cis-infection of HIV-1-exposed DC used in trans-infection experiments, the HIV-1-pulsed DC types were also cultured with media alone and supernatants harvested for HIV-1 core Ag ELISA on d 8. Extracellular core Ag was consistently below the lower limit of detection by ELISA in all DC conditions, including iDC, DC1, and DC2. In accordance with a previous study investigating differential transmission of HIV-1 by iDC and mature DC types [113], DC1 displayed an enhanced ability to infect autologous $CD4^+$ T cells in trans compared to DC2, while iDC possessed an intermediate trans-infecting ability (Figure 19).

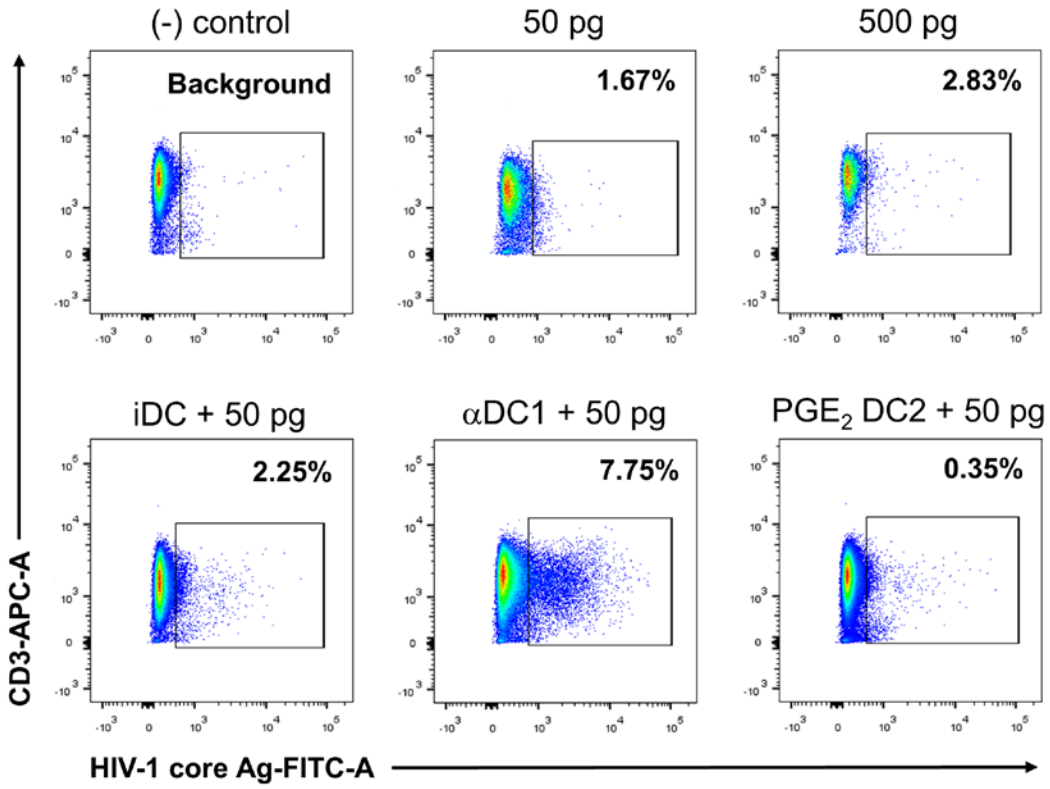

Immature DC and representative mature DC1 and DC2 generated using the αDC1 or PGE_2-based cytokine cocktails were exposed to 50 pg HIV-1 R5 BaL for 2 h and washed extensively prior to co-culture with autologous pre-activated $CD4^+$ T cells. Depicted above are the pseudo-colored dot plots generated from $CD4^+$ T cells harvested at d 6 and stained intracellularly with anti-HIV-1 core Ag mAb, followed by flow cytometry. Controls include $CD4^+$ T cells + media alone or $CD4^+$ T cells + 50 or 500 pg virus (upper panel, left to right). Percentage of HIV-1 core Ag+ $CD4^+$ T cells reflects the raw percentage+ minus the background ($CD4^+$ T cells + media).

Figure 19. DC1 display an enhanced ability to trans-infect $CD4^+$ T cells compared to DC2.

4.3.1.2 Similar to reticulation, enhanced HIV-1 trans-infection is a general trait of DC1

We established in Aim 1 that alternative strategies for generating differentially polarized DC show the same pattern of responsiveness to CD40L, with DC1 displaying a dramatically enhanced ability to reticulate, DC2 being highly refractory to induction of this process, and DC0 displaying an intermediate phenotype. We therefore utilized the maturation factor R848 (TLR7/8) alone, or in combination with IFN-γ or PGE_2, to generate DC0, DC1, and DC2, respectively, and tested their ability to trans-infect autologous $CD4^+$ T cells using 50 pg of input virus. In accordance with the two previously published studies of differentially programmed mature DC trans-infection [113, 115], DC1 generated by alternate methods displayed a heightened ability to trans-infect $CD4^+$ T cells, while DC2 were highly inefficient, and DC0 displayed an intermediate trans-infecting capacity (Figure 20). Enhanced HIV-1 trans-infection, similar to reticulation, indeed appears to be a general characteristic of DC matured by mediators of type-1 immunity.

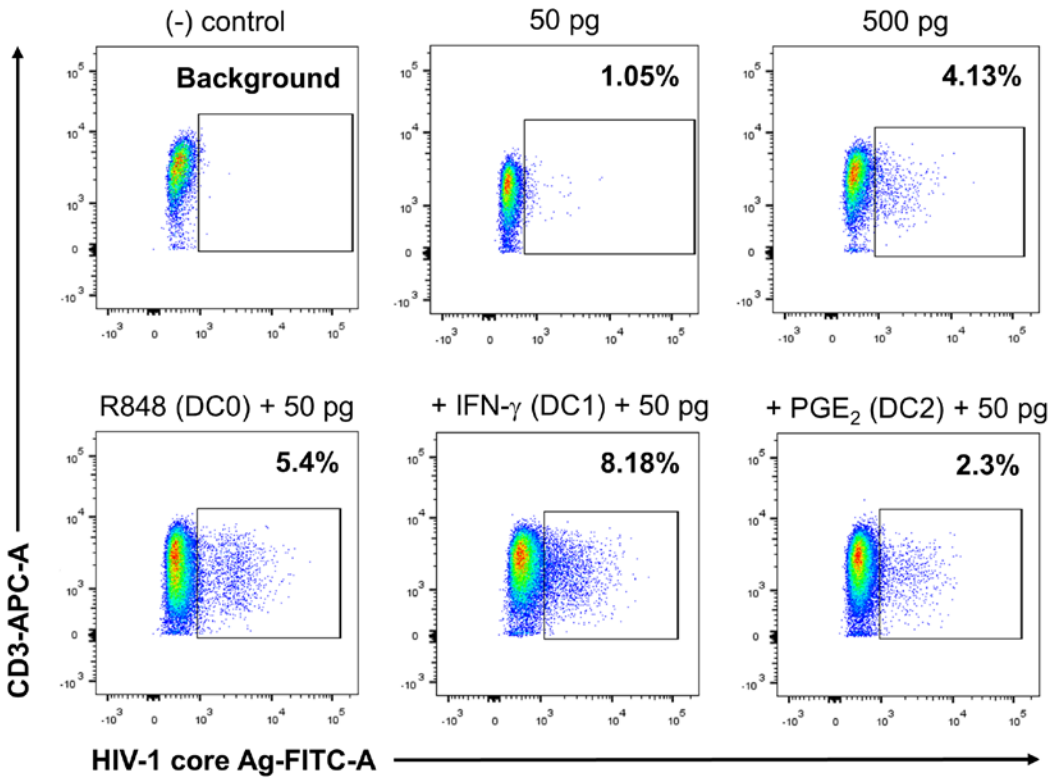

$CD4^+$ T cells alone were exposed to media only (- control), 50 pg, or 500 pg of HIV-1 R5 BaL, as described previously (upper panel, left to right). R848 alone or in combination with IFN-γ or PGE_2, was used as an alternate means to generate DC0, DC1, and DC2, respectively, and exposed to 50 pg virus prior to co-culture with $CD4^+$ T cells (lower panel). Depicted are the pseudo-colored dot plots generated from $CD4^+$ T cells harvested at d 6 and stained intracellularly with mAb specific for HIV-1 core Ag, followed by flow cytometry. As with CD40L-induced reticulation and IL-12p70 production, R848-programmed DC1 demonstrate a differential ability to trans-infect $CD4^+$ T cells compared to DC0 and DC2.

Figure 20. Enhanced HIV-1 trans-infection of $CD4^+$ T cells is a common trait of DC1, while DC0 display an intermediate trans-infection ability.

4.3.1.3 Efficient DC1 trans-infection is evident using extremely low amounts of input virus

Although HIV-1-exposed DC1 in the previous experiments were washed extensively prior to co-culture with $CD4^+$ T cells, 50 pg of input virus also supported low level cis-infection in the $CD4^+$ T cell only control conditions. Although unlikely, the possibility of direct cis-infection of T cells by contaminating unbound virus in DC-T cell co-cultures could therefore not be completely eliminated. A fore-mentioned study assessing differentially matured DC ability to transmit HIV-1 to $CD4^+$ T cells used 150 pg of input virus and core Ag ELISA as the readout of infectivity [113], while another investigation exposed DC to a whopping 15,000 pg of virus prior to co-culture with T cells and used both ICS and core Ag ELISA detection in a single cycle transmission assay. Previous studies of B cell- and iDC-mediated HIV-1 trans-infection conducted in our laboratory utilized extremely small amounts of input virus (3 pg) at a multiplicity of infection below that which is required for direct cis-infection of $CD4^+$ T to eliminate the uncertainty of cis-infection in the HIV-1-exposed APC-T cell co-cultures [93, 110, 119]. Considering this, we next investigated the ability of differentially matured DC to transmit a similarly low dose of virus (5 pg) to $CD4^+$ T cells in multiple donors. In a representative experiment of TNF-α + IL-1β matured DC0, αDC1, and standard PGE_2-matured DC2, we demonstrated dramatically enhanced DC1-mediated trans-infection compared to DC0 or DC2 (Figure 21). Furthermore, trans-infections using 5 pg input virus from 3 HIV-1-naïve donors independently tested revealed a highly significant difference between DC1- and DC2-mediated trans-infection (p-value = 0.0085) (Figure 22). As expected, cis-infection at 5 pg was negligible (0.325%), while there was a striking nearly 3-fold difference in the percentage of ICS core Ag+ $CD4^+$ T cells when infection was mediated by DC1 (8.18%) compared to direct cell-free cis-infection of T cells (2.91%) using 100 times more input virus.

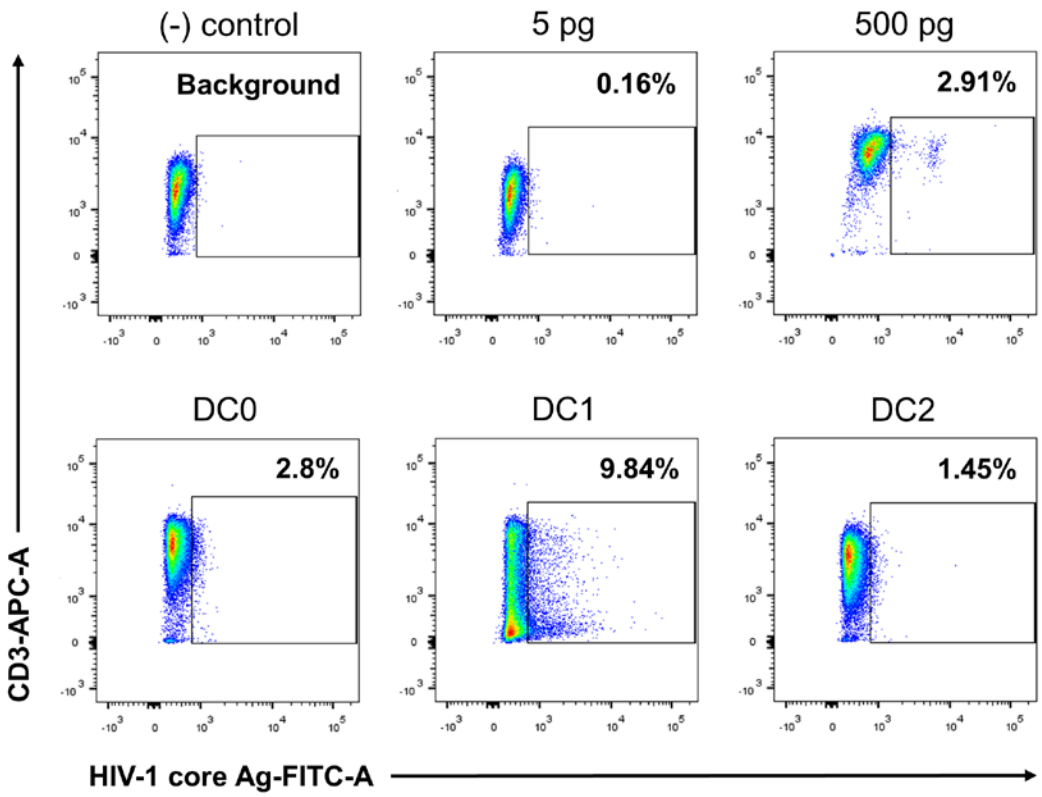

Trans-infections were repeated using an extremely low amount of input virus (5 pg), below that which induces cis-infection of $CD4^+$ T cells. Depicted here are the pseudo-colored dot plots generated from intracellular HIV-1 core Ag staining and flow cytometry at d 6. Controls include $CD4^+$ T cells + media only (background), $CD4^+$ T cells + 5 pg, and $CD4^+$ T cells + 500 pg virus (upper panel, left to right). The lower panel indicate representative DC0, DC1, or DC2 each exposed to 5 pg HIV-1 prior to co-culture with autologous pre-activated $CD4^+$ T cells, as before (lower panel, left to right). Flow data is from one representative donor, with each condition set-up in triplicate, of 3 donors independently tested.

Figure 21. DC1 mediate enhanced HIV-1 trans-infection using extremely low amounts of input virus.

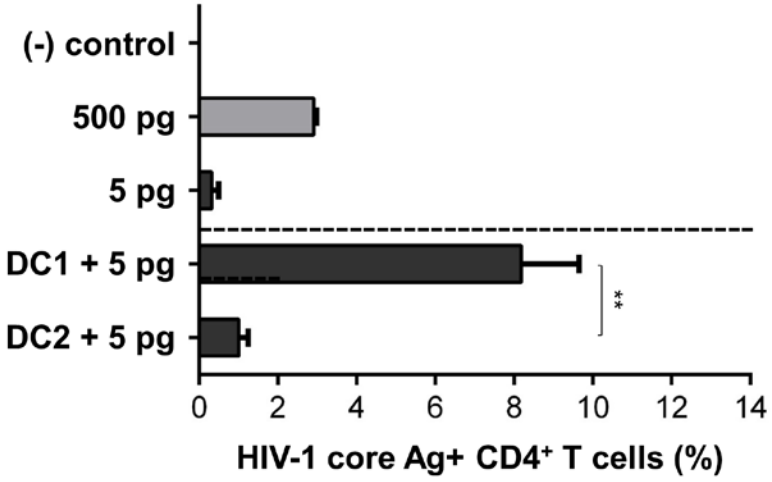

Trans-infections experiments were conducted on 3 HIV-1-naïve donors independently tested. DC1 vs. DC2 trans-infection was measured as before by intracellular HIV-1 core Ag staining and flow cytometric analysis using 5 pg of input virus. Bars above the dashed line indicate $CD4^+$ T cell only controls, while bars below the line are the experimental DC + $CD4^+$ T cell conditions. Data are represented as mean percentage of HIV-1 core Ag+ T cells ± SE. Statistical analysis was performed using an unpaired student t test and ** indicates a p-value of < 0.01.

Figure 22. DC1 display an enhanced HIV-1 trans-infection ability compared to DC2 in multiple donors tested.

4.3.2 Aim 3b. Multiple mechanisms contribute to enhanced DC1-mediated HIV-1 trans-infection

4.3.2.1 Polarized DC differentially express HIV-1 capture molecules and ICAM-1

A previous study found no substantial correlation between DC-SIGN surface expression, a C-type lectin that was initially thought to be the primary HIV-1 capture molecule utilized by DC [131] , and differences in trans-infection capabilities displayed by polarized DC [113]. They concluded that the observed differences were instead related to the later stage of HIV-1 trans-infection, in which DC hand-off virions to $CD4^+$ T cells, rather than initial virus acquisition. They also demonstrated a role for ICAM-1, which facilitates close cell-cell interactions with LFA-1-expressing T cells, in enhanced DC1 trans-infection. More recent studies indicate that mature DC acquire HIV-1 primarily via the lectin-like adhesion molecule, Siglec-1, which captures HIV-1 by interacting with sialyllactose moieties of viral membrane gangliosides, rather than DC-SIGN, which is down-regulated on DC upon maturation [89]. Furthermore, Siglec-1 is significantly up-regulated upon LPS maturation or type-I IFN treatment of mature DC. This molecule, however, has not yet been investigated in the context of differentially matured DC trans-infection.

We sought to rule out the possibility that enhanced DC1 trans-infection was related to differential Siglec-1 expression on the DC types, and also to confirm high ICAM-1 expression on DC1 in our system. We first investigated DC-SIGN, Siglec-1, and ICAM-1 gene expression levels from representative DC1 and DC2 using a genome-wide transcriptional profiling approach. VST-normalized mRNA expression levels were more than 10-fold higher on DC1 compared on DC2, nearly 5-fold higher for Siglec-1, and almost 20-fold higher for ICAM-1 (Figure 23).

We next stained differentially programmed DC with mAbs specific for DC-SIGN, Siglec-1, and ICAM-1, in addition to maturation markers (d.n.s.), and determined their surface expression by flow cytometry. These data revealed that both DC1 and DC2 express DC-SIGN, which was higher on DC1 compared to DC2 (Figure 24), in contrast to the current literature. Strikingly, Siglec-1 expression was nearly undetectable on DC2, but highly up-regulated on DC1 (Figure 24). ICAM-1 was highly expressed on both DC1 and DC2, with substantially higher expression displayed by DC1 (Figure 24). Furthermore, TNF-α + IL-1β-matured DC0 displayed intermediate levels of these markers, and the same overall pattern was observed when using the R848-based strategy to generate DC0, DC1, and DC2 (d.n.s.). These results are in accordance with our previous observation that fewer labeled HIV-1-like particles could be detected on DC2 compared to DC1, after exposing them to the same amount of virus and imaging with standard confocal methods (d.n.s.). Although confirmation of these results in multiple donors as well as blocking studies are required to definitively link low expression of HIV-1 capture molecules to inhibited DC2 trans-infection in our system, these data imply that DC1 acquire HIV-1 more efficiently than DC2.

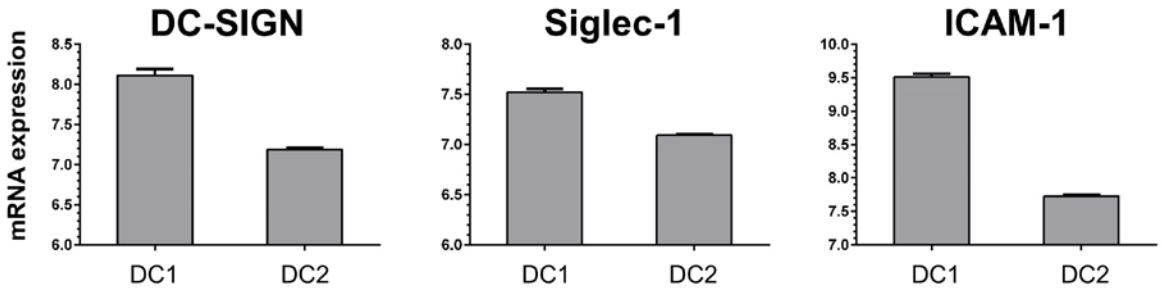

Representative DC1 and DC2 were generated as described previously and mRNA extracted for direct hybridization using the Ilumina HumanT-12 Expression BeadChip Kit, as described previously. Data analysis was conducted using Genome Studio software, and the data were VST-transformed to obtain normalized mRNA expression levels. Importantly, a 1 unit difference (i.e. 7.0 to 8.0) represents nearly a 10-fold difference in gene expression. DC-SIGN expression levels were more than 10-fold higher on DC1 compared on DC2 and nearly 5-fold higher for Siglec-1, and nearly 20-fold higher for ICAM-1. The graphs represent 2 replicate sample values ± SE.

Figure 23. DC1 express greater mRNA levels of HIV-1 capture molecules and DC-T cell interaction-promoting ICAM-1 compared to DC2.

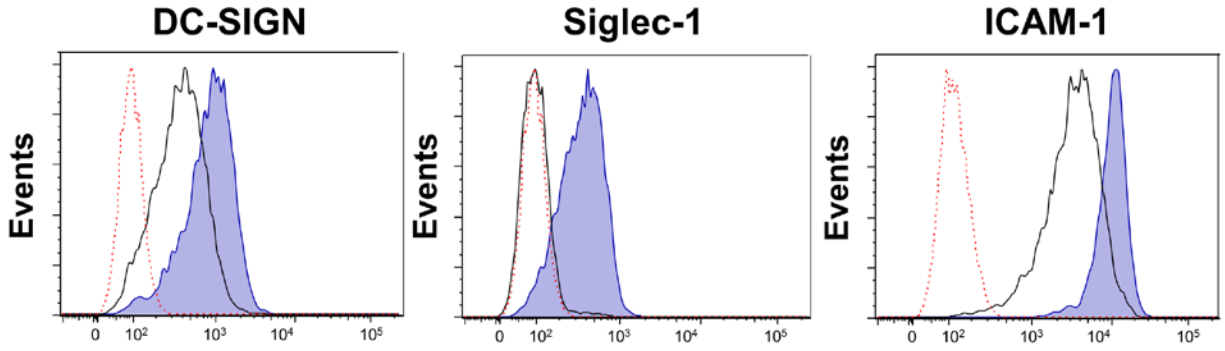

Representative mature DC0 (d.n.s.), DC1, and DC2 were stained with labeled mAbs specific for DC-SIGN, Siglec-1, or ICAM-1, or respective isotype control mAb. Following flow cytometric analysis, over-laid histograms were generated, in which DC1 are represented by blue histograms, and DC2 are represented by transparent histograms outlined in black, and isotype controls are distinguished by empty histograms outline by the red-dashed line.

Figure 24. DC1 display higher levels of cell surface HIV-1 capture molecules and ICAM-1 than DC2.

4.3.2.2 CD40L is critical for DC1-mediated trans-infection

The striking correlation between CD40L-induced reticulation, or formation of TNT networks, and DC1 trans-infection ability prompted us to investigate the role of CD40L in DC1-mediated transmission of HIV-1 to CD40L-expressing T cells. A previous study demonstrated that treatment with stimulatory anti-CD40 mAb increased iDC-mediated transmission of HIV-1, suggesting a role for $CD4^+$ T cell-associated CD40L in trans-infection [111], but the importance of the CD40-CD40L pathway in DC1-instigated transmission remains to be explored. In our system, CD40L-specific blocking mAb substantially abrogated inducible DC1 reticulation compared to treatment with an irrelevant control mAb (Figure 25A), and CD40L-specific mAb treatment resulted in a substantial decline in the ability of DC1 to produce IL-12p70 (Figure 25B). Next, we tested the ability of CD40L-blocking mAb to inhibit DC1-mediated trans-infection, and revealed an almost complete abolition of trans-infection from 13.91% to 0.49% when using 12.5 pg of input virus, an amount which also failed to induce substantial cis-infection (Figure 25C). These data provide a rationale for further exploration of the role of CD40L-induced reticulation in facilitating DC1 mediated HIV-1 trans-infection.

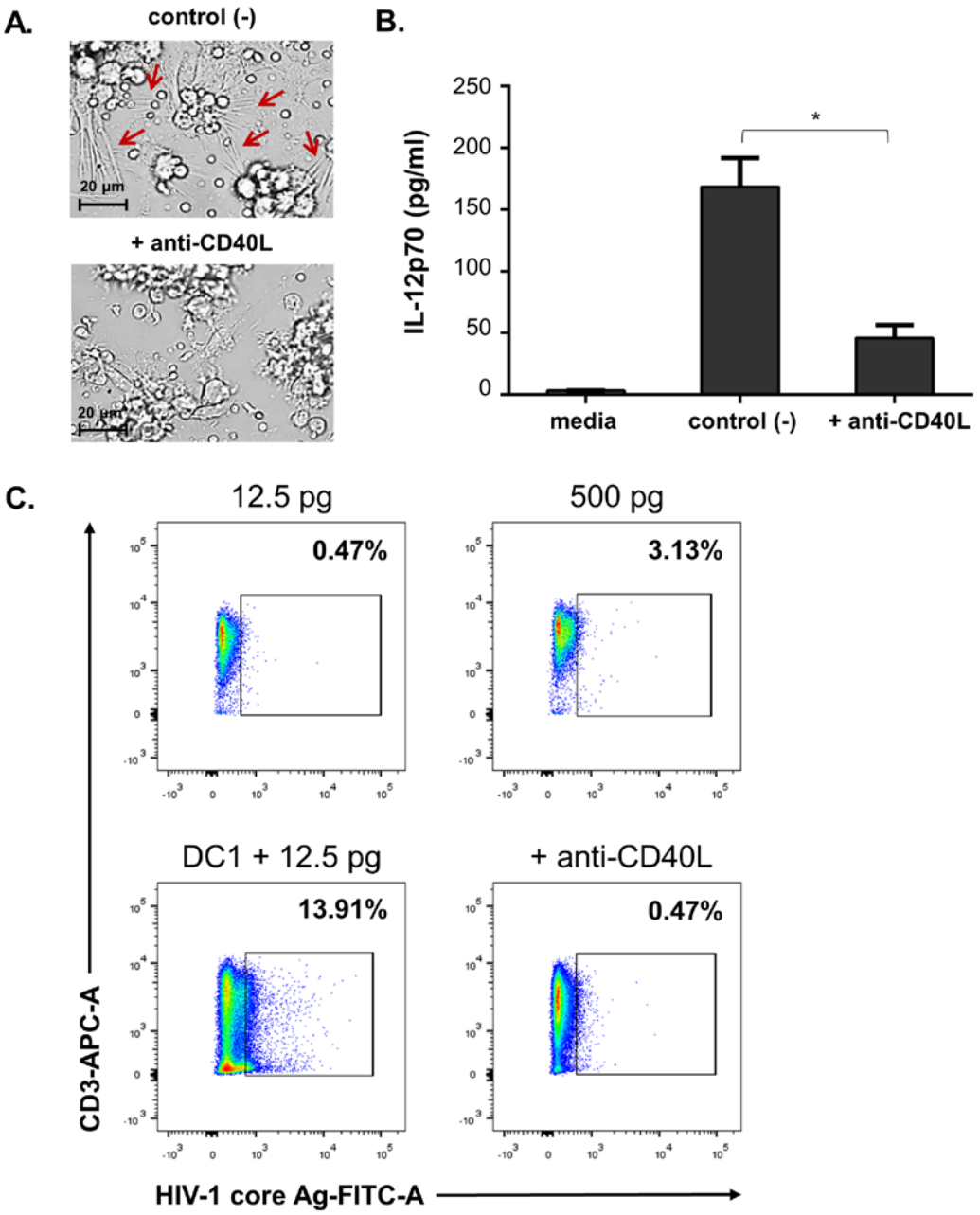

(A) Ag-loaded DC1-CD4$^+$ T cell co-cultures were treated with anti-CD40L blocking mAb or control mAb for 24 h prior to imaging. (B) In addition to inhibiting reticulation, anti-CD40L mAb treatment substantially decreased IL-12p70 production in DC1, as measured by standard IL-12p70 ELISA. Data are indicative of 2 replicate experiments and * indicates a p-value < 0.05. (C) Pseudo-colored dot plots derived from d 6 HIV-1 core Ag-stained CD4$^+$ T cell only controls exposed to 12.5 or 500 pg of input virus (upper panel, left to right), or HIV-1- exposed DC1 (12.5 pg) co-cultured with CD4$^+$ T in the presence or absence of blocking anti-CD40L mAb (lower panel).

Figure 25. Blockage of CD40L signaling inhibits DC1-mediated HIV-1 trans-infection.

4.3.2.3 A role for cholesterol in HIV-1 transmission from DC1 to $CD4^+$ T cells

A previous study highlighted that cholesterol-sphingomyelin membrane nanodomains are likely required for TNT formation, as these domains were detected along the length of TNTs, which were also destabilized upon membrane cholesterol depletion [47]. Intriguingly, our research group recently revealed a probable link between HIV-1 disease progression and trans-infection when we showed that APC from NP are unable to trans-infect autologous or heterologous $CD4^+$ T cells due to altered cholesterol metabolism, while APC from PR and HIV-1-naïve donors trans-infect efficiently [110]. Furthermore, reconstitution of cellular cholesterol restored trans-infection ability of iDC and B cells in NP, and cholesterol depletion in these cell types with reductase inhibitors (statins) inhibited trans-infection in PR and HIV-1 naïve donors. Reduced cellular cholesterol could conceivably inhibit trans-infection at various stages, but we considered the possibility that this finding was in part related to TNT-mediated HIV-1 transmission. Abrogated cholesterol could also impact exosome-mediated HIV-1 transmission, but the current literature and our visual observations of DC1 reticulation by SEM support the concept that TNT- and exosome-mediated communication pathways are linked [69]. SEM micrographs of DC1-derived TNTs revealed exosome-like vesicles trailing off from the tips of TNT-like projections or TNT formation following the trail of exosomes (Figure 26). Although the evidence of a link between exosomes and TNTs shown here is preliminary, this intriguing possibility will be a future area of research in our laboratory.

To investigate a possible connection between the reticulation process, HIV-1 trans-infection, and disease progression, we next tested the ability of differentially matured DC1 and DC2 from 2 NP and 3 PR subjects used in the previous study to develop TNT networks upon exposure to CD40L. DC1 from both of the NP expressed abnormally low levels of TNTs, while

DC1 from 2 out of 3 PR expressed normally high levels and 1 PR had a moderate level of TNT expression. The percentage reticulation positive DC1 from a representative NP and PR donor pair was quantitated as described previously, and the DC1 from NP displayed substantial inhibition of DC1 reticulation (Figure 27A). These striking findings could not be attributed simply to a failure of DC from NP to polarize, considering that DC types displayed the normal pattern of IL-12p70 production in response to CD40L (Figure 27B). Taken together, these data support our hypothesis that reduced cholesterol content in the membranes of APC from NP donors inhibits their capacity to reticulate, which subsequently impacts their trans-infection ability.

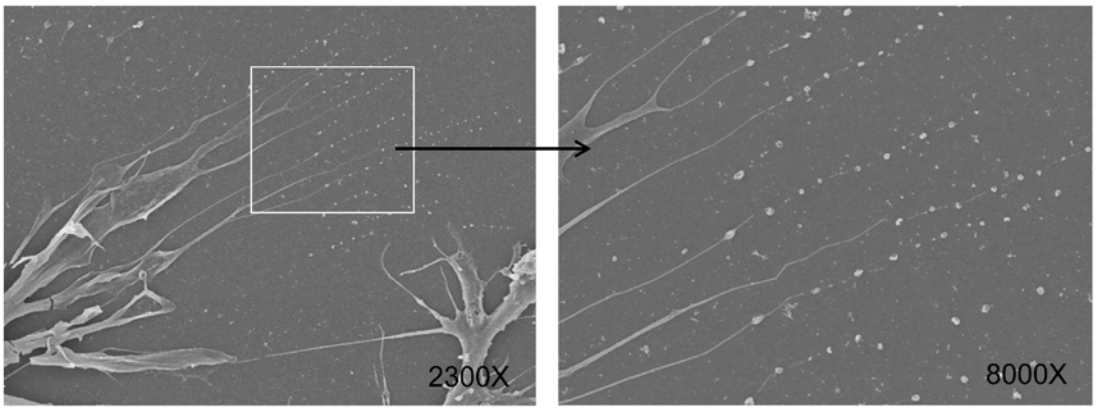

SEM micrographs of reticulating DC1 reveal exosome-like vesicles trailing off from the tips of TNT-like processes, or TNTs following a trail of exosomes. Further study is required to confirm the identity of the vesicles and the manner in which these 2 forms of intercellular communication are linked in the context of DC1 reticulation.

Figure 26. TNT- and exosome-driven modes of intercellular communication may be linked.

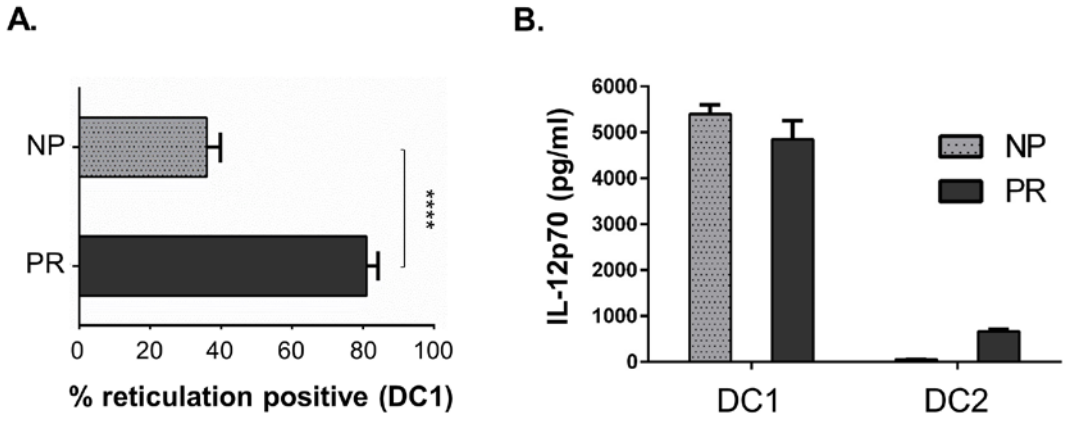

DC1 and DC2 were generated from monocytes isolated from NP and PR PBMCs collected post-seroconversion and stimulated as described previously with rhCD40L. (A) The percentage of reticulation+ CD40L-stimulated DC1 was assessed, and a highly significant difference in the ability of NP and PR to develop TNT networks was noted. Similar to HIV-1 naïve donors, DC1 from a representative PR reticulated efficiently, while the process was strongly inhibited in NP. (B) Supernatants from rhCD40L-stimulated DC1 and DC2 generated from the same NP and PR were collected and tested for IL-12p70 production as described previously. IL-12p70 production by DC1 was similar to that of HIV-1 naïve donors (d.n.s.) and the difference between NP and PR IL-12p70 levels was not statistically significant (p-value = 0.350). These data indicate that DC1 and DC2 from NP and PR were functionally polarized. Data are from one representative donor pair and expressed as percentage reticulation+ ± SE, and p-values of < 0.0001 are indicated by ****.

Figure 27. Inefficient DC trans-infection displayed by NP corresponds with inhibited DC reticulation.

A thorough investigation of the relationships between TNT networks, DC1 trans-infection, and HIV-1 disease progression is beyond the scope of this dissertation. However, the correlation between inhibited reticulation and trans-infection in a subset of NP provided further support of a role for inducible cholesterol-enriched TNTs in DC1-mediated trans-infection. Simvastatin is a specific inhibitor of HMG-CoA reductase, the enzyme that catalyzes the conversion of HMG-CoA to mevalonate, which inhibits an early step in cholesterol biosynthesis [120]. We first tested the ability of this clinically-approved drug to inhibit CD40L-induced reticulation, and found that pre-treatment at a concentration of 20 μM resulted in a highly significant reduction in the percentage of reticulation+ DC1 (p-value < 0.0001) in a representative donor (Figure 28). Next we investigated the impact of this drug on DC1-mediated trans-infection, by pre-treating DC1 with simvastatin during maturation and washing it out prior to exposing the treated DC1 or DC1 + media only to 12.5 pg of HIV-1, and then co-culturing them with autologous $CD4^+$ T cells as before. We observed a striking abrogation of DC1-mediated trans-infection as a result of simvastatin pre-treatment (Figure 29), providing further evidence of a role for inducible TNT networks in this process. However, these findings could not completely eliminate the possibility that cholesterol inhibition acted on another stage of DC1 trans-infection.

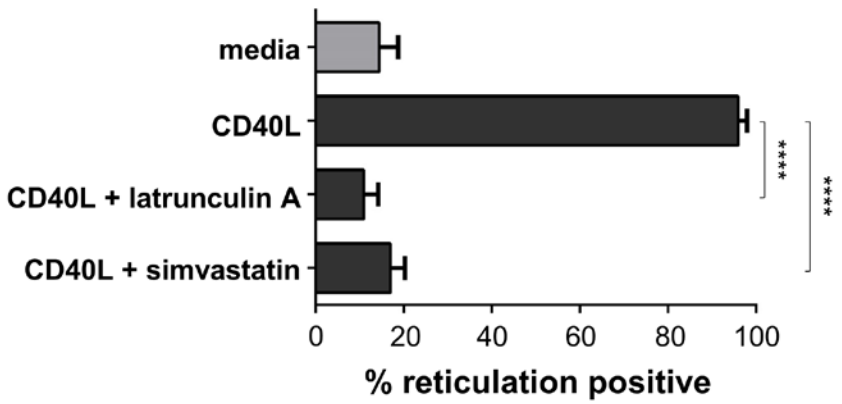

Mature DC1 were exposed to media only or rhCD40L, prior to collection of at least 10 image fields used to obtain the percentage of reticulation+ cells, as described previously. Alternatively, DC1 were treated with 100 nM latrunculin A, an F-actin depolymerization drug commonly used to block TNT formation, or 20 µM simvastatin, and again scored for reticulation. Quantitation was performed on one representative of 3 donors independently tested and displayed as mean ± SE. P-values < 0.0001 are represented by ****.

Figure 28. Drugs that target cholesterol and actin polymerization inhibit DC1 reticulation.

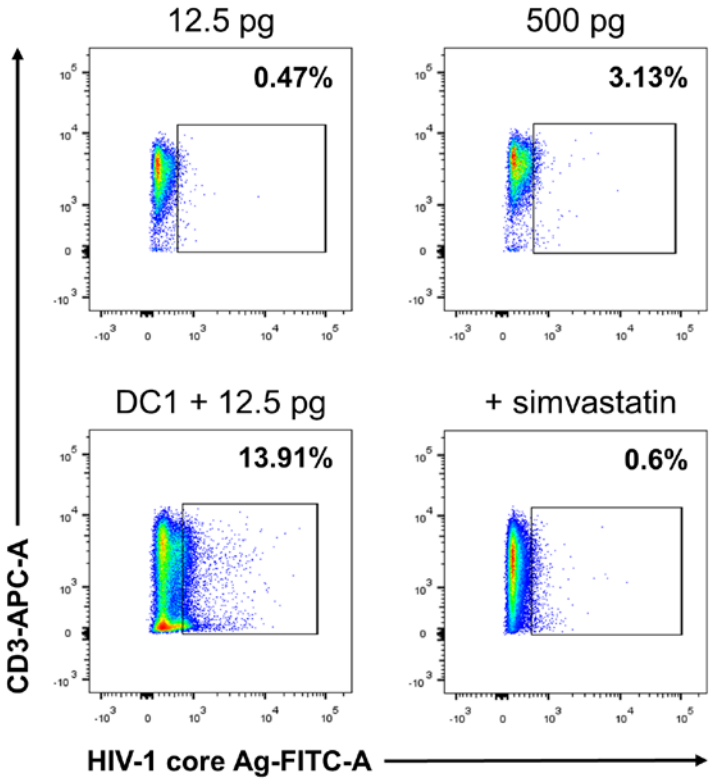

DC1 were treated with media only or pre-treated with 20 μM simvastatin, a concentration that also strongly inhibited the reticulation process, prior to washing extensively and exposing DC1 to 12.5 pg virus, and co-culturing them with $CD4^+$ T cells as described previously. Depicted are pseudo-colored dot plots of $CD4^+$ T cells harvested at d 6 post-co-culture and stained with HIV-1 core Ag-specific mAb as before. $CD4^+$ T cell only controls (upper panel) or DC1 + T cell conditions (lower panels) are shown. Data are from 1 representative donor, with experiments set-up in triplicate.

Figure 29. Inhibition of cholesterol synthesis abrogates DC1-mediated trans-infection.

4.3.2.4 An actin depolymerization drug blocks DC1- but not DC2-mediated trans-infection

In addition to blocking cellular cholesterol, previous studies have utilized actin-depolymerizing drugs including latrunculin A [49, 58, 76] and latrunculin B [38, 57] to inhibit TNT formation and TNT-mediated trafficking of various cargoes. We chose to evaluate varying doses of latrunculin A, which sequesters G-actin and prevents F-actin assembly, on inducible DC1 reticulation and trans-infection due to its lack of impact on cell viability [132]. We found that the relatively low dose of 100 nM resulted in highly significant abrogation of reticulation (Figure 28), while this dosage did not inhibit IL-12p70 production (d.n.s.), indicating that other aspects of DC function were preserved. In order to eliminate the possibility that latrunculin A could act on the T cells, we pre-treated HIV-1-exposed DC1 or DC2 with 100 nM latrunculin A for 1 h and then washed the cells extensively to remove residual drug prior to co-culture with $CD4^+$ T cells in our trans-infection system. This strategy revealed a striking reduction in trans-infection in the DC1 condition, while DC2-mediated trans-infection was completely unaffected (Figure 30), indicating a role of F-actin-mediated processes in DC1 trans-infection. Taken together, these data support our supposition that TNTs represent an important pathway for virus transmission from DC1 to $CD4^+$ T cells.

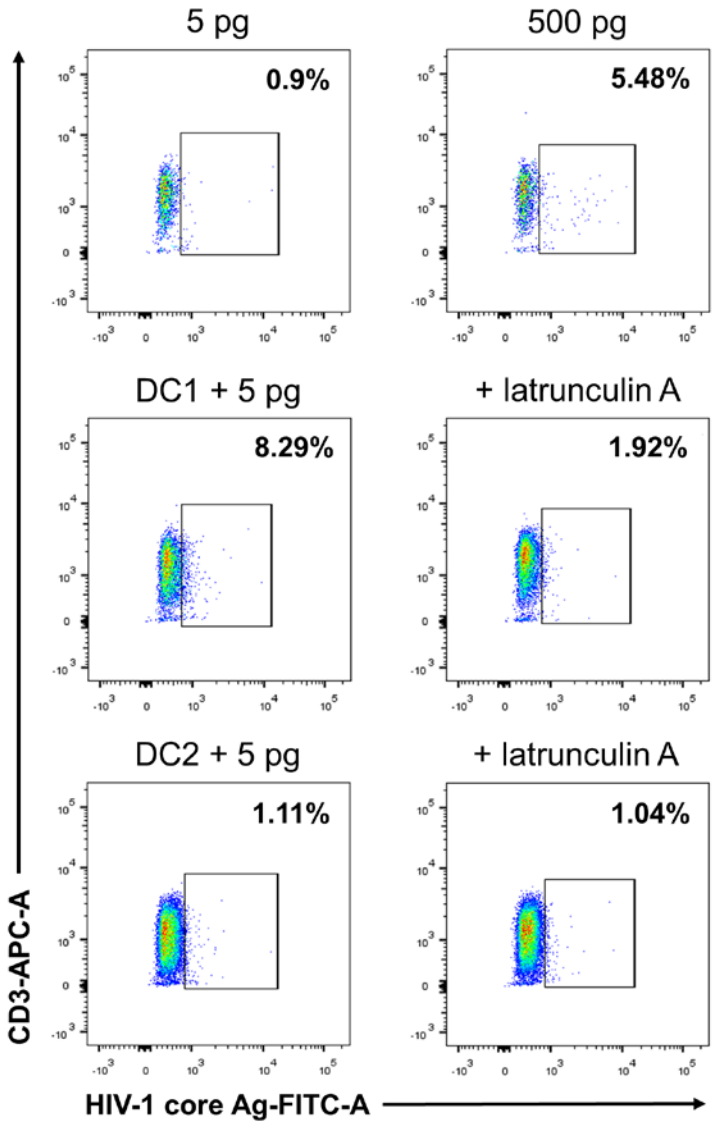

DC1 and DC2 were generated and exposed to 5 pg HIV-1 R5 Bal as described previously, and then pre-treated with a low dose of latrunculin A (100 nM), an actin-depolymerizing drug frequently used to block TNT formation, which also substantially inhibited the reticulation process. DC were washed extensively prior to co-culture to eliminate the possibility of latrunculin A acting directly on the T cells. Depicted here are pseudo-colored dot plots of $CD4^+$ T cell only controls (upper panel) and T cell + DC1 (middle panel) or T cell + DC2 (lower panel) co-cultures in which DC were pre-treated with media or latrunculin A. Data are from 1 representative donor, with experiments set-up in triplicate.

Figure 30. Latrunculin A pre-treatment inhibits DC1- but not DC2-mediated trans-infection.

4.3.3 Aim 3c. Visualizing DC1-CD4$^+$ T cell HIV-1 transmission via inducible TNT networks

4.3.3.1 CD4$^+$ T cells can form uropods for acquisition of HIV-1 from the DC surface

In support of CD40L- and TNT-blocking studies described in the previous section, we next endeavored to find visual evidence of TNT-mediated HIV-1 transmission to CD4$^+$ T cells in the setting of reticulation using live-cell super-resolution SIM. Cy5-labeled DC1 were exposed to EGFP-expressing HIV-1-like particles as described previously for 2 h, washed extensively to remove unbound virus, and plated to imaging dishes. In order to recapitulate a setting where the DC form an interconnected network of thin and thick TNTs, we exposed DC1 to CD40L for 10-12 h prior to co-culturing them with autologous Cy3-labeled PHA- and IL-2 activated CD4$^+$ T cells and imaging. Super-resolution techniques allowed us to visualize reticulation in even greater detail than high-resolution confocal allowed in previous experiments. In accordance with confocal imaging, CD40L induced an interlacing network of TNTs, which increased in complexity over time (Figure 31). We also found visual evidence of CD4$^+$ T cell uropods and filopodia-like structures probing into HIV-1-like particle-enriched regions of the DC membrane, and particle localization to the T cell-derived structures (Figure 32A-32B), similar to previous studies of DC-T cell dynamics of the virologic synapse [97, 106]. Particles rapidly localized to the T cell projections, within 1-2 h of co-culture. Furthermore, complex DC membrane folds could occasionally be observed at least partially enveloping T cells at the interface between the 2 cells (Figure 32B). T cells also displayed ruffles, which appeared to maximize the contact zone between interposed cells, and DC-derived TNT-like projections could also be seen interacting with the T cell membrane.

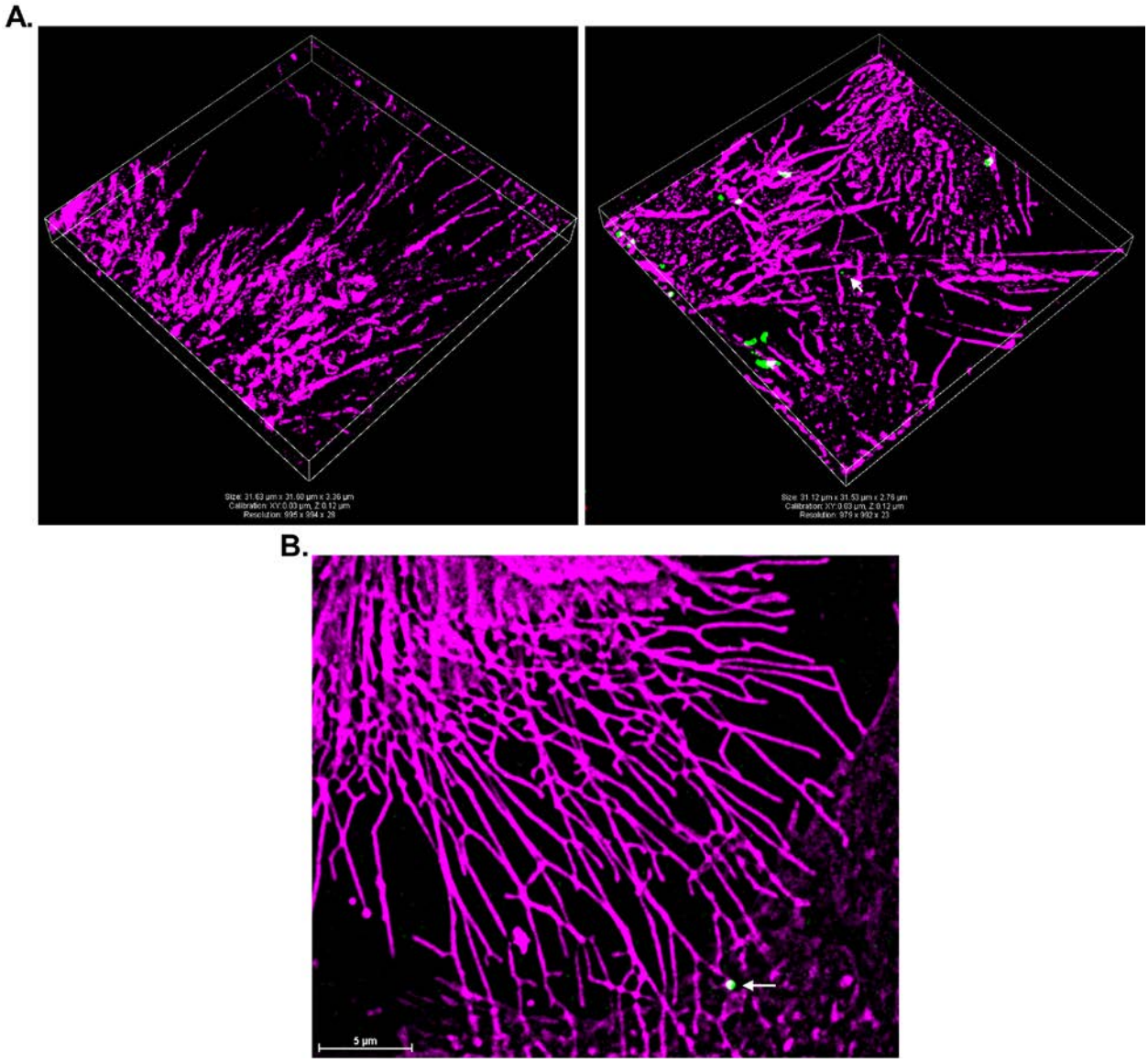

Live, Cy5-labeled DC1 (magenta) were exposed to rhCD40L and imaged using super-resolution SIM, revealing a complex network of interlacing TNTs. (A) DC1 were exposed to media only (left) as a negative control or HIV-1-like particles (right) and imaged in both green and far-red channels by SIM after 10-12 h treatment with rhCD40L. Individual TNTs took a relatively straight or winding path, and the latter appeared to be a means of bypassing obstructions posed by other membrane protrusions. (B) DC1 were exposed to HIV-1-like particles as before and imaged after 18-20 h of rhCD40L treatment, which induced an even more intricate network of TNTs. An individual particle (green, white arrows) can be seen at the interface between TNT and the membrane of the connected DC1.

Figure 31. Super-resolution SIM reveals an intricate network of TNTs displayed by DC1.

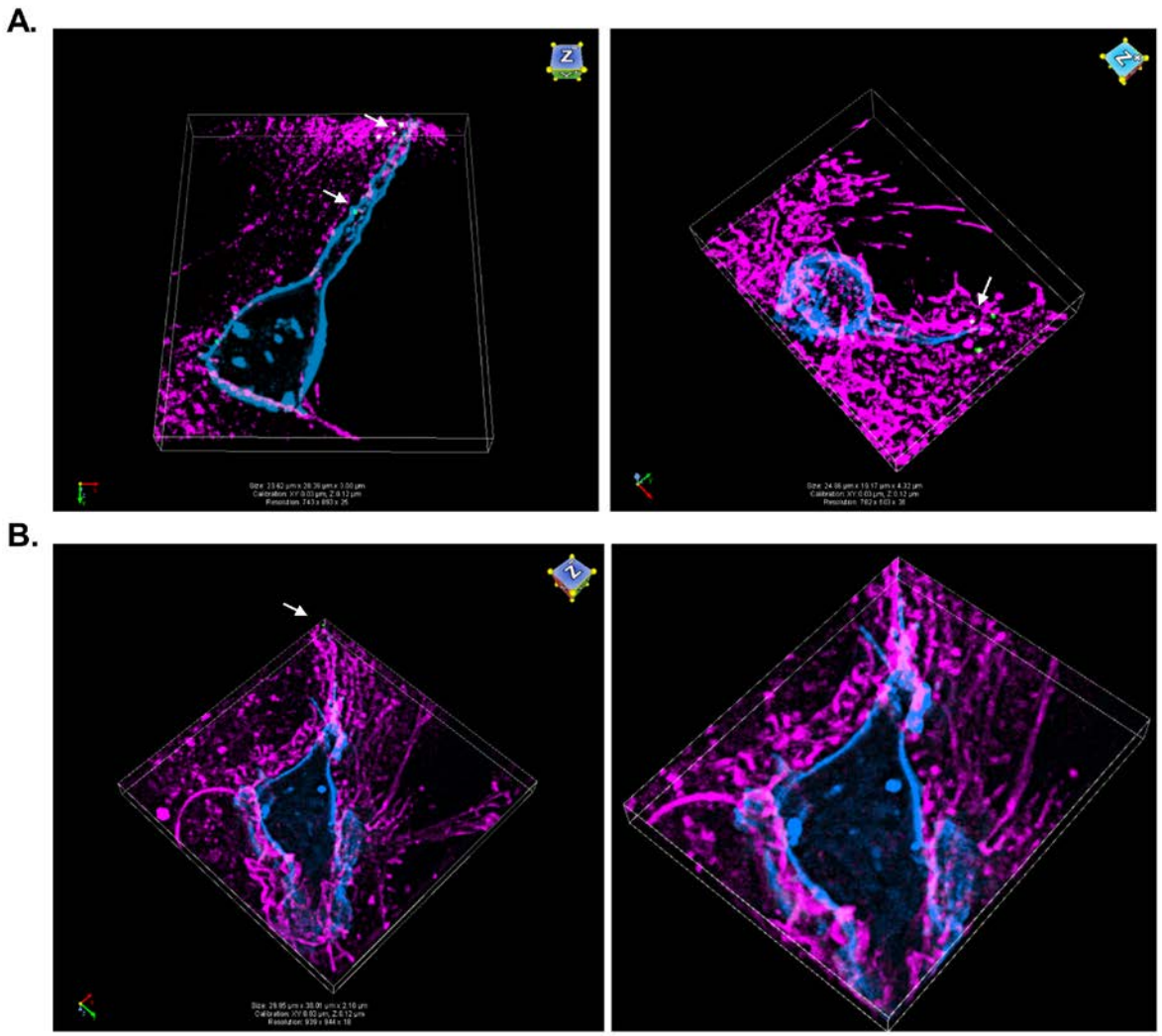

Cy5-labeled DC1 were pulsed with EGFP-expressing HIV-1-like particles for 2 h and washed extensively to remove unbound virus. DC1 were plated to imaging dishes and exposed to rhCD40L as described previously and then co-cultured with Cy3-labeled pre-activated autologous $CD4^+$ T cells (blue). (A) $CD4^+$ T cells formed uropod- and filopodia-like projections that appeared directed toward HIV-1-like particle-enriched regions of the DC membrane, and these T cell-derived extensions rapidly acquired particles. (B) Complex ruffle-like DC membrane projections occasionally partially enveloped interacting $CD4^+$ T cells. T cells also displayed ruffles, which appeared to maximize the contact zone between interposed cells. TNT-like extensions could also be seen apparently interacting with the T cell membrane. White arrows highlight the location of HIV-1-like particles.

Figure 32. $CD4^+$ T cells can form uropods for acquiring HIV-1 from DC membranes.

4.3.3.2 $CD4^+$ T cells can interact with the DC1 network via thick and thin TNTs, which also facilitate virus transmission

We next investigated the ability of $CD4^+$ T cells to interact with the DC1-derived TNT network, and also searched for visual evidence of direct virus transmission to interconnected $CD4^+$ T cells via these structures using live-cell SIM. Short filopodia-like projections derived from Cy3-labeled $CD4^+$ T cells appeared to interdigitate with DC1-derived TNTs, which not only facilitated DC1-DC1 contacts, but also supported additional contact between DC1 and closely interacting $CD4^+$ T cells, as well as between T cells and adjacent interconnected DC1 (Figure 33). DC-derived TNTs often appeared to slide along the T cell surface, but we failed to uncover evidence of direct interaction between T cell-derived and DC1-origin TNTs, nor did we observe membrane mixing between the 2 cell types. Future investigations may yet reveal this interaction, but culture conditions optimized for development of T cell-derived TNTs and/or utilization of a basement membrane matrix to better recapitulate the 3D in vivo extracellular matrix in lymph nodes should be considered [133].

Nevertheless, we uncovered striking evidence of DC1-derived TNTs mediating direct HIV-1 transmission to $CD4^+$ T cells. Within 1 h of co-culture, $CD4^+$ T cells localized to DC1 cell bodies as well as regions of the membrane containing many thin and thick TNTs, and multiple HIV-1-like particles were also observed at the interface between the 2 closely interacting cells (Figure 34). Thick TNTs that connected adjacent cells provided additional contact sites for multiple T cells along the length of individual structures, and many HIV-1-like particles were again observed at the interface between the DC1 and T cells, which presumably represents a virologic synapse (Figure 35A). A rotated view and a magnified view of the same image allowed better visualization of one T cell-DC contact zone, and revealed a thin TNT

emanating from a third DC1 interacting with the T cell (Figure 35B). Several HIV-1-like particles could be clearly seen on the T cell side of the interface between the thin TNT and the T cell. Furthermore, the T cell appeared to be stretched along the length of the thick TNT, apparently to maximize surface area of the T cell-DC contact zone. Finally, very large vesicle-like structures also emanated from this T cell, and these were closely opposed with the thick TNT surface, where virus particles were also detected. Taken together, these data provide strong evidence in support of direct and rapid HIV-1 transmission via inducible DC1-derived TNTs, which provide sites for close interaction with multiple T cells and facilitate additional contacts between T cells and adjacent DC1 that are part of a vast intercellular DC network.

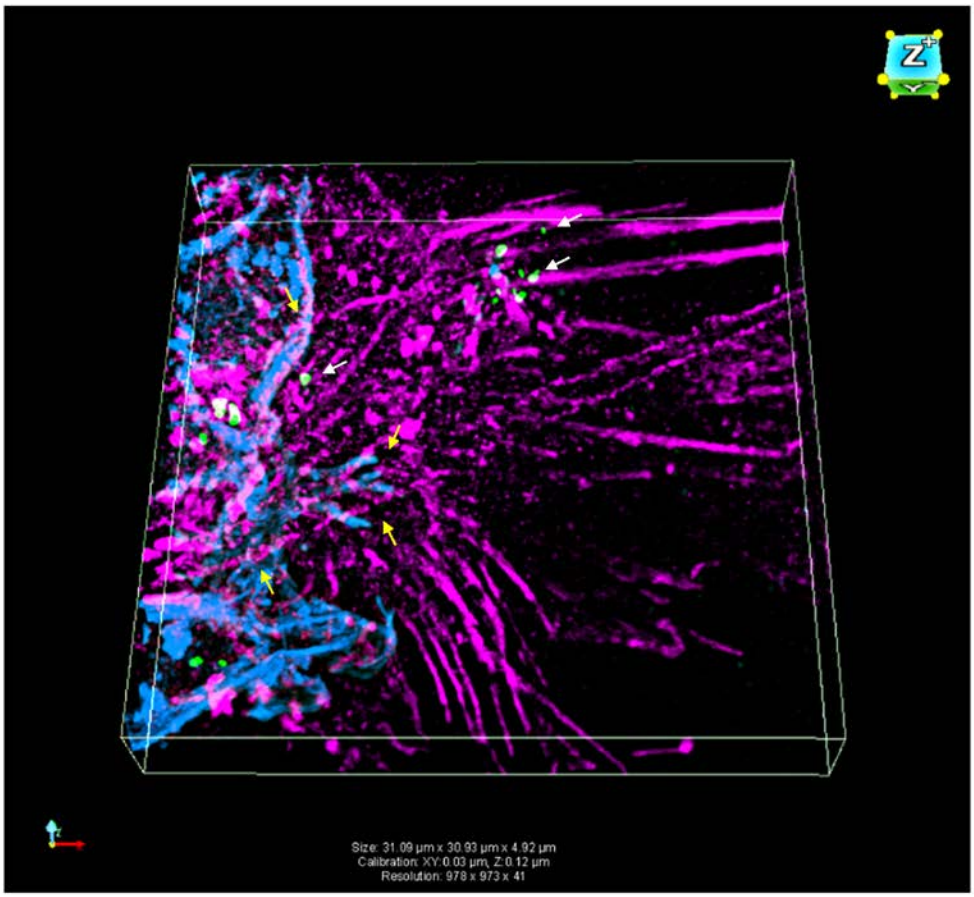

Depicted here are live-cell SIM images of Cy5-labeled HIV-1-like particle-exposed DC1 that formed a complex inducible intercellular network of TNTs, which facilitated contact between Cy3-labeled $CD4^+$ T cells and multiple interconnected DC1. Short filopodia-like projections derived from the Cy3-labeled $CD4^+$ T cells appeared to interdigitate with DC1 TNTs. Strikingly, the DC1-derived projections facilitated direct interaction between $CD4^+$ T cells in close contact, but also between T cells and adjacent cells, as well as contact between neighboring DC1. Yellow arrows highlight the zones of TNT-mediated contact between DC1 and T cells. White arrows indicate HIV-1-like particles localizing to TNTs.

Figure 33. DC1-derived TNTs facilitate contact between $CD4^+$ T cells and a multicellular DC network.

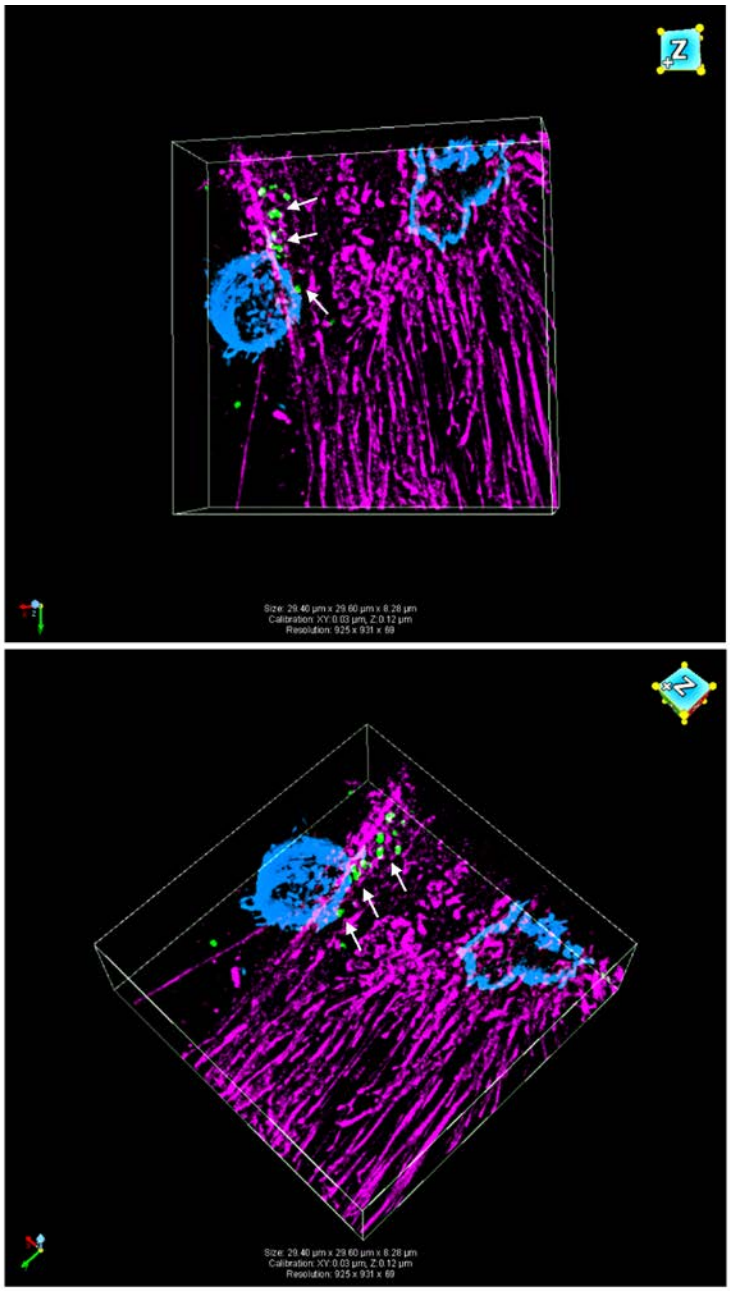

Shown are Cy5-labeled, HIV-1-exposed, reticulating DC1 interacting with Cy5-labeled $CD4^+$ T cells. $CD4^+$ T cells rapidly localized cell bodies of DC1 as well as areas of the DC1 membrane containing many thin and thick TNTs. Multiple HIV-1-like particles (white arrows) can be observed at the interface between the DC-derived TNTs and the interacting T cell membrane.

Figure 34. $CD4^+$ T cells interact with and acquire HIV-1 from complex TNTs formed by DC1.

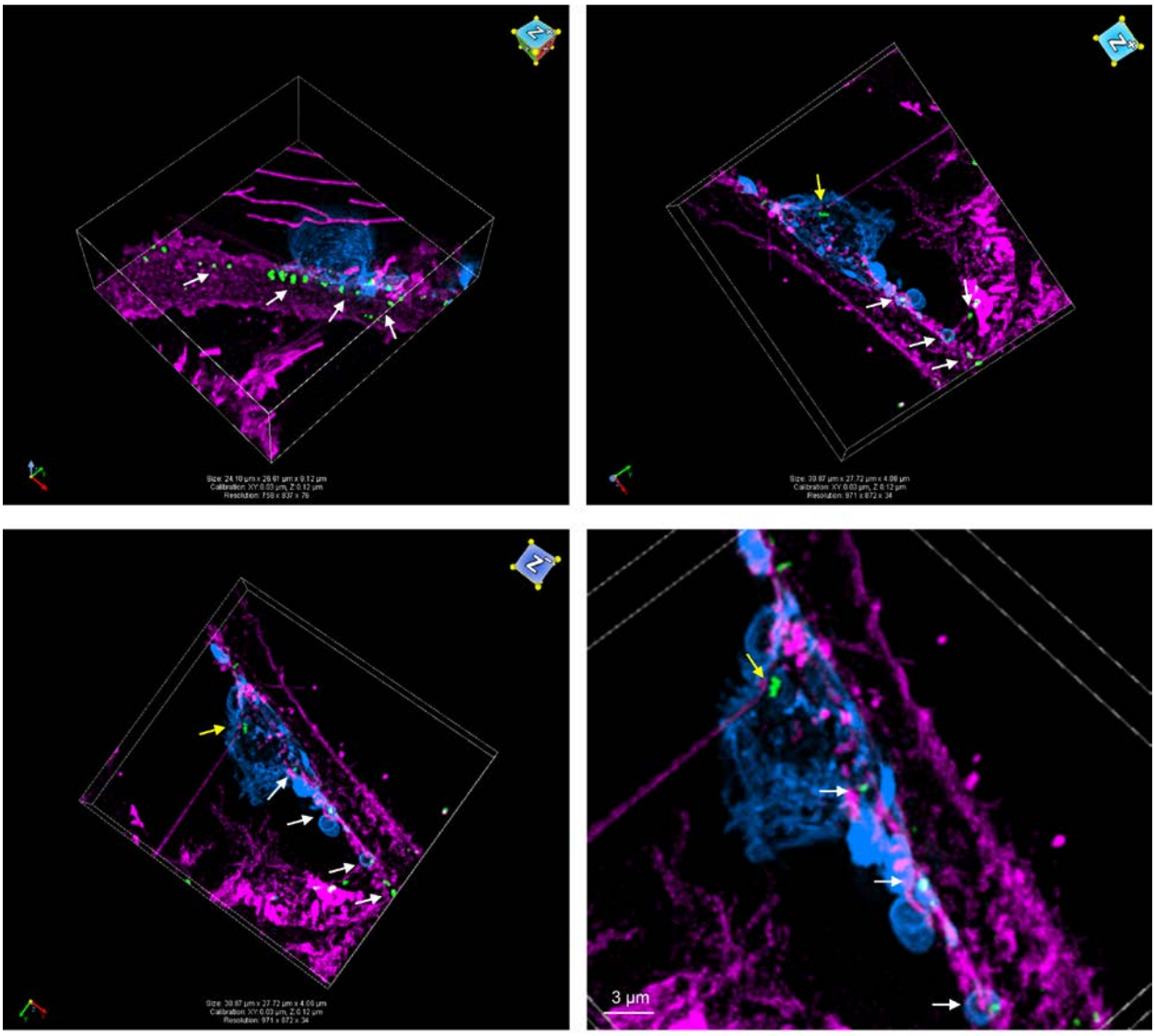

HIV-1-like-particle-exposed DC1 were co-cultured with Cy3-labeled $CD4^+$ T cells in the setting of reticulation and imaged using SIM. Multiple $CD4^+$ T cells were observed interacting with a thick TNT connecting 2 adjacent DC1, and many HIV-1-like particles localized to the interface between the DC-derived extension and T cells (upper panel, left to right). A rotated view (lower left) and a magnified view of the same rotated image (lower right) allows better visualization of the T cell-thick TNT interface, as well as the T cell interaction with a thin TNT emanating from a 3rd cell and several HIV-1-like particles on the T cell side of that contact zone (yellow arrows). Large vesicle-like structures also emanated from the T cell, which appeared stretched to maximize the DC-T cell contact zone.

Figure 35. DC1-derived thick TNTs provide contact sites for multiple $CD4^+$ T cells, and both thin and thick TNTs provide a pathway for direct HIV-1 transmission.

4.3.3.3 ICAM-1 and HIV-1-like particles localize to F-actin-based TNTs expressed by DC1

We next utilized a novel F-actin probe, SiR actin, which combines the unique features of cell permeability, fluorogenic character, and compatibility with super-resolution STED and SIM, to study the interaction of HIV-1 with F-actin-based TNTs and surface ICAM-1. Briefly, unlabeled DC1 were stained with a polyclonal Ab specific for ICAM-1 and a 555-conjugated secondary mAb or secondary mAb alone as a control (Figure 36A). DC were again exposed to HIV-1-like particles, washed and stimulated with CD40L in imaging dishes, and 1 µM SiR-actin was added prior to imaging live cells. Using this strategy, we detected localization of individual HIV-1-like particles to TNT-like F-actin filaments in live cells using STED (Figure 36A) and SIM (Figure 36B). Strikingly, these formations occasionally displayed a highly curved morphology (Figure 36B), which was previously unrecognizable when staining the cell surface. Furthermore, ICAM-1 was detected in distinct clusters on the surface of DC1, and these often localized to the base of TNTs (Figure 37, upper), and occasionally to the length of these structures (Figure 37, lower). Importantly, an HIV-1-like particle could clearly be observed co-localizing with an ICAM-1 puncta on the surface of a DC1-derived TNT (Figure 37, lower). ICAM-1 puncti localization to CD40L-inducible TNTs likely promotes close interaction with LFA-1-expressing T cells along these HIV-1 enriched structures, thereby also facilitating direct TNT-mediated HIV-1 transmission from DC1 to $CD4^+$ T cells.

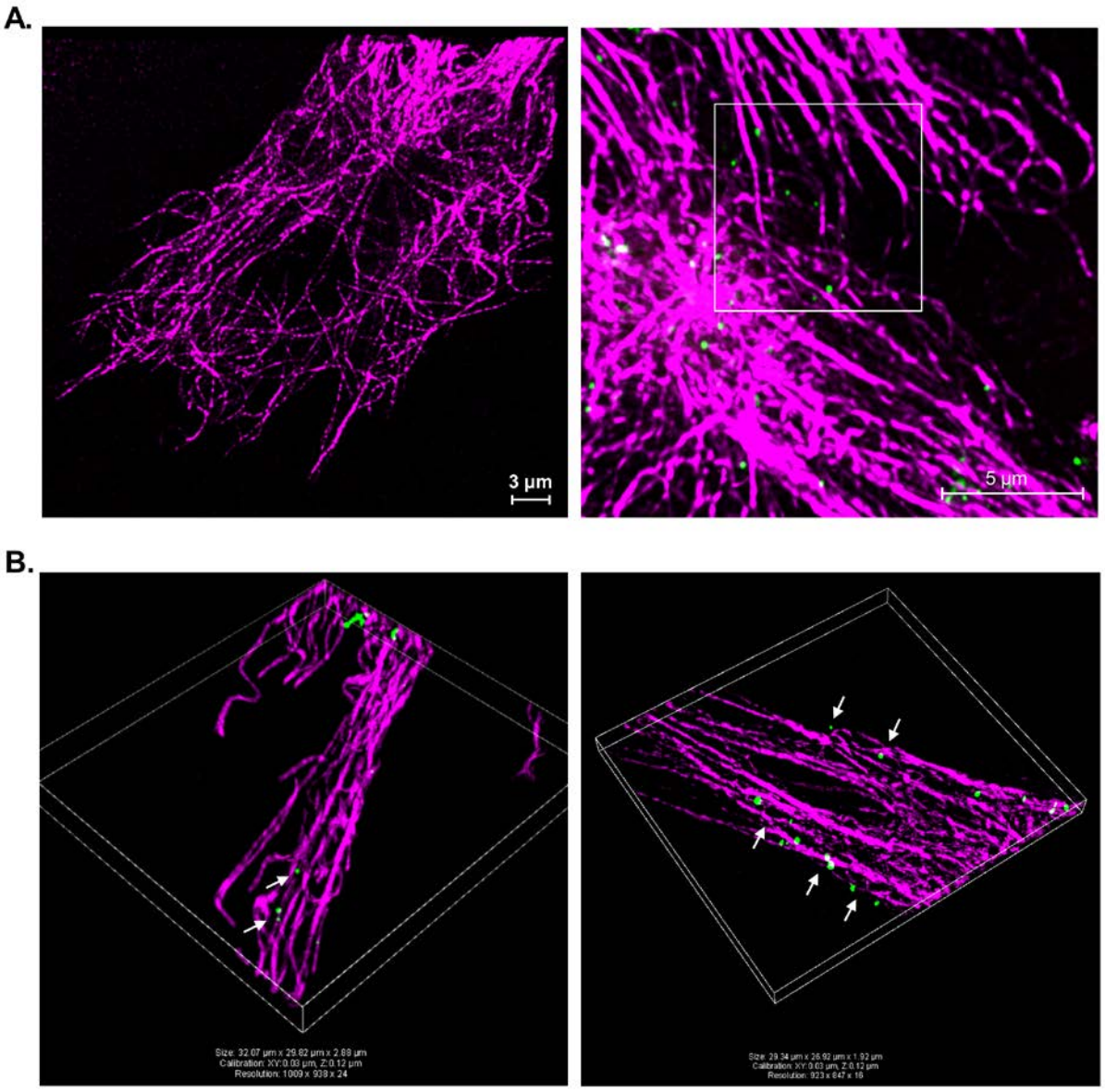

Live DC1 were exposed to HIV-1-like particles as before and reticulation induced with rhCD40L in imaging dishes prior to staining them with SiR-actin to illuminate F-actin-based TNTs. (A) DC1 were labeled with the secondary 555-conjugated mAb alone, which was used to label ICAM-1-specific primary Ab, and imaged in green, red, and far-red channels using STED as a negative control for the remaining experiments (left). A magnified STED image of HIV-1-like particle-exposed DC1 shows particles localization to thin TNT-like structures connecting 2 cells (right). (B) SIM-acquired images showing the concentration of HIV-1-like particles to highly curved (left), as well as straight TNTs (right) displayed by reticulating DC1.

Figure 36. STED and SIM reveal HIV-1 trafficking along F-actin-based TNTs in DC1.

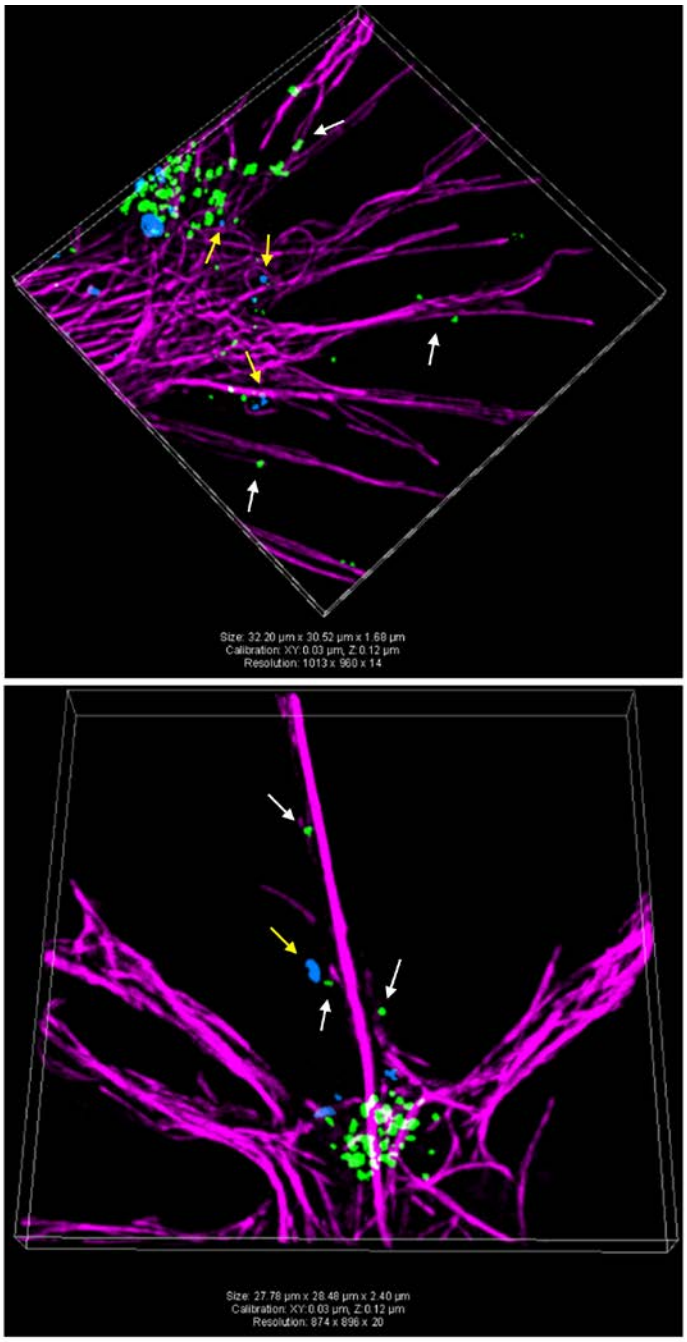

Live, HIV-1-like particle-exposed, reticulating DC1 were immunolabeled with Ab specific for ICAM-1 and then stained with SiR-actin to illuminate F-actin-based TNTs. HIV-1-like particles (white arrows) can be seen along the length of thin TNTs, while ICAM-1 puncti localize closer to the base of these structures (upper panel). An ICAM-1 puncta can clearly be visualized co-localizing with an HIV-1-like particle (white arrow) on the surface of a thick TNT (lower panel).

Figure 37. ICAM-1 clusters and HIV-1 can co-localize to inducible TNTs displayed by DC1.

5.0 DISCUSSION

5.1 TNT NETWORKS AND DC1-DRIVEN IMMUNE RESPONSES IN LYMPH NODES

I describe in this report the induction of the immune process of 'reticulation', a novel aspect of CD40L-mediated $CD4^+$ T cell help that results in the formation of dynamic networks of TNT-like membrane extensions between proximal and remote DC [134]. I determined that the ability of human myeloid DC to reticulate is imprinted by specific combinations of pathogen- and host-derived inflammatory signals that they receive during maturation. Importantly, migratory, high IL-12p70-producing DC1 appear to be 'licensed' to reticulate in response to CD40 ligation, while DC2 are refractory to this process.

Current research suggests a multifarious role for TNTs in intercellular communication, but their mode of induction and function in the context of DC-mediated immunity has not been fully elucidated. Studies using iDC have demonstrated that TNTs induced by mechanical stimulation or *E. coli* supernatants support cell-to-cell propagation of calcium fluxes, which are integral in the regulation of DC activation [55]. A recent investigation showed that MHC class II^+ DC in mouse corneas form TNTs in response to trauma or LPS activation, highlighting a potential link between inflammation and TNT formation for the first time in vivo [59]. I showed that DC matured under type-1 inflammatory conditions display an enhanced number of

unbranched ultrafine TNTs compared to DC2 in their resting state prior to in secondary activation, which could indicate a role for TNTs in pathogen sensing in tissues. However, the distinctive responsiveness of pre-programmed DC1 to secondary CD40L stimulation, or DC0 to concomitant CD40L and IFN-γ stimulation, results in the formation of a far more extensive and complex network of TNTs. Although CD40L-induces both thin and thick TNTs appear similar to those described in macrophages due to their heterogeneous structure [57], they typically exhibit a branching pattern that is distinct from TNTs observed in other cell types, and this results in a highly complex, interconnected web of DC.

Since the initial description of TNTs by Rustom et al. [38] in 2004, TNTs have been shown to facilitate the direct transfer of cytosolic and membrane components, such as endosome- and lysosome-associated vesicles, mitochondria, and MHC molecules [35, 37, 58]. Previous in vivo studies have also shown that non-migratory lymph node-residing DC specializing in cross-presentation acquire Ag and Ag-loaded MHC molecules from migratory DC for the efficient induction of CTL responses [21, 22]. While Ag acquisition by DC has been demonstrated through a number of alternate mechanisms [23, 24, 135], I reveal that the reticulation process can facilitate intercellular Ag exchange for the enhancement of Ag-specific T cell responses, which likely represents an additional novel mechanism by which the acquisition occurs in vivo.

Recent in situ imaging advances have provided evidence of dynamic DC membrane extensions forming intercellular networks in lymph nodes or facilitating probing for microbial pathogens in non-lymphoid tissues. In lymph nodes, resident DC are positionally fixed in a distributed manner along a complex fibroblastic reticular network, which defines the T cell zones and guides T cell migration and scanning of DC [136]. These DC are linked by the tips of extended membrane processes, which also facilitate rapid and pervasive probing [137].

Migratory DC that travel to the T cell areas of regional lymph nodes undergo frequent changes in morphology, including the formation of dendrite-like extensions, and become sessile within 2 d as they are likely integrated into the resident DC network [26, 137]. These studies collectively provide in vivo evidence of a meshwork of DC fixed on the fibroblastic reticular network (FRN) of lymph nodes. This study demonstrates the unique ability of CD40L-expressing Th cells to regulate the formation of intercellular TNT networks in differentially polarized DC, and highlights the possibility that CD40L-induced reticulation facilitates integration of DC1 into the existing resident DC network in lymph nodes.

While DC found in vivo in lymph nodes display many interdigitating membrane projections that form an interconnected network on the stromal scaffold [136], most in vitro DC studies have been conducted with standard DC, which display a ruffled membrane morphology and very few dendrites [27]. I demonstrated herein that the dramatically different membrane morphologies displayed by PGE_2-matured DC2 and IFN-γ-programmed DC1 are determined by the unique maturation program induced by these 2 opposing polarization factors. Migratory DC programming may determine not only their ability to response to CD40L by developing TNT networks, but may also dictate their localization and behavior in the lymph node.

Two photon imaging of steady state DC in inguinal lymph nodes of a CD11c-EYFP mouse model revealed that the vast majority of DC are sessile due to their integration into intercellular networks, yet sparse fast-moving DC could be detected in each of the DC-containing regions. DC located in the subcapsular sinus displayed only sparse dendrites and many large ruffles, which rapidly extended and contracted, and the authors suggested that these DC had recently migrated to the nodes [137]. DC in the paracortical region were interspersed with T cells, and entrenched in vast networks, but extensively probed their surroundings via

extended membrane processes. Three distinct populations of DC were observed in the B cell follicles. Perifollicular DC seemed positioned for Ag acquisition and exhibited slow probing motions, while DC at the border of the T and B cell zones formed clusters and dynamic membrane extensions that captured and drew in nearby lymphocytes, and sparse DC in the follicles were highly motile. These data demonstrate the DC in the lymph nodes form discrete groups with differing motility and probing behavior for interacting with their surroundings. Interestingly, when differentially labeled DC1 and DC2 were imaged their interaction during CD40L stimulation, DC1 becoming sessile as they developed an intercellular TNT-based network of TNTs, while DC2 rapidly migrated around the DC1 networks and repeatedly probed the networks by contacting the dynamic DC1 membrane extensions via their own shorter projections. The impact of differential DC programming on migratory DC compartmentalization and behavior in the lymph nodes remains to be determined. Nevertheless, I propose that CD40L stimulation of DC1 in a 3D culture system could together be used to generate a model of the multicellular reticulated DC network, in order to study coordinated rather than individual DC functions in vitro.

DC reticulation may help or harm depending on the context in which it is induced, yet this phenomenon likely represents a fundamental aspect of DC effector function. The increased surface area and spatial reach afforded by this dynamic process can enhance not only the ability of IFN-γ-polarized DC1 to directly transfer activation signals or Ags to other DC subsets, but can also provide DC a greater opportunity to encounter rare cognate T cells for the efficient initiation of adaptive immune responses. While elevated IL-12p70 production in part explains why DC1 are highly effective inducers of $CD8^+$ T cell responses [8, 125], their ability to reticulate and

maximize opportunities for critical contact with T cells as well as exchange Ags between interconnected DC are also likely contributing factors.

In addition to demonstrating that pre-programmed DC1 respond to CD40L by forming TNT networks, I showed that CD40L and the cytokine IFN-γ can co-stimulate reticulation in mature, non-polarized DC0. These data collectively provide support for the existence of a positive feedback loop wherein successful DC1-driven IFN-γ responses from Th1, CTL, and/or NK cell immune effectors in turn promote continued DC1 polarization [11], and therefore reticulation (Figure 38). Conversely, exposure of DC to the chronic inflammatory mediator PGE_2 during early stages of maturation generates DC2 that not only have a diminished capacity to produce IL-12p70 and promote type-1 immunity [8, 12, 13], but also fail to reticulate in response to CD40 ligation. Furthermore, the Th2 cell-associated cytokine IL-4 substantially inhibits this CD40L-induced process in both DC0 and DC1, suggesting a Th2-driven negative feedback mechanism for inhibiting the reticulation process. Although further study is required to fully understand the regulation and immunologic activity of DC reticulation in vivo, these findings advance our basic comprehension of the mechanisms by which DC bridge innate and adaptive immunity. These results also have important implications in the ongoing quest for therapies to combat cancer and viral pathogens such as HIV-1.

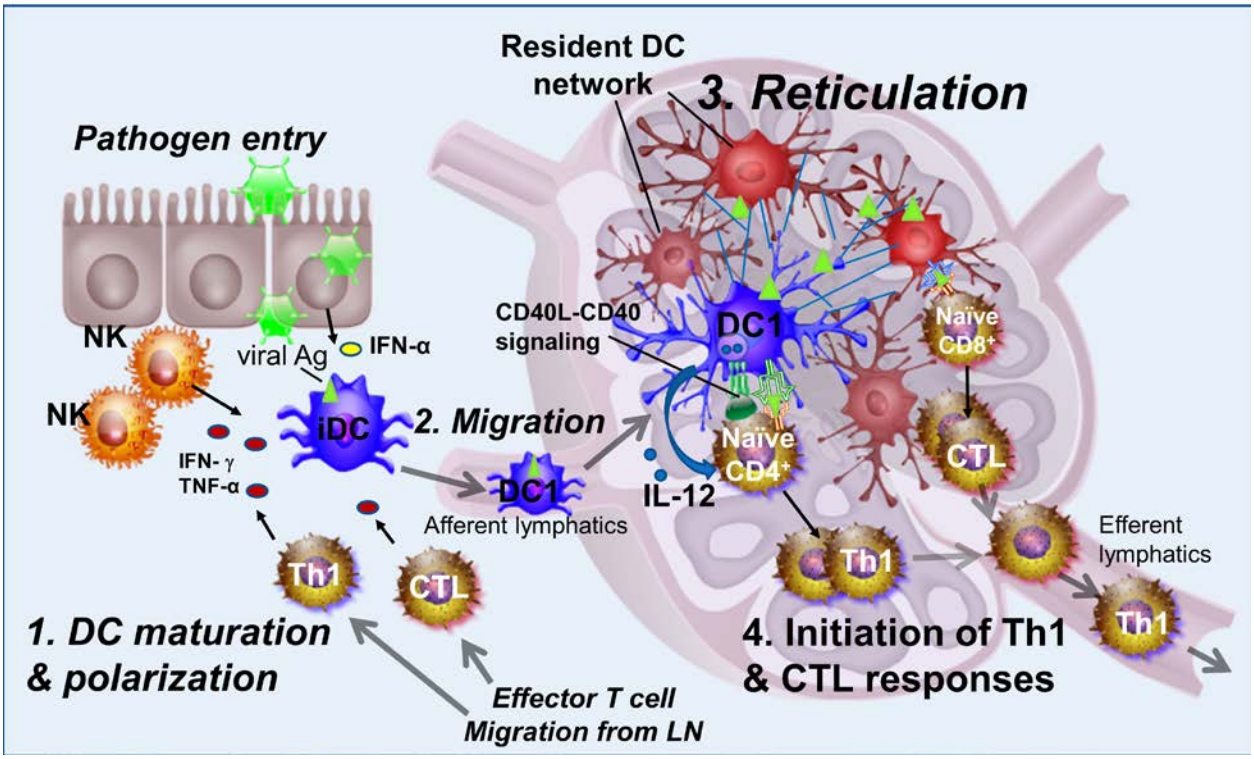

(1) Immature DC are uniquely programmed in the periphery by exposure to pathogen- and host-derived acute inflammatory mediators. (2) Maturing DC1 migrate to the regional lymph node, where they interact with cognate naïve $CD4^+$ T cells. (3) CD40-CD40L signaling mediates bi-directional cross-talk between DC1 and interacting T cells. In addition high IL-12p70 production, CD40L induces uniquely in DC1 the process of reticulation, wherein DC1 develop an extensive network of TNT-like processes. Reticulation likely allows migratory DC1 to integrate in the multicellular resident DC network, and facilitates the direct hand off of Ag to interconnected DC, for amplification of Ag-specific immune responses. The increased surface area and reach afforded by CD40L-induced reticulation also provides additional opportunities for direct contact between DC and T cells. (4) High IL-12p70 production by DC1 results in polarization of Th1- and CTL-driven Ag-specific immune responses. Effector T cells are programmed to migrate from the lymph node to the initial site of infection, where the produce key inflammatory mediators such as IFN-γ and TNF-α upon secondary Ag stimulation, thereby promoting the polarization of additional DC1.

Figure 38. DC1 reticulation induces a positive IFN-γ-driven feedback loop that promotes type-1 responses.

5.2 TNT-MEDIATED INTERCELLULAR COMMUNICATION IN TISSUES

In addition to facilitating integration of migratory into resident DC networks in lymph nodes, TNT-like extensions may also assist pathogen acquisition by sentinel DC in the periphery. My results demonstrate that DC matured under type-1 inflammatory conditions display an enhanced number of ultrafine TNTs prior to secondary CD40L activation, which could indicate a role for TNTs in pathogen sensing in tissues. Watkins and Salter demonstrated that TNT networks induce rapid and extensive calcium fluxes between iDC in response to mechanical stimulation or E. coli supernatants [55], providing convincing evidence of a functional role for TNTs in pathogen sensing. Chinnery et al. [59] revealed that LPS or trauma induced TNT networks between sparse DC residing in the central region of the mouse cornea, supporting a role for TNTs in acute inflammation in specialized tissues close to the external environment. Interestingly, intravital imaging of the lamina propria has revealed an increase in dynamic trans-epithelial DC extensions upon introduction of enteric bacterial pathogens [77]. I have shown that DC exposed to signals from pathogens such as LPS in combination with type-1 inflammatory mediators can develop TNTs, and speculate that interaction with CD40L-expressing effector Th cells could further enhance the number of pathogen-probing extensions formed by DC in the mucosa.

An unpublished intravital imaging study conducted by Blanco and Saban has revealed a vast and intricate TNT network between mononuclear phagocytes, including DC, and nerve axon terminals in the cornea, skin, intestine, and peritoneum of the mouse [60]. Interestingly, TNTs share some morphological and functional qualities with nerve axons, as they both facilitate the formation of vast intercellular networks as well as gap junction-mediated transmission of electrical signals [73, 138]. Although the purpose of this TNT-mediated DC-nerve cell

communication is an open question, sensory nerves have been shown to drive inflammation in a setting of psoriasis and asthma [139, 140]. Nociceptive sensory neurons of the skin induced interlinked dermal DC to produce IL-23, which in turn instigated skin inflammation and psoriasis [139]. Instruction of tissue DC by sensory neurons could represent a defense mechanism to induce inflammation to protect against pathogen invasion or trauma, and a novel mechanism of neuro-immune intercellular communication. Although the function of TNT-comprised intercellular networks between DC and nerve cells remains to be explored, these findings could spur an exciting new area of TNT-related research with important implications in the field of psychoneuroimmunology.

5.3 MECHANISMS OF TNT DEVELOPMENT IN DC

TNTs can be formed between immune cells de novo, when an outgrowth of a filopodia-like protrusion fuses with a target cell membrane, or when two cells make contact at an immunological synapse and subsequently diverge, drawing out the membrane tether [35]. Based on time-lapse imaging of live cells, I conclude that TNT formation in the setting of reticulation relies primarily on the filopodia-driven model, although we also occasionally visualized TNTs being drawn out after close contact between 2 cells. Further study is needed to determine the actin dynamics and the role of molecular motors such as myosin-X in these 2 distinct modes of TNT formation in DC1. My observations support the concept that TNTs actively seek nearby and distant cell targets, as opposed to being randomly put forth, and an in vivo study of TNT development by DC in the mouse cornea supports this assertion [59]. Taken together, these data imply some type of chemotactic direction of TNT movement, and I consider this to be an

important unanswered question in the field of TNT research. A recent study showed that exogenous melanoma-derived exosomes enhanced TNT formation in lipid raft-enriched melanoma cells, and TNTs facilitated their direct cell-cell transfer [69]. I speculate that chemokine or exosome secretion by DC1 plays a role in directing TNT development by providing chemotactic stimuli. My SEM data has provided initial visual evidence of a possible link between the TNT and exosome communication pathways in inflammatory DC1, and I propose a convergence of the exocytic and TNT pathways upon interaction with LST1 and the RalA-exocyst complex. Further investigation is required to delineate the relationship between these 2 modes of intercellular communication, which could also have important implications in the context of HIV-1 trans-infection.

5.4 TNT NETWORKS AND DC1-MEDIATED HIV-1 TRANS-INFECTION

While DC1 reticulation is likely important for direct communication between immune cells, this process may conversely facilitate progression of chronic diseases such as HIV-1 or cancer. TNTs can be hijacked by intracellular pathogens to enhance rapid spread to distant cells, while avoiding the inhospitable extracellular milieu. HIV-1 was shown to induce TNTs in infected macrophages and utilize them for high-speed transmission to neighboring uninfected macrophages [86-88], and utilize existing TNTs displayed by $CD4^+$ T cells to support the direct virus transfer from infected to uninfected T cells over long distances [67]. While DC are resistant to cis-infection by HIV-1, they can act as a 'Trojan horse' by sequestering intact virions and mediating trans-infection of $CD4^+$ T cells upon transmission of virions across the virologic synapse [90]. Herein, I investigated the ability of differentially programmed mature DC to

mediate HIV-1 trans-infection to $CD4^+$ T cells. In accordance with other reports [113, 115], DC1 displayed a dramatically enhanced capacity for trans-infection compared to DC2, which were inefficient, and DC0, which displayed an intermediate ability to transmit HIV-1 similar to iDC.

While the C-type lectin DC-SIGN was initially thought to be responsible for the acquisition of HIV-1 by both iDC and mature DC, recent studies have shown that Siglec-1, which interacts with sialyllactose moieties of viral membrane gangliosides, is the primary capture molecule in mature DC [89]. Siglec-1 is upregulated on the DC surface upon LPS maturation or exposure to type-I IFNs, and I therefore investigated the possibility of differential expression of Siglec-1 on polarized DC. Both DC-SIGN and Siglec-1 were highly expressed on DC1, while DC2 expressed less DC-SIGN and almost undetectable levels of Siglec-1. Furthermore, DC0 displayed an intermediate expression of these capture molecules, in accordance with their intermediate trans-infection ability. Furthermore, microarray-based analysis of mRNA expression by DC1 and DC2 detected similar dramatic differences in mRNA levels of these 2 capture molecules. Although blocking studies are needed to confirm the role of these capture molecules in our trans-infection system, I nevertheless provided striking evidence that DC1 possess a superior ability to capture HIV-1 prior to transmission to $CD4^+$ T cells compared to DC2, which likely contributes to enhanced DC1 trans-infection.

I next investigated the role of the CD40L-induced reticulation process, which results in the formation of an extensive intercellular network of TNT-like processes, in DC1-mediated trans-infection. The inhibition of CD40L-CD40 signaling with blocking anti-CD40L mAb almost completely abrogated DC1 trans-infection, providing a rationale for further investigation of CD40L-inducible TNTs in this process. Cholesterol-rich lipid rafts are critical for the stability

of TNTs [47], and our research group recently found that altered cholesterol metabolism restricts the ability of APC from a subset HIV-1^+ NP to transmit virus to $CD4^+$ T cells [110]. Therefore, I next assessed the ability of simvastatin, a specific inhibitor of an early step in cholesterol biosynthesis, to inhibit the reticulation process and DC1-mediated trans-infection. Pre-treatment of DC1 with simvastatin or an F-actin depolymerization drug latrunculin A, which is typically used to block TNTs, indeed almost completely abrogated DC1 trans-infection. Taken together, these data provide further evidence of a role for CD40L-inducible TNTs in DC1-mediated trans-infection. Furthermore, my live-cell super-resolution imaging studies provided striking visual confirmation of HIV-1 transmission from DC1 to $CD4^+$ T cells via both thin and thick TNTs in the setting of reticulation. TNT networks also readily supported the exchange of HIV-1 between interconnected DC1, which could serve to amplify the viral reservoir in lymph nodes. Furthermore, I confirmed higher expression of ICAM-1 on the surface of DC1 compared to DC2, in accordance with a previous study that linked differential expression of this molecule to enhanced DC1 trans-infection [113]. Again, microarray showed differential mRNA expression levels of ICAM-1 in representative DC1 and DC2. Finally, additional live-cell super-resolution studies revealed the localization of ICAM-1 clusters, a key molecule in promoting interaction between DC and T cells, to the surface of TNTs and co-localization of HIV-1-like particles with ICAM-1 puncti. I propose that ICAM-1 clusters on the TNT surface can provide additional sites for close contact with $CD4^+$ T cells in the nodes, and CD40L-inducible DC1-derived membrane protrusions can directly transmit the virus to interacting $CD4^+$ T cells.

The research presented herein provides an improved understanding of the mechanisms that facilitate enhanced DC1 trans-infection. I envision 4 distinct mechanisms whereby unique features of DC1 promote HIV-1 transmission in the context of early infection (Figure 39).

Firstly, iDC respond to acute inflammatory signals in the periphery that induce maturation and DC1 polarization as well as concomitant up-regulation of Siglec-1, which in turn mediates efficient capture of HIV-1 in the periphery. After initial virus acquisition, the DC carry intact virions in complex, surface-accessible crypts on the membrane as they migrate to the regional lymph node. The current literature has shown that DC1 secrete high levels of chemokines such as CCL5 for attracting $CCR5^+$ susceptible $CD4^+$ T cells [141]. In the second phase, we therefore hypothesize that chemokine secretion by DC1 results in homing susceptible T cells to DC1, followed by engagement of LFA-1 on the T cell via clusters of ICAM-1 on the DC1 surface, which brings the 2 cells into close contact. Thirdly, subsequent CD40-CD40L bidirectional signaling induces in DC1 both high IL-12p70 production and the development of an extensive network of TNTs. We postulate that virus is shuttled from crypts along these DC-derived membrane protrusions in association with Siglec-1. Finally, ICAM-1 clusters on the surface of TNTs facilitate additional direct DC1-T cell interactions, and promote HIV-1 transmission from TNTs to interdigitated T cells membranes by a receptor-dependent mechanism. Alternatively, $CD4^+$ T cells can form uropods or filopodia to acquire HIV-1 directly from virus-enriched crypts [97, 106]. In addition to providing a direct conduit for HIV-1 dissemination from migratory DC1 to susceptible T cells in acute infection, I propose that reticulation facilitates viral spread from migratory to interlinked lymph node-residing DC, thereby amplifying the proportion of cells harboring and able to transmit the virus.

In the setting of chronic infection, the reticulated DC network in the nodes could conceivably serve as a long-term HIV-1 reservoir, and contribute to disease progression. Importantly, our research recently showed that CTL-driven epitope divergence results in surviving HIV-1 epitope variants that can selectively utilize CTL helper activity in the absence

of killing to induce and program DC1 capable of efficiently mediating HIV-1 trans-infection of $CD4^+$ T cells [93, 94]. The current study demonstrates that $CD8^+$ T cell-matured DC1 also reticulate in response to CD40L. Taken together, these data imply that HIV-1 can facilitate TNT-mediated viral spread during chronic infection by inducing dysfunctional, cross-reactive CTL that promote DC1. IFN-γ-programmed DC1 likely perpetuate a positive feedback loop wherein DC1 drive Th1 and CTL responses, which in turn induce more DC1 in an IFN-γ-dependent manner.

Additionally, studies have shown that the HIV-1 accessory protein Nef can directly promote TNT development in infected macrophages via interaction with the exocyst complex, which is critical for both TNT formation and vesicle secretion at the plasma membrane [43, 92]. Nef-induced TNTs can promote Nef-mediated B cell dysfunction by directly transferring this multifunctional molecule from macrophages to B cells in lymphoid tissues, as well as providing an avenue for HIV-1 spread. Importantly, HIV-1 can acquire CD40L as it buds from $CD4^+$ T cells, and promote B cell activation and dysfunction through sustained stimulation of CD40 in the B cell-containing compartments of lymph nodes [142]. Taken together, these results infer that CD40L-expressing HIV-1 virions may directly instigate a CD40L-driven positive feedback loop that induces TNT networks in DC1 for enhanced DC-mediated virus transmission in vivo. In summary, HIV-1 appears to utilize multiple novel aspects of DC1 phenotype and function for enhanced cell-cell spread, which could be relevant in the setting of both acute and chronic infection. Although questions remain regarding the importance of trans-infection in natural infection, this dissertation demonstrates that CD40L-inducible DC1 reticulation is a double-edged sword in the context of HIV-1 infection and highlights this process as a potential target for interrupting viral transmission in vivo.

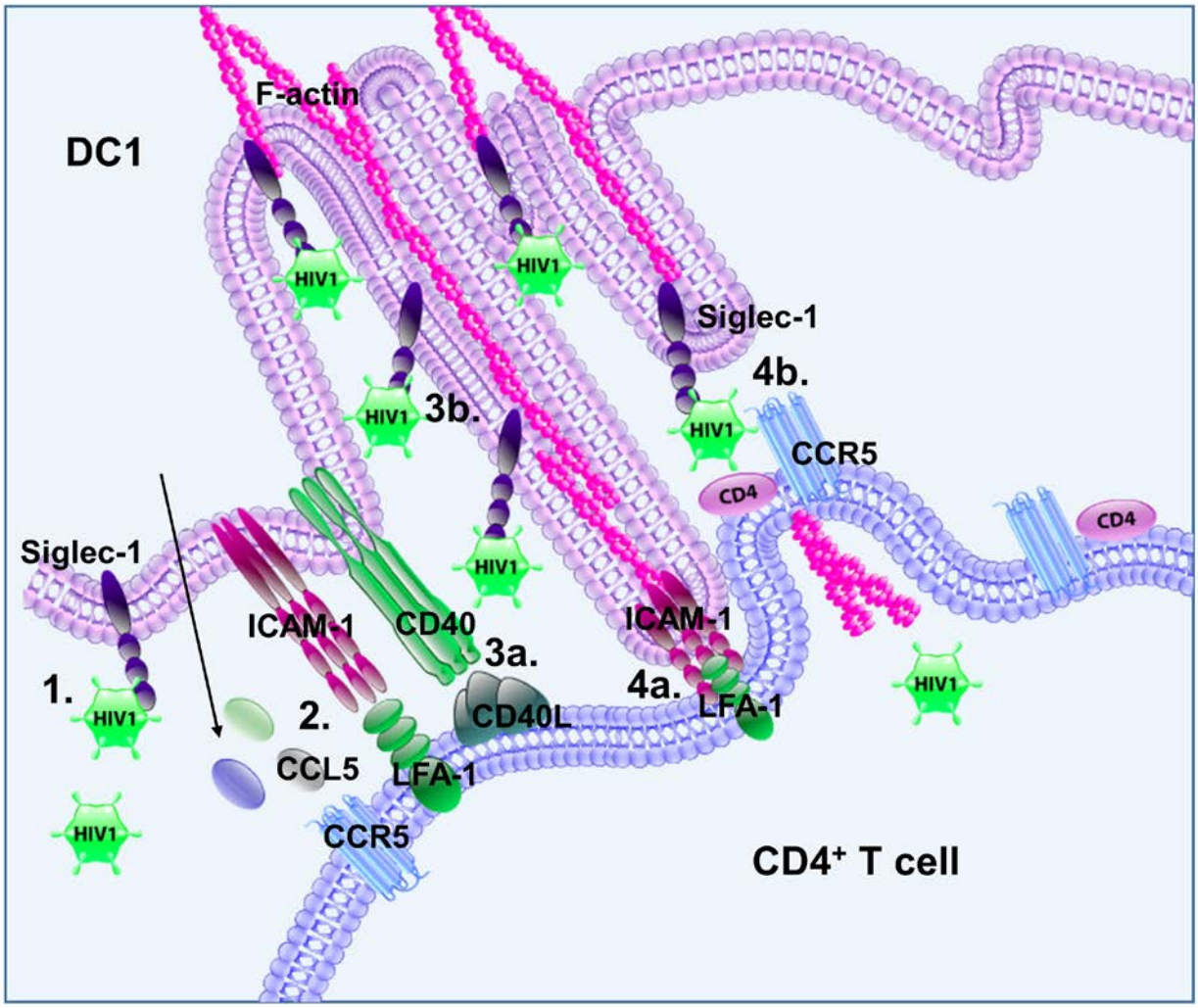

Represented are 4 distinct mechanisms that enhance DC1-mediated HIV-1 transmission to $CD4^+$ T cells in the context of early infection. (1) In the periphery, iDC are polarized by acute inflammatory signals and maturing DC1 exhibit high expression of Siglec-1, which participates in HIV-1 acquisition. After initial virus capture, the DC1 carry intact virus in complex, surface-accessible crypts on the membrane as they migrate to the regional lymph node. (2) DC1 reach the lymph node where they secrete chemokines that attract susceptible $CD4^+$ T cells, and ICAM-1 clusters on the DC1 surface engage LFA-1 on the T cell, bringing the 2 cells into close contact. (3) CD40-CD40L bidirectional signaling induces the development of an extensive network of TNT-like membrane protrusions by DC1 (a), and the virus is shuttled from the crypts along these protrusions in association with Siglec-1 (b). (4) ICAM-1 clusters on the surface of TNTs facilitate additional direct interactions between DC1 and T cells (a), and promote direct HIV-1 transmission from TNTs to interdigitated T cell membranes by a receptor-dependent mechanism (b).

Figure 39. Diverse mechanisms of DC1-mediated HIV-1 trans-infection of $CD4^+$ T cells.

6.0 IMPLICATIONS TO PUBLIC HEALTH

6.1 DC1-BASED VACCINES: A ROLE FOR TNTS?

Ex vivo generated Ag-bearing αDC1 are currently being utilized as cancer vaccines due to their selective induction of tumor-specific Th1 cells and CTLs that are capable of homing to tumor sites in vivo [141, 143]. The αDC1 cocktail was originally developed in order to induce high IL-12p70-producing DC1 ex vivo in serum free media for clinical applications [8]. Tumor-Ag loaded αDC1 are capable of inducing tumor-specific CTL responses 20-70 times higher than that of PGE_2-programmed DC2. Aside from their high IL-12 production, which is critical for inducing Th1- and CTL-driven responses, these polarized DC1 also secrete high levels of chemokines such as CCL5 and CXCL10, for attracting effector T cells, and they induce T cells expression of chemokine receptors for homing to the location of tumors in vivo [141]. Herein, I have demonstrated the unique ability of DC1 to respond to Th cell-associated CD40L by forming vast networks of TNTs, which in turn facilitate the direct transfer of Ag from donor to recipient DC for the efficient induction of Ag-specific T cell responses [134]. Another recent study demonstrated that TNTs can mediate the direct transfer of MHC class I molecules [58]. I assert that inducible TNT networks represent an important pathway for the transfer of Ag from migratory to resident DC for the efficient induction of NK-, CTL-, and Th1-driven immune

responses, which represents an additional characteristic of DC1 that contributes to their efficacy as cancer immunotherapies.

DC-derived exosomes, a mechanism of intercellular communication that may be directly linked with TNTs, are currently being investigated as treatments for cancer and neurological disorders. I propose that the next wave of research into nanoscale therapies will likely seek to harness the power of TNTs. DC-derived exosomes vary in function depending on the activation state of the originating cell, and these structures can induce either immune activation or tolerance [71]. Exosome-induced programming of DC is emerging as a useful technique for priming T cell responses that suppress cancer cell proliferation as well as eliminating tumors [144]. A recent report by Kraig and colleagues demonstrated that IFN-γ-treated DC release microRNA-containing exosomes that can increase baseline myelination, reduce oxidative stress, and induce remyelination in hippocampal slice cultures [145]. Furthermore, nasal administration of exosomes facilitated CNS myelination in vivo, indicating that polarized exosomes could be used to promote remyelination for treatment of multiple sclerosis and other dysmyelinating disorders. TNT-mediated transfer of genetic materials is not well understood, however one study demonstrated that TNTs can mediate the direct transfer of microRNAs between tumor and stromal cells [78]. While many of the current studies are focused on cell-free nanoscale exosome therapies, TNTs could provide an additional direct mechanism for delivering polarized exosomes or microRNAs to tumors or the CNS in order to treat cancer or neurological disorders, respectively, as well as certain infectious diseases.

6.2 TNT-MEDIATED RESCUE OF TISSUES BY MITOCHONDRIAL DNA TRANSFER

Although cell-cell organelle transfer via TNTs has been observed in various cell types including T cells, macrophages, NRK cells, epithelial cells, and myocardial cells since their discovery in 2004 [35, 37], the ramifications of this exchange are still under investigation. The cell-cell exchange of mitochondria is thought to be a general mechanism for rescuing stressed or damaged cells, and TNTs may provide a direct pathway for such exchange. In 2014, Yan and colleagues demonstrated that TNTs mediate unidirectional transfer of mitochondria from mesenchymal stem cells to injured human vascular endothelial cells, which results in the rescue of aerobic respiration and protection from apoptosis by an unknown mechanism [146]. Wang and Gerdes published a report in early 2015 demonstrating that UV-treated PC12 cells can be rescued from the early stages of apoptosis upon TNT-mediated acquisition of functional mitochondria from healthy PC12 cells [147]. Unlike healthy cells, TNTs formed by stressed cells contained microtubule tracks that facilitated mitochondria transport, demonstrating that these stress-induced TNTs possess a distinctive cytoskeletal composition and unique biophysical properties. Importantly, a disorganized microtubule network coupled with mitochondrial damage are considered to be hallmarks of neurodegenerative disorders such as Parkinson's disease [148]. TNTs could provide a future therapeutic delivery system for mitochondria-mediated rescue of stressed or damaged cells, particularly those that do not regenerate or proliferate slowly, such as cardiomyocytes and neurons.

6.3 TNTS AND CHRONIC DISEASES: A DOUBLE-EDGED SWORD

6.3.1 Cancer biology

Current literature and my own investigation together suggest that TNT-mediated intercellular communication can be detrimental, particularly in the context of chronic diseases such as cancer and HIV-1 infection. The bi-directional transfer of vesicles, proteins, and mitochondria via TNTs was recently observed between malignant human pleural mesothelioma cells and lung adenocarcinoma tumor specimens [57], suggesting that tumors utilize TNTs to support their development. The possible roles for TNTs in cancer biology include the transfer and subsequent dissemination of chemotherapy resistance proteins or genes, similar to the propagation of antibiotic resistance genes observed between both closely and distantly related bacterial species [74]. Furthermore, TNT formation between malignant cells and surrounding stromal cells may support tumor development and progression in advance of tumor invasion and metastasis [39]. On the other hand, the presence of TNTs in tumors could represent an avenue for delivery of biological agents or small molecule inhibitors into tumors, which are difficult to penetrate using current methods. The study of TNTs in the context of cancer will therefore likely be another area of intensive research in the coming years.

6.3.2 DC-mediated trans-infection and HIV-1 disease progression

Our previous work revealed that iDC and B cells isolated from a subset of HIV-1 infected NP, who can control virus infection for many years in the absence of ART, fail to mediate HIV-1 trans-infection due to alterations in cellular cholesterol metabolism resulting from increased

activity of the cholesterol transporter, ABCA-1 [110]. This ability can be restored by reconstitution of cellular cholesterol or inhibited in PR and HIV-1 naïve donors by treatment of APC with statins. The current study has revealed that multiple mechanisms contribute to enhanced trans-infection of $CD4^+$ T cells by DC1, which are generated in the setting of acute inflammation, and this process may be important for promoting HIV-1 persistence in vivo. I observed a striking inhibition of CD40L-induced reticulation in DC1 derived from these same NP, which correlates with their inability to trans-infect $CD4^+$ T cells, while DC1 generated from PR and HIV-1 naïve donors reticulate and trans-infect efficiently. In support of a role for TNTs in APC-mediated trans-infection, simvastatin pre-treatment completely abolished DC1 trans-infection at a concentration that also inhibited reticulation.

A previous study demonstrated that statins decrease viral loads in chronically infected patients as well as in HIV-1 infected cells in vitro due to inhibition of HIV-1 binding to target cells and viral fusion [149]. I propose that alterations in cellular cholesterol metabolism inhibit HIV-1 infection on multiple levels, including TNT- and exosome-mediated APC trans-infection. The genetic link and the exact mechanisms by which altered cholesterol metabolism inhibit DC trans-infection in NP remain to be elucidated. Aside from genomic and epigenomic studies in NP and PR cohorts, our research group aims to conduct mechanistic studies to explore a potential link between reduced cholesterol content in the cell membrane of APC and their reduced ability to form TNTs and release exosomes, which could together represent an important pathway for HIV-1 transmission.

6.3.3 Future directions of TNT research

These findings demonstrate that iDC are programmed by combinations of host- and pathogen-derived acute inflammatory signals to reticulate, or develop extensive networks of TNTs, upon interaction with cognate CD40L-expressing $CD4^+$ Th cells. Reticulation likely results in integration of migratory DC1 into the vast intercellular network of resident DC built on the stromal infrastructure in lymph nodes. Furthermore, the reticulation process may allow a coordinated multicellular response between migratory DC matured in a setting of acute inflammation and interlinked resident DC by facilitating Ag exchange for the efficient induction of Th1 and CTL responses. This unique ability to develop TNT networks, in addition to their ability to produce high levels of the Th1 polarizing cytokine IL-12p70 and chemokines for attracting appropriate T cell subsets, could contribute to the current and future success of DC1-based immunotherapies for cancer [141].

Reticulation also likely promotes a positive feedback loop wherein effector Th1 cells home to infected tissues and secrete DC1-inducing cytokines at the sight of infection, which induce the polarization of tissue iDC to DC1. In support of this, I also showed that the reticulation process is positively regulated by the Th1 cytokine, IFN-γ, and negatively regulated by the Th2 cytokine, IL-4. Taken together, these data illuminate the intriguing possibility that ex vivo generated Ag-bearing DC1 could be used in induce TNT-expressing migratory DC at the primary site of infection, thereby amplifying a primary adaptive immune responses to viral or cancer-relevant Ags. Intriguingly, cutting edge research has revealed a bidirectional communication network between nerve axons and myeloid-origin immune sentinels in MALT-associated tissues [60]. These data indicate a role for DC-derived TNTs in tissues in the steady state, in addition to my findings that are applicable in the setting of acute inflammation. The full

ramifications of a TNT-mediated interface between the immune and neurological systems in tissues and CD40L-inducible reticulation in the context of an immune response in lymph nodes remain to be explored. Nevertheless, I have clearly demonstrated a role for CD40L-inducible TNT networks in the orchestration of Th1- and CTL-biased adaptive immune responses by DC programmed by acute mediators of type-1 immunity. On the other hand, this process can be hijacked by HIV-1 for enhanced DC1-mediated high-speed transmission to $CD4^+$ T cells, and may also be linked to disease progression. Conceivably, many other viruses may utilize TNTs for cell-cell spread, and future investigations are sorely needed to identify these pathogens and to explore TNTs as a target for interrupting viral transmission.

Cutting-edge research laboratories are currently working to harness other forms of DC-mediated intercellular communication such as exosomes to treat certain chronic diseases, and TNTs represent the logical next step in this area of research. These versatile conduits can incorporate aspects of all the other known modes of direct and indirect intercellular communication, as they form receptor-ligand complexes, immunologic synapses, and gap junctions at the point of contact with target cell membranes, and can also directly mediate the rapid exchange of membrane vesicles, electrical signals, and calcium fluxes between distant interconnected cells [35, 37, 73]. The research herein has revealed mechanisms of TNT network induction and regulation in migratory DC by $CD4^+$ Th cells in the context of an immune response, providing clues that could someday enable us to utilize this powerful and multifarious mode of intercellular communication to treat certain cancers, neurological disorders, and infectious diseases.

BIBLIOGRAPHY

1. Steinman, R.M. and J. Banchereau, *Taking dendritic cells into medicine.* Nature, 2007. **449**(7161): p. 419-26.
2. Kalinski, P., et al., *T-cell priming by type-1 and type-2 polarized dendritic cells: the concept of a third signal.* Immunol Today, 1999. **20**(12): p. 561-7.
3. Kapsenberg, M.L., *Dendritic-cell control of pathogen-driven T-cell polarization.* Nat Rev Immunol, 2003. **3**(12): p. 984-93.
4. Bennett, S.R., et al., *Help for cytotoxic-T-cell responses is mediated by CD40 signalling.* Nature, 1998. **393**(6684): p. 478-80.
5. Schoenberger, S.P., et al., *T-cell help for cytotoxic T lymphocytes is mediated by CD40-CD40L interactions.* Nature, 1998. **393**(6684): p. 480-3.
6. Ridge, J.P., F. Di Rosa, and P. Matzinger, *A conditioned dendritic cell can be a temporal bridge between a CD4+ T-helper and a T-killer cell.* Nature, 1998. **393**(6684): p. 474-8.
7. Koguchi, Y., et al., *Preformed CD40 ligand exists in secretory lysosomes in effector and memory CD4+ T cells and is quickly expressed on the cell surface in an antigen-specific manner.* Blood, 2007. **110**(7): p. 2520-7.
8. Mailliard, R.B., et al., *alpha-type-1 polarized dendritic cells: a novel immunization tool with optimized CTL-inducing activity.* Cancer Res, 2004. **64**(17): p. 5934-7.
9. Mailliard, R.B., et al., *Dendritic cells mediate NK cell help for Th1 and CTL responses: two-signal requirement for the induction of NK cell helper function.* J Immunol, 2003. **171**(5): p. 2366-73.
10. Trinchieri, G., *Interleukin-12 and the regulation of innate resistance and adaptive immunity.* Nat Rev Immunol, 2003. **3**(2): p. 133-46.
11. Kalinski, P. and M. Moser, *Consensual immunity: success-driven development of T-helper-1 and T-helper-2 responses.* Nat Rev Immunol, 2005. **5**(3): p. 251-60.
12. Vieira, P.L., et al., *Development of Th1-inducing capacity in myeloid dendritic cells requires environmental instruction.* J Immunol, 2000. **164**(9): p. 4507-12.
13. Kalinski, P., *Regulation of immune responses by prostaglandin E2.* J Immunol, 2012. **188**(1): p. 21-8.
14. Mailliard, R.B., et al., *Complementary dendritic cell-activating function of CD8+ and CD4+ T cells: helper role of CD8+ T cells in the development of T helper type 1 responses.* J Exp Med, 2002. **195**(4): p. 473-83.
15. Lanzavecchia, A., *Mechanisms of antigen uptake for presentation.* Curr Opin Immunol, 1996. **8**(3): p. 348-54.

16. Banchereau, J. and R.M. Steinman, *Dendritic cells and the control of immunity.* Nature, 1998. **392**(6673): p. 245-52.
17. Joffre, O.P., et al., *Cross-presentation by dendritic cells.* Nat Rev Immunol, 2012. **12**(8): p. 557-69.
18. Jongbloed, S.L., et al., *Human CD141+ (BDCA-3)+ dendritic cells (DCs) represent a unique myeloid DC subset that cross-presents necrotic cell antigens.* J Exp Med, 2010. **207**(6): p. 1247-60.
19. Villadangos, J.A. and K. Shortman, *Found in translation: the human equivalent of mouse CD8+ dendritic cells.* J Exp Med, 2010. **207**(6): p. 1131-4.
20. den Haan, J.M., S.M. Lehar, and M.J. Bevan, *CD8(+) but not CD8(-) dendritic cells cross-prime cytotoxic T cells in vivo.* J Exp Med, 2000. **192**(12): p. 1685-96.
21. Allan, R.S., et al., *Migratory dendritic cells transfer antigen to a lymph node-resident dendritic cell population for efficient CTL priming.* Immunity, 2006. **25**(1): p. 153-62.
22. Qu, C., et al., *MHC class I/peptide transfer between dendritic cells overcomes poor cross-presentation by monocyte-derived APCs that engulf dying cells.* J Immunol, 2009. **182**(6): p. 3650-9.
23. Albert, M.L., B. Sauter, and N. Bhardwaj, *Dendritic cells acquire antigen from apoptotic cells and induce class I-restricted CTLs.* Nature, 1998. **392**(6671): p. 86-9.
24. Andre, F., et al., *Exosomes as potent cell-free peptide-based vaccine. I. Dendritic cell-derived exosomes transfer functional MHC class I/peptide complexes to dendritic cells.* J Immunol, 2004. **172**(4): p. 2126-36.
25. Harshyne, L.A., et al., *A role for class A scavenger receptor in dendritic cell nibbling from live cells.* J Immunol, 2003. **170**(5): p. 2302-9.
26. Bousso, P., *T-cell activation by dendritic cells in the lymph node: lessons from the movies.* Nat Rev Immunol, 2008. **8**(9): p. 675-84.
27. Swetman, C.A., et al., *Extension, retraction and contraction in the formation of a dendritic cell dendrite: distinct roles for Rho GTPases.* Eur J Immunol, 2002. **32**(7): p. 2074-83.
28. Commins, S.P., L. Borish, and J.W. Steinke, *Immunologic messenger molecules: cytokines, interferons, and chemokines.* J Allergy Clin Immunol, 2010. **125**(2 Suppl 2): p. S53-72.
29. Robbins, P.D. and A.E. Morelli, *Regulation of immune responses by extracellular vesicles.* Nat Rev Immunol, 2014. **14**(3): p. 195-208.
30. Neijssen, J., B. Pang, and J. Neefjes, *Gap junction-mediated intercellular communication in the immune system.* Prog Biophys Mol Biol, 2007. **94**(1-2): p. 207-18.
31. Joly, E. and D. Hudrisier, *What is trogocytosis and what is its purpose?* Nat Immunol, 2003. **4**(9): p. 815.
32. Dustin, M.L., *A dynamic view of the immunological synapse.* Semin Immunol, 2005. **17**(6): p. 400-10.
33. Salter, R.D., et al., *Rapid and extensive membrane reorganization by dendritic cells following exposure to bacteria revealed by high-resolution imaging.* J Leukoc Biol, 2004. **75**(2): p. 240-3.
34. Mattila, P.K. and P. Lappalainen, *Filopodia: molecular architecture and cellular functions.* Nat Rev Mol Cell Biol, 2008. **9**(6): p. 446-54.
35. Davis, D.M. and S. Sowinski, *Membrane nanotubes: dynamic long-distance connections between animal cells.* Nat Rev Mol Cell Biol, 2008. **9**(6): p. 431-6.

36. Wang, X. and H.H. Gerdes, *Long-distance electrical coupling via tunneling nanotubes.* Biochim Biophys Acta, 2012. **1818**(8): p. 2082-6.
37. Marzo, L., K. Gousset, and C. Zurzolo, *Multifaceted roles of tunneling nanotubes in intercellular communication.* Front Physiol, 2012. **3**: p. 72.
38. Rustom, A., et al., *Nanotubular highways for intercellular organelle transport.* Science, 2004. **303**(5660): p. 1007-10.
39. Lou, E., et al., *Tunneling Nanotubes: A new paradigm for studying intercellular communication and therapeutics in cancer.* Commun Integr Biol, 2012. **5**(4): p. 399-403.
40. Pasquier, J., et al., *Preferential transfer of mitochondria from endothelial to cancer cells through tunneling nanotubes modulates chemoresistance.* J Transl Med, 2013. **11**: p. 94.
41. Hase, K., et al., *M-Sec promotes membrane nanotube formation by interacting with Ral and the exocyst complex.* Nat Cell Biol, 2009. **11**(12): p. 1427-32.
42. Kimura, S., K. Hase, and H. Ohno, *The molecular basis of induction and formation of tunneling nanotubes.* Cell Tissue Res, 2013. **352**(1): p. 67-76.
43. Mukerji, J., et al., *Proteomic analysis of HIV-1 Nef cellular binding partners reveals a role for exocyst complex proteins in mediating enhancement of intercellular nanotube formation.* Retrovirology, 2012. **9**: p. 33.
44. Schiller, C., et al., *LST1 promotes the assembly of a molecular machinery responsible for tunneling nanotube formation.* J Cell Sci, 2013. **126**(Pt 3): p. 767-77.
45. Gousset, K., et al., *Myo10 is a key regulator of TNT formation in neuronal cells.* J Cell Sci, 2013. **126**(Pt 19): p. 4424-35.
46. Lokar, M., A. Iglic, and P. Veranic, *Protruding membrane nanotubes: attachment of tubular protrusions to adjacent cells by several anchoring junctions.* Protoplasma, 2010. **246**(1-4): p. 81-7.
47. Lokar, M., et al., *The role of cholesterol-sphingomyelin membrane nanodomains in the stability of intercellular membrane nanotubes.* Int J Nanomedicine, 2012. **7**: p. 1891-902.
48. Wang, Y., et al., *Tunneling-nanotube development in astrocytes depends on p53 activation.* Cell Death Differ, 2011. **18**(4): p. 732-42.
49. Fifadara, N.H., et al., *Interaction between activated chemokine receptor 1 and FcepsilonRI at membrane rafts promotes communication and F-actin-rich cytoneme extensions between mast cells.* Int Immunol, 2010. **22**(2): p. 113-28.
50. Chauveau, A., et al., *Membrane nanotubes facilitate long-distance interactions between natural killer cells and target cells.* Proc Natl Acad Sci U S A, 2010. **107**(12): p. 5545-50.
51. Gerdes, H.H., N.V. Bukoreshtliev, and J.F. Barroso, *Tunneling nanotubes: a new route for the exchange of components between animal cells.* FEBS Lett, 2007. **581**(11): p. 2194-201.
52. Gurke, S., J.F. Barroso, and H.H. Gerdes, *The art of cellular communication: tunneling nanotubes bridge the divide.* Histochem Cell Biol, 2008. **129**(5): p. 539-50.
53. Austefjord, M.W., H.H. Gerdes, and X. Wang, *Tunneling nanotubes: Diversity in morphology and structure.* Commun Integr Biol, 2014. **7**(1): p. e27934.
54. Gerdes, H.H. and R.N. Carvalho, *Intercellular transfer mediated by tunneling nanotubes.* Curr Opin Cell Biol, 2008. **20**(4): p. 470-5.
55. Watkins, S.C. and R.D. Salter, *Functional connectivity between immune cells mediated by tunneling nanotubules.* Immunity, 2005. **23**(3): p. 309-18.

56. Smith, I.F., J. Shuai, and I. Parker, *Active generation and propagation of Ca2+ signals within tunneling membrane nanotubes.* Biophys J, 2011. **100**(8): p. L37-9.
57. Onfelt, B., et al., *Structurally distinct membrane nanotubes between human macrophages support long-distance vesicular traffic or surfing of bacteria.* J Immunol, 2006. **177**(12): p. 8476-83.
58. Schiller, C., et al., *Tunneling nanotubes enable intercellular transfer of MHC class I molecules.* Hum Immunol, 2013. **74**(4): p. 412-6.
59. Chinnery, H.R., E. Pearlman, and P.G. McMenamin, *Cutting edge: Membrane nanotubes in vivo: a feature of MHC class II+ cells in the mouse cornea.* J Immunol, 2008. **180**(9): p. 5779-83.
60. Blanco, T. and D. Saban, *Intravital multiphoton visualization identifies inter-working between nerves and bone marrow-derived cells of the mouse cornea*. 2014, Duke University.
61. Knop, E. and N. Knop, *The role of eye-associated lymphoid tissue in corneal immune protection.* J Anat, 2005. **206**(3): p. 271-85.
62. Bangert, C., P.M. Brunner, and G. Stingl, *Immune functions of the skin.* Clin Dermatol, 2011. **29**(4): p. 360-76.
63. Turner, J.R., *Intestinal mucosal barrier function in health and disease.* Nat Rev Immunol, 2009. **9**(11): p. 799-809.
64. Onfelt, B., et al., *Cutting edge: Membrane nanotubes connect immune cells.* J Immunol, 2004. **173**(3): p. 1511-3.
65. Stinchcombe, J.C., et al., *The immunological synapse of CTL contains a secretory domain and membrane bridges.* Immunity, 2001. **15**(5): p. 751-61.
66. Arkwright, P.D., et al., *Fas stimulation of T lymphocytes promotes rapid intercellular exchange of death signals via membrane nanotubes.* Cell Res, 2010. **20**(1): p. 72-88.
67. Sowinski, S., et al., *Membrane nanotubes physically connect T cells over long distances presenting a novel route for HIV-1 transmission.* Nat Cell Biol, 2008. **10**(2): p. 211-9.
68. Rainy, N., et al., *H-Ras transfers from B to T cells via tunneling nanotubes.* Cell Death Dis, 2013. **4**: p. e726.
69. Thayanithy, V., et al., *Tumor exosomes induce tunneling nanotubes in lipid raft-enriched regions of human mesothelioma cells.* Exp Cell Res, 2014. **323**(1): p. 178-88.
70. Mineo, M., et al., *Exosomes released by K562 chronic myeloid leukemia cells promote angiogenesis in a Src-dependent fashion.* Angiogenesis, 2012. **15**(1): p. 33-45.
71. Gutierrez-Vazquez, C., et al., *Transfer of extracellular vesicles during immune cell-cell interactions.* Immunol Rev, 2013. **251**(1): p. 125-42.
72. Wiley, R.D. and S. Gummuluru, *Immature dendritic cell-derived exosomes can mediate HIV-1 trans infection.* Proc Natl Acad Sci U S A, 2006. **103**(3): p. 738-43.
73. Abounit, S. and C. Zurzolo, *Wiring through tunneling nanotubes--from electrical signals to organelle transfer.* J Cell Sci, 2012. **125**(Pt 5): p. 1089-98.
74. Dubey, G.P. and S. Ben-Yehuda, *Intercellular nanotubes mediate bacterial communication.* Cell, 2011. **144**(4): p. 590-600.
75. Peralta, B., et al., *Mechanism of membranous tunnelling nanotube formation in viral genome delivery.* PLoS Biol, 2013. **11**(9): p. e1001667.
76. Lou, E., et al., *Tunneling nanotubes provide a unique conduit for intercellular transfer of cellular contents in human malignant pleural mesothelioma.* PLoS One, 2012. **7**(3): p. e33093.

77. Ady, J.W., et al., *Intercellular communication in malignant pleural mesothelioma: properties of tunneling nanotubes.* Front Physiol, 2014. **5**: p. 400.
78. Thayanithy, V., et al., *Tumor-stromal cross talk: direct cell-to-cell transfer of oncogenic microRNAs via tunneling nanotubes.* Transl Res, 2014. **164**(5): p. 359-65.
79. Gousset, K. and C. Zurzolo, *Tunnelling nanotubes: a highway for prion spreading?* Prion, 2009. **3**(2): p. 94-8.
80. Langevin, C., et al., *Characterization of the role of dendritic cells in prion transfer to primary neurons.* Biochem J, 2010. **431**(2): p. 189-98.
81. McCune, J.M., *The dynamics of CD4+ T-cell depletion in HIV disease.* Nature, 2001. **410**(6831): p. 974-9.
82. World Health Organization. *Global Health Observatory (GHO) data*. 2014 2015 February 23, 2015]; Available from: http://www.who.int/gho/hiv/en/.
83. Rudnicka, D. and O. Schwartz, *Intrusive HIV-1-infected cells.* Nat Immunol, 2009. **10**(9): p. 933-4.
84. Piguet, V. and R.M. Steinman, *The interaction of HIV with dendritic cells: outcomes and pathways.* Trends Immunol, 2007. **28**(11): p. 503-10.
85. Collman, R.G., et al., *HIV and cells of macrophage/dendritic lineage and other non-T cell reservoirs: new answers yield new questions.* J Leukoc Biol, 2003. **74**(5): p. 631-4.
86. Eugenin, E.A., P.J. Gaskill, and J.W. Berman, *Tunneling nanotubes (TNT) are induced by HIV-infection of macrophages: a potential mechanism for intercellular HIV trafficking.* Cell Immunol, 2009. **254**(2): p. 142-8.
87. Kadiu, I. and H.E. Gendelman, *Macrophage bridging conduit trafficking of HIV-1 through the endoplasmic reticulum and Golgi network.* J Proteome Res, 2011. **10**(7): p. 3225-38.
88. Kadiu, I. and H.E. Gendelman, *Human immunodeficiency virus type 1 endocytic trafficking through macrophage bridging conduits facilitates spread of infection.* J Neuroimmune Pharmacol, 2011. **6**(4): p. 658-75.
89. Izquierdo-Useros, N., et al., *HIV-1 capture and transmission by dendritic cells: the role of viral glycolipids and the cellular receptor Siglec-1.* PLoS Pathog, 2014. **10**(7): p. e1004146.
90. Rinaldo, C.R., *HIV-1 Trans Infection of CD4(+) T Cells by Professional Antigen Presenting Cells.* Scientifica (Cairo), 2013. **2013**: p. 164-203.
91. Landi, A., et al., *One protein to rule them all: modulation of cell surface receptors and molecules by HIV Nef.* Curr HIV Res, 2011. **9**(7): p. 496-504.
92. Xu, W., et al., *HIV-1 evades virus-specific IgG2 and IgA responses by targeting systemic and intestinal B cells via long-range intercellular conduits.* Nat Immunol, 2009. **10**(9): p. 1008-17.
93. Mailliard, R.B., et al., *Selective Induction of CTL Helper Rather Than Killer Activity by Natural Epitope Variants Promotes Dendritic Cell-Mediated HIV-1 Dissemination.* J Immunol, 2013. **191**(5): p. 2570-80.
94. Zaccard, C.R., et al., *HIV's ticket to ride: Cytotoxic T-lymphocyte-activated dendritic cells exploited for virus intercellular transfer.* AIDS Res Hum Retroviruses, 2014. **30**(11): p. 1023-4.
95. Dimitrov, D.S., et al., *Quantitation of human immunodeficiency virus type 1 infection kinetics.* J Virol, 1993. **67**(4): p. 2182-90.

96. Feldmann, J. and O. Schwartz, *HIV-1 Virological Synapse: Live Imaging of Transmission.* Viruses, 2010. **2**(8): p. 1666-80.
97. McDonald, D., *Dendritic Cells and HIV-1 Trans-Infection.* Viruses, 2010. **2**(8): p. 1704-17.
98. Garcia, E., et al., *HIV-1 trafficking to the dendritic cell-T-cell infectious synapse uses a pathway of tetraspanin sorting to the immunological synapse.* Traffic, 2005. **6**(6): p. 488-501.
99. Yu, H.J., M.A. Reuter, and D. McDonald, *HIV traffics through a specialized, surface-accessible intracellular compartment during trans-infection of T cells by mature dendritic cells.* PLoS Pathog, 2008. **4**(8): p. e1000134.
100. Rinaldo, C., *HIV-1 Trans Infection of CD4+ T Cells by Professional Antigen Presenting Cells.* Scientifica, 2013. **Volume 2013 (2013)**(Article ID 164203): p. 30 pages.
101. Cavrois, M., J. Neidleman, and W.C. Greene, *The achilles heel of the trojan horse model of HIV-1 trans-infection.* PLoS Pathog, 2008. **4**(6): p. e1000051.
102. Cavrois, M., et al., *In vitro derived dendritic cells trans-infect CD4 T cells primarily with surface-bound HIV-1 virions.* PLoS Pathog, 2007. **3**(1): p. e4.
103. Izquierdo-Useros, N., et al., *Capture and transfer of HIV-1 particles by mature dendritic cells converges with the exosome-dissemination pathway.* Blood, 2009. **113**(12): p. 2732-41.
104. Izquierdo-Useros, N., et al., *HIV and mature dendritic cells: Trojan exosomes riding the Trojan horse?* PLoS Pathog, 2010. **6**(3): p. e1000740.
105. Nikolic, D.S., et al., *HIV-1 activates Cdc42 and induces membrane extensions in immature dendritic cells to facilitate cell-to-cell virus propagation.* Blood, 2011. **118**(18): p. 4841-52.
106. Felts, R.L., et al., *3D visualization of HIV transfer at the virological synapse between dendritic cells and T cells.* Proc Natl Acad Sci U S A, 2010. **107**(30): p. 13336-41.
107. Kalinski, P., et al., *Prostaglandin E2 induces the final maturation of IL-12-deficient CD1a+CD83+ dendritic cells: the levels of IL-12 are determined during the final dendritic cell maturation and are resistant to further modulation.* J Immunol, 1998. **161**(6): p. 2804-9.
108. Poropatich, K. and D.J. Sullivan, Jr., *Human immunodeficiency virus type 1 long-term non-progressors: the viral, genetic and immunological basis for disease non-progression.* J Gen Virol, 2011. **92**(Pt 2): p. 247-68.
109. Hadi, K., et al., *Human immunodeficiency virus type 1 Vpr polymorphisms associated with progressor and nonprogressor individuals alter Vpr-associated functions.* J Gen Virol, 2014. **95**(Pt 3): p. 700-11.
110. Rappocciolo, G., et al., *Alterations in cholesterol metabolism restrict HIV-1 trans infection in nonprogressors.* MBio, 2014. **5**(3): p. e01031-13.
111. Pinchuk, L.M., et al., *The role of CD40 and CD80 accessory cell molecules in dendritic cell-dependent HIV-1 infection.* Immunity, 1994. **1**(4): p. 317-25.
112. Vanham, G., et al., *Decreased CD40 ligand induction in CD4 T cells and dysregulated IL-12 production during HIV infection.* Clin Exp Immunol, 1999. **117**(2): p. 335-42.
113. Sanders, R.W., et al., *Differential transmission of human immunodeficiency virus type 1 by distinct subsets of effector dendritic cells.* J Virol, 2002. **76**(15): p. 7812-21.
114. Comrie, W.A., et al., *The dendritic cell cytoskeleton promotes T cell adhesion and activation by constraining ICAM-1 mobility.* J Cell Biol, 2015. **208**(4): p. 457-73.

115. Groot, F., et al., *Differential susceptibility of naive, central memory and effector memory T cells to dendritic cell-mediated HIV-1 transmission.* Retrovirology, 2006. **3**: p. 52.
116. Goulder, P.J., et al., *Evolution and transmission of stable CTL escape mutations in HIV infection.* Nature, 2001. **412**(6844): p. 334-8.
117. Jonuleit, H., et al., *Pro-inflammatory cytokines and prostaglandins induce maturation of potent immunostimulatory dendritic cells under fetal calf serum-free conditions.* Eur J Immunol, 1997. **27**(12): p. 3135-42.
118. Keating, S.M., et al., *Durable human memory T cells quantifiable by cultured enzyme-linked immunospot assays are induced by heterologous prime boost immunization and correlate with protection against malaria.* J Immunol, 2005. **175**(9): p. 5675-80.
119. Rappocciolo, G., et al., *DC-SIGN on B lymphocytes is required for transmission of HIV-1 to T lymphocytes.* PLoS Pathog, 2006. **2**(7): p. e70.
120. Tobert, J.A., *Lovastatin and beyond: the history of the HMG-CoA reductase inhibitors.* Nat Rev Drug Discov, 2003. **2**(7): p. 517-26.
121. Snijders, A., et al., *High-level IL-12 production by human dendritic cells requires two signals.* Int Immunol, 1998. **10**(11): p. 1593-8.
122. Nielsen, J.S., et al., *An in vitro-transcribed-mRNA polyepitope construct encoding 32 distinct HLA class I-restricted epitopes from CMV, EBV, and Influenza for use as a functional control in human immune monitoring studies.* J Immunol Methods, 2010. **360**(1-2): p. 149-56.
123. Balachandran, R., et al., *Human immunodeficiency virus isolates from asymptomatic homosexual men and from AIDS patients have distinct biologic and genetic properties.* Virology, 1991. **180**(1): p. 229-38.
124. Pan, J., et al., *Interferon-gamma is an autocrine mediator for dendritic cell maturation.* Immunol Lett, 2004. **94**(1-2): p. 141-51.
125. Ten Brinke, A., et al., *The clinical grade maturation cocktail monophosphoryl lipid A plus IFNgamma generates monocyte-derived dendritic cells with the capacity to migrate and induce Th1 polarization.* Vaccine, 2007. **25**(41): p. 7145-52.
126. Napolitani, G., et al., *Selected Toll-like receptor agonist combinations synergistically trigger a T helper type 1-polarizing program in dendritic cells.* Nat Immunol, 2005. **6**(8): p. 769-76.
127. Cheong, C., et al., *Microbial stimulation fully differentiates monocytes to DC-SIGN/CD209(+) dendritic cells for immune T cell areas.* Cell, 2010. **143**(3): p. 416-29.
128. Yang, H., et al., *Improved quantification of HIV-1-infected CD4+ T cells using an optimised method of intracellular HIV-1 gag p24 antigen detection.* J Immunol Methods, 2013. **391**(1-2): p. 174-8.
129. Holzer, T.J., et al., *Frequency of cells positive for HIV-1 p24 antigen assessed by flow cytometry.* AIDS, 1993. **7 Suppl 2**: p. S3-5.
130. Guan, Y., et al., *Self-protection of individual CD4+ T cells against R5 HIV-1 infection by the synthesis of anti-viral CCR5 ligands.* PLoS One, 2008. **3**(10): p. e3481.
131. Geijtenbeek, T.B., et al., *DC-SIGN, a dendritic cell-specific HIV-1-binding protein that enhances trans-infection of T cells.* Cell, 2000. **100**(5): p. 587-97.
132. Liu, X., et al., *Low dose latrunculin-A inhibits dexamethasone-induced changes in the actin cytoskeleton and alters extracellular matrix protein expression in cultured human trabecular meshwork cells.* Exp Eye Res, 2003. **77**(2): p. 181-8.

133. Sowinski, S., et al., *Optimized methods for imaging membrane nanotubes between T cells and trafficking of HIV-1.* Methods, 2011. **53**(1): p. 27-33.
134. Zaccard, C.R., et al., *CD40L induces functional tunneling nanotube networks exclusively in dendritic cells programmed by mediators of type 1 immunity.* J Immunol, 2015. **194**(3): p. 1047-56.
135. Harshyne, L.A., et al., *Dendritic cells acquire antigens from live cells for cross-presentation to CTL.* J Immunol, 2001. **166**(6): p. 3717-23.
136. Kastenmuller, W., M.Y. Gerner, and R.N. Germain, *The in situ dynamics of dendritic cell interactions.* Eur J Immunol, 2010. **40**(8): p. 2103-6.
137. Lindquist, R.L., et al., *Visualizing dendritic cell networks in vivo.* Nat Immunol, 2004. **5**(12): p. 1243-50.
138. Hormuzdi, S.G., et al., *Electrical synapses: a dynamic signaling system that shapes the activity of neuronal networks.* Biochim Biophys Acta, 2004. **1662**(1-2): p. 113-37.
139. Riol-Blanco, L., et al., *Nociceptive sensory neurons drive interleukin-23-mediated psoriasiform skin inflammation.* Nature, 2014. **510**(7503): p. 157-61.
140. Veres, T.Z., et al., *Spatial interactions between dendritic cells and sensory nerves in allergic airway inflammation.* Am J Respir Cell Mol Biol, 2007. **37**(5): p. 553-61.
141. Kalinski, P. and H. Okada, *Polarized dendritic cells as cancer vaccines: directing effector-type T cells to tumors.* Semin Immunol, 2010. **22**(3): p. 173-82.
142. Imbeault, M., et al., *Acquisition of host-derived CD40L by HIV-1 in vivo and its functional consequences in the B-cell compartment.* J Virol, 2011. **85**(5): p. 2189-200.
143. Palucka, K., J. Banchereau, and I. Mellman, *Designing vaccines based on biology of human dendritic cell subsets.* Immunity, 2010. **33**(4): p. 464-78.
144. Tan, A., H. De La Pena, and A.M. Seifalian, *The application of exosomes as a nanoscale cancer vaccine.* Int J Nanomedicine, 2010. **5**: p. 889-900.
145. Pusic, A.D., et al., *IFNgamma-stimulated dendritic cell exosomes as a potential therapeutic for remyelination.* J Neuroimmunol, 2014. **266**(1-2): p. 12-23.
146. Liu, K., et al., *Mesenchymal stem cells rescue injured endothelial cells in an in vitro ischemia-reperfusion model via tunneling nanotube like structure-mediated mitochondrial transfer.* Microvasc Res, 2014. **92**: p. 10-8.
147. Wang, X. and H.H. Gerdes, *Transfer of mitochondria via tunneling nanotubes rescues apoptotic PC12 cells.* Cell Death Differ, 2015.
148. Esteves, A.R., I. Gozes, and S.M. Cardoso, *The rescue of microtubule-dependent traffic recovers mitochondrial function in Parkinson's disease.* Biochim Biophys Acta, 2014. **1842**(1): p. 7-21.
149. del Real, G., et al., *Statins inhibit HIV-1 infection by down-regulating Rho activity.* J Exp Med, 2004. **200**(4): p. 541-7.